Variation, adaptation and evolution of the nasal cavity and the nasal airway

Laura Marechal

THÈSE PRÉSENTÉE
POUR OBTENIR LE GRADE DE

DOCTEURE DE L'UNIVERSITÉ DE BORDEAUX

ÉCOLE DOCTORALE N°304 SCIENCES ET ENVIRONNEMENTS
SPÉCIALITÉ ANTHROPOLOGIE BIOLOGIQUE

Par Laura MARÉCHAL

Variation, adaptation et évolution de la cavité nasale et de la voie aérienne nasale

Sous la direction de : Yann HEUZÉ

Soutenue le 6 juin 2023

Membres du jury :

Mme Christine COUTURE-VESCHAMBRE, PU, Université de Bordeaux	Présidente
M. Robert G. FRANCISCUS, Professor, University of Iowa	Rapporteur
M. Philipp GUNZ, Research Group Leader, MPI for Evolutionary Anthropology	Rapporteur
Mme Claire MAJOUFRE, PU-PH, CHU de Bordeaux	Examinatrice
Mme Neus MARTINEZ-ABADIAS, Professor, Universitat de Barcelona	Examinatrice
M. Yann HEUZÉ, Chargé de recherche, CNRS, Université de Bordeaux	Directeur
M. Jean DUMONCEL, Ingénieur de recherche, CNRS	Invité

Variation, adaptation et évolution de la cavité nasale et de la voie aérienne nasale

La diversité climatique à l'échelle du globe a façonné l'évolution de l'espèce humaine : depuis l'émergence du genre *Homo*, les populations se sont installées dans des niches englobant toutes les régions habitables. La question de l'adaptation aux environnements changeants est une question clé en évolution humaine, car de nombreux traits caractérisant notre espèce ont été interprétés comme des adaptations climatiques. Il a notamment été démontré que la morphologie de la cavité nasale variait en fonction de facteurs éco-géographiques (ex. température, humidité). Dans ce travail doctoral, nous tentons de comprendre comment les facteurs climatiques ont impacté la morphologie nasale humaine.

Le premier axe de ce projet vise à quantifier la variation de la voie aérienne nasale dans des populations humaines actuelles. Alors que la cavité nasale (volume négatif défini par l'os) a été largement étudiée, les chercheurs ont accordé peu d'attention à la voie aérienne nasale (volume négatif délimité par la muqueuse nasale). Pourtant, la muqueuse nasale est le principal tissu impliqué dans les fonctions physiologiques mises en lien avec l'adaptation climatique de la morphologie nasale. Par ailleurs, la co-variation stricte entre tissus osseux et tissus mous de la région nasale n'a pas été démontrée, ce qui questionne la pertinence des interprétations physiologiques basées sur la seule étude de crânes secs. A travers l'étude de 195 scans *in vivo* collectés dans 5 régions géographiques, nous quantifions la variation morphologique de la voie aérienne nasale chez l'humain moderne. Nos résultats mettent en évidence des différences de conformation subtiles mais significatives entre nos 5 échantillons. Nous n'enregistrons aucune différence de volume entre les groupes, ce qui questionne l'influence climatique sur les demandes métaboliques en oxygène. Par ailleurs, nous ne détectons aucun effet de l'âge ou du sexe sur la conformation de la voie aérienne nasale ; en revanche, ces facteurs en influencent le volume. Les hommes présentent des voies aériennes nasales plus volumineuses que les femmes, probablement pour répondre à des besoins énergétiques plus importants. Le volume a également tendance à augmenter avec l'âge, en raison d'une rétraction de la muqueuse nasale.

Le deuxième axe de ce projet vise à comprendre les mécanismes qui relient les variations climatiques et morphologiques. Il a été démontré que la relation entre le climat et la morphologie du corps humain est partiellement déterminée par une sélection naturelle pour

des phénotypes adaptés au froid. Cependant, de plus en plus d'éléments suggèrent que l'adaptation au climat peut également relever de la plasticité phénotypique, induisant une variation qui résulte d'un stress environnemental et qui se produit au cours de la vie d'un individu. Dans ce travail, nous essayons d'évaluer le rôle de cette plasticité phénotypique liée à la température, ainsi que celui de la dureté de la nourriture, sur la variation cranio-faciale de souris consanguines élevées dans différentes conditions de température. Nos résultats démontrent un effet de la plasticité phénotypique lié à la température : le volume de la cavité nasale des deux groupes de souris élevées au froid (10°C) est significativement plus petit que celui des groupes contrôle (20°C) et thermoneutralité (26°C). Nous soulignons également que la dureté de la nourriture a un effet majeur sur la conformation de la cavité nasale, ce qui brouille par ailleurs le signal d'une potentielle variation de conformation liée à la température. Ces observations peuvent être mises en relation avec des différences de forces masticatrices, liées à la dureté et à la quantité de la nourriture ingérée.

Grâce à ce travail, nous apportons une contribution originale aux recherches sur l'adaptation humaine au climat et soulignons la pertinence de l'utilisation de données modernes et expérimentales pour apporter une nouvelle perspective à ces questions.

Mots clés : Adaptation climatique ; Morphométrie géométrique ; Imagerie 3D; Morphologie nasale ; Plasticité phénotypique

Variation, adaptation and evolution of the nasal cavity and the nasal airway

The diversity of climatic conditions on a global scale has shaped the evolution of the human species: since the emergence of the genus *Homo*, populations have moved into niches encompassing all habitable regions, including some extreme environments. The question of the adaptation to these changing environments is a key issue in the study of human evolution, as many traits characterizing our species have been interpreted as climatic adaptations. More specifically, the nasal cavity morphology has been shown to vary according to ecogeographic factors (e.g. temperature, humidity). In this doctoral thesis, we join the collective research endeavor to understand how climatic factors have impacted nasal morphology in humans.

The first axis of this project seeks to quantify modern variability for the nasal airway in extant *Homo sapiens* populations. While nasal cavity (*i.e.,* the negative volume defined by bone) has been extensively studied, researchers have to date paid little attention to the nasal airway (*i.e.,* the negative volume delimited by the nasal mucosa). Yet, nasal mucosa is the main tissue involved in the physiological functions thought to underlie climate-related variation of the nasal morphology. Furthermore, no study has yet demonstrated a strict covariation between hard and soft tissues in the nasal region, which questions the relevance of physiologic interpretations based on the study of dry skulls alone. Through the study of 195 *in vivo* CT scans collected in 5 geographical regions, we proceed to a quantification of the morphological variation of the nasal airway in modern humans. Our results highlight subtle but statistically significant shape differences between the nasal airways of our 5 samples. Interestingly, we record no between-group differences in nasal airway volume, which questions the climate-related metabolic demands in oxygen. We do not detect any effect of age or sex on the shape of the nasal airway, but these factors are shown to influence nasal airway volume. Males display larger nasal airways than females, presumably to meet higher energetic demands. The nasal airway volume also tends to increase with age, probably because of a shrinkage of the nasal mucosa with age.

The second axis of this project aims at understanding the mechanisms connecting climatic and morphological variation. It has been showed that the relation between climate and human body morphology is partially driven by natural selection for cold-adapted phenotypes over successive generations. However, an increasing amount of evidence suggests that adaptation to climate can also go through an acclimatization, or phenotypic plasticity, *i.e.,* the

physiological and morphological variation that results from an environmental stress and occurs between the conception and the maturity of an organism. To date, little is known about such phenotypic plasticity of the nasal region. Here, we try to evaluate the role of such temperature-related phenotypic plasticity, but also of food hardness, on the craniofacial variation of inbred mice reared under different temperature conditions. Our results demonstrate an effect of developmental plasticity in response to temperature: the nasal cavity volume of the two groups of cold-reared mice (10°C) is significantly smaller than in the control (20°C) and thermoneutrality (26°C) groups. We also highlight that food hardness has a major effect on the shape of the nasal cavity, critically blurring the signal of a potential response to temperature on this feature of the morphology. These observations can be linked to differences in masticatory forces, probably due to both food hardness and food intake.

Through this work, we provide an original contribution to discuss human adaptation to climate and highlight the relevance of using modern and experimental data to bring a fresh perspective to these long-standing research questions.

Keywords: Climatic adaptation; Geometric Morphometrics; 3D Imaging; Nasal morphology; Phenotypic plasticity

RÉSUMÉ DÉTAILLÉ

Le climat est une composante fondamentale et omniprésente de l'environnement naturel, qui évolue lentement au cours des temps géologiques et agit, par ses fluctuations, comme une force de sélection naturelle sur les organismes vivants. La diversité des conditions climatiques à l'échelle de notre planète a notamment façonné l'évolution des populations humaines, dont certaines différences biologiques peuvent s'expliquer en partie par des interactions écologiques avec leur environnement physique (James 2010 ; Beall et al. 2012 ; Winder et al. 2015 ; Degroot et al. 2022). Depuis l'émergence du genre *Homo*, les populations humaines se sont installées dans des niches écologiques englobant toutes les régions climatiques habitables, y compris certains environnements extrêmes (e.g. Potts & Faith 2015).

En anthropologie biologique, l'intérêt pour les variations morphologiques humaines résultant de processus de sélection naturelle date des années 1950 (e.g. Washburn, 1951). À partir de ces premiers travaux, les chercheurs ont tenté de comprendre comment et pourquoi des caractéristiques phénotypiques spécifiques, mais aussi certaines variations génétiques (e.g. Hancock et al. 2011 ; Kalyakulina et al. 2020), sont apparues au sein de certains groupes humains et comment ces variations pourraient être partiellement expliquées par la capacité d'adaptation environnementale de ces groupes humains. L'adaptation de l'homme au climat a impliqué un mélange complexe d'évolution biologique et culturelle, au point qu'aujourd'hui, le résultat de ce long processus lie inextricablement ces deux facteurs. Au-delà de l'intérêt purement scientifique de ces questions, l'étude de l'adaptation climatique des populations humaines dans le passé nous donne également un aperçu de la manière dont le corps humain et les sociétés humaines, tant dans leurs aspects biologiques que culturels, réagissent à des environnements changeants et/ou extrêmes. Ce sujet de recherche fournit donc des informations essentielles à appliquer dans notre monde moderne, afin de nous protéger des conditions climatiques extrêmes que l'avenir nous réserve (IPCC 2023).

Dans le présent travail, nous nous concentrons spécifiquement sur l'adaptation morphologique aux températures froides. Plusieurs règles éco-géographiques ont été explorées pour expliquer l'adaptation de la morphologie liée au climat. Au XIX^{e} siècle, Bergmann

(1847, traduit dans James, 1970) et Allen (1877) ont observé des relations entre le climat, la taille du corps adulte et la morphologie chez les espèces homéothermes. Les paléoanthopologues ont ensuite confirmé que ces règles peuvent également s'appliquer à l'espèce humaine, car elles expliquent en partie la variation morphologique dans les populations vivant dans différents écosystèmes (par exemple, Ruff, 1994 ; Katzmarzyk & Leonard, 1998). Une autre règle éco-géographique formulée à l'époque (Thomson 1913) concerne la cavité nasale humaine, qui présente une morphologie relativement plus étroite lorsque le climat est plus frais et plus sec (voir également Thomson & Buxton, 1923). Des études ultérieures, basées sur diverses collections archéologiques et anatomiques et axées sur la morphologie nasale, ont confirmé son association avec des facteurs environnementaux. Ces études ont montré que dans les environnements plus froids et plus secs, les humains ont tendance à présenter une cavité nasale plus profonde, plus haute et plus étroite (Franciscus 1995 ; Churchill et al. 2004 ; Doorly et al. 2008 ; Yokley 2009 ; Holton et al. 2011, 2013 ; Evteev & Grosheva 2019). Cette morphologie améliorerait deux fonctions physiologiques assurées par le nez : le conditonnement de l'air, c'est-à-dire le processus par lequel l'air inspiré atteint la température centrale du corps et une saturation complète en vapeur d'eau (e.g. Wolf et al., 2004 ; Elad et al., 2008) et l'énergétique respiratoire, c'est-à-dire la régulation de la quantité d'air inhalé pour assurer la libération d'une quantité suffisante d'énergie pour le travail métabolique (e.g. Churchill et al., 2004 ; Hall, 2005 ; Froehle et al., 2013). Ces deux fonctions physiologiques pouvant être influencées par des facteurs climatiques, les structures nasales internes sont des zones anatomiques clés pour comprendre l'adaptation climatique de l'espèce humaine.

Dans ce contexte, nous avons décidé de nous joindre à l'effort collectif de recherche pour comprendre comment les facteurs climatiques ont impacté la morphologie nasale de l'espèce humaine. Ce projet doctoral se concentre plus spécifiquement sur deux axes de recherche, chacun basé sur un échantillon différent.

Le premier axe vise à quantifier la variabilité moderne de la voie aérienne nasale au sein de populations actuelles d'*Homo sapiens*. Si la cavité nasale (c'est-à-dire le volume négatif défini par l'os) a été largement étudiée, les anthropologues ont jusqu'à présent accordé peu d'attention à la voie aérienne nasale (c'est-à-dire le volume négatif à l'intérieur de la cavité nasale, délimité par la muqueuse nasale). Pourtant, la muqueuse nasale est le principal tissu impliqué dans les fonctions physiologiques supposément à l'origine des variations de la

morphologie nasale liées au climat. De plus, aucune étude n'a encore démontré une co-variation stricte entre les tissus durs et les tissus mous dans la région nasale. Ceci doit, à notre avis, inciter à la prudence dans l'application d'explications fonctionnelles aux variations climatiques de la morphologie des voies respiratoires supérieures, à travers l'unique étude de la morphologie de la cavité nasale osseuse.

Dans cette optique, nous avons mis en place un protocole basé sur des tomographies médicales collectées au Cambodge, au Chili, en France, en Russie et en Afrique du Sud. L'étude de ces données a été réalisée par des techniques d'imagerie 3D et de morphométrie. Nous explorons l'hypothèse selon laquelle la diversité génétique et géographique des populations modernes serait responsable d'une variation de la morphologie de la voie aérienne nasale. Notre approche vise également à explorer la variation intra-populationnelle de la morphologie de la voie aérienne nasale en relation avec la saisonnalité, le sexe et/ou l'âge. Nos résultats démontrent des différences de conformation subtiles mais significatives entre les voies aériennes nasales de nos cinq échantillons. Nous n'observons aucune différence de volume de la voie aérienne nasale en fonction des groupes, ce qui soulève la question de l'influence du climat sur les demandes métaboliques. Nous ne détectons aucun effet de l'âge ou du sexe sur la conformation de la voie aérienne. En revanche, ces facteurs influencent le volume de la voie aérienne nasale. Les hommes présentent en effet une voie aérienne nasale plus volumineuse que les femmes afin de répondre à des demandes énergétiques plus importantes. Le volume de la voie aérienne tend éagelement à augmenter avec l'âge, probablement en raison d'une rétraction de la muqueuse nasale.

Notre deuxième axe vise à comprendre les mécanismes qui relient les variations climatiques et morphologiques. Il a été démontré que la relation entre le climat et la morphologie du corps humain est régie par des mécanismes génétiques (Katzmarzyk & Leonard 1998 ; Serrat et al. 2008), impliquant par exemple une sélection naturelle, au cours des générations, pour des phénotypes adaptés au froid. Selon cette hypothèse, les stress climatiques peuvent avoir conduit à des adaptations qui ne sont plus essentielles à la survie de l'homme moderne. Cependant, de plus en plus d'éléments suggèrent que l'adaptation au climat peut également passer par une acclimatation, ou plasticité phénotypique (également appelée plasticité développementale), c'est-à-dire la variation physiologique et morphologique qui résulte d'un stress environnemental et qui se produit entre la conception et la maturité d'un

organisme (Rae et al. 2006 ; Serrat et al. 2008). Par définition, ces mécanismes épigénétiques ne durent que le temps de la vie de l'organisme, mais peuvent néanmoins avoir une importance biologique capitale (voir par exemple Gluckman & Hanson 2006).

L'utilisation d'approches expérimentales dans des environnements contrôlés est susceptible de nous permettre de distinguer les causes génétiques de la variation phénotypique liée au climat. Pour répondre à notre deuxième axe de recherche, nous avons choisi de travailler sur des images micro-tomographiques de souris (*Mus musculus*) élevées dans différentes conditions de température : soit à 26˚C (thermoneutralité), soit à 22˚C (contrôle), soit à 10˚C (froid). Les souris étudiées étant consanguines, cet échantillon permet de s'affranchir artificiellement du signal de sélection naturelle. Notre approche vise également à tester l'effet des forces masticatoires sur la morphologie nasale, puisque nous avons nourri les deux groupes de souris élevées au froid avec des palettes de dureté différente. Ce facteur peut avoir son importance, car les animaux vivant dans des conditions froides ont tendance à augmenter leur consommation de nourriture afin de répondre aux demandes énergétiques plus élevées requises par leur environnement. Nos résultats démontrent un effet de plasticité phénotypique en réponse à la température : le volume de la cavité nasale des deux groupes de souris élevées au froid est significativement plus petit que celui des groupes contrôle et thermoneutralité. Nous soulignons que la dureté de la nourriture a un effet majeur sur la conformation de la cavité nasale, ce qui brouille sensiblement le signal d'une réponse potentielle à la température. Cela peut être lié à une variation des forces masticatrices, due à la fois à la consistance de la nourriture et à sa quantité. En effet, les souris élevées au froid ont consommé plus de nourriture, en particulier lorsque la nourriture est ramollie, ce qui est possiblement lié à une nécessité plus forte d'usure dentaire. Enfin, nous n'observons aucune différence significative pour la morphologie externe du squelette cranio-facial.

À la fin de ce travail, nous fournissons une synthèse générale de tous nos résultats. Nous commençons par les replacer dans le contexte de l'adaptation de l'homme au climat et discutons de la pertinence de l'utilisation de données modernes et expérimentales pour apporter une nouvelle perspective à ces questions de recherche de longue date. Enfin, nous suggérons d'autres pistes de recherche qui, selon nous, mériteraient d'être explorées à l'avenir.

ORIGINAL PUBLICATIONS
PUBLICATIONS ORIGINALES

This work is a thesis by publication, based on the following peer reviewed papers:

1. Maréchal L. and Heuzé Y. **2022**
   Interaction Between Environmental Temperature and Craniofacial Morphology in Human Evolution: A Focus on Upper Airways. In *Evolutionary Cell Processes in Primates: Genes, Skin, Energetics, Breathing, and Feeding*, Volume II, eds. M. K. Pitirri and J. T. Richtsmeier, CRC Press: Boca Raton and London

2. Maréchal L., Dumoncel J., Santos F., Astudillo Encina W., Evteev A., Prevost A., Toro-Ibacache V., Venter R.G., Heuzé Y. **2023**
   New insights into the variability of upper airway morphology in modern humans. *Journal of Anatomy* 242(5): 787-795.

3. Maréchal L., Magne L., Santos F., Devlin M., Heuzé Y. **In preparation**
   Food hardness and cold stress influence on the craniofacial and nasal morphology of inbred mice.

The present manuscript was written following the bibliographic standards of the Journal of Anatomy. Unless stated otherwise, all the illustrations are original and made by the author of this thesis.

ACKNOWLEDGEMENTS
REMERCIEMENTS

Upon completion of this doctoral project, I would like to thank many people without whom this experience would have been impossible and/or infinitely more unpleasant. I could not bring myself to choose a language for these acknowledgements, so I decided to express my gratitude in a language that corresponds to each one. Hopefully the purists will forgive me for these linguistic acrobatics.

Mes premiers mots vont à mon directeur de thèse, Yann Heuzé. Il y a quatre ans, tu m'as proposé d'embarquer pour cette aventure et, puisses-tu me le re-proposer cent fois, pas une fois je ne reviendrais sur ma décision. La façon dont cette thèse s'est déroulée te revient autant qu'à moi, car elle a été guidée par ta bienveillance et ton soutien. Je tiens donc à te remercier du fond du cœur pour ton accompagnement scientifique, qui m'a aidée à développer une richesse de compétences et de réflexions relevant de tous les aspects de la recherche, ainsi que pour ta confiance sans failles, qui a rapiécé la mienne à diverses reprises, et qui m'a surtout permis de m'épanouir sereinement dans cette thèse. Bien que ces mots semblent peu de chose, puisses-tu prendre la mesure de l'étendue et de la sincérité de ma gratitude.

I would like to express my sincere gratitude to Robert Franciscus and Philipp Gunz, who accepted to be the reviewers of this doctoral thesis, but also to Christine Couture, Neus Martínez-Abadías and Claire Majoufre for accepting to participate in my jury.

Cette thèse de doctorat n'aurait pu être menée à bien sans le soutien financier et administratif de nombreuses institutions, à commencer par le Ministère de l'Enseignement Supérieur et de la Recherche, qui m'a accordé en 2019 une bourse doctorale. Je remercie également le projet Erasmus+ Bakeng se Afrika qui a participé à mon environnement de thèse et qui m'a notamment offert l'opportunité d'un déplacement en Afrique du Sud. Merci au LabEx Sciences Archéologiques de Bordeaux pour son soutien financier dans la mise en place du protocole expérimental ayant généré une partie des données traitées dans cette thèse. De plus, je remercie Bordeaux Métropole pour m'avoir accordé une bourse de soutien à la mobilité, qui m'a permis de présenter les résultats de mes recherches au colloque 2022 de l'American

Association of Biological Anthropologists à Denver (USA). Je remercie également le Service Développement des Compétences de l'Université de Bordeaux qui, à deux reprises, m'a accordé un financement de formation individuelle. Merci à l'école doctorale « Sciences et Environnements » de l'Université de Bordeaux pour son soutien administratif. Enfin, je remercie la direction (actuelle et précédente) du laboratoire PACEA pour m'avoir fourni un environnement de travail favorable, l'équipement nécessaire à la réalisation de ma recherche, mais aussi pour l'aide financière ponctuelle apportée lors de mes déplacements et formations. Merci également à l'équipe de gestion administrative et financière pour leur soutien dans toutes mes démarches administratives.

J'adresse également mes sincères remerciements aux membres de mon comité de suivi de thèse pour avoir suivi ce travail doctoral avec bienveillance : Bruno Maureille, Priscilla Bayle, Thomas Colard et Nicolas Navarro, ainsi qu'aux invité·e·s qui ont ponctuellement assisté à nos discussions : Isabelle Crevecoeur, Neus Martínez-Abadías, et Markus Bastir.

My warmest thanks also go to the collaborators with whom I have had the privilege of working during the past three years. En particulier, je souhaite remercier Jean Dumoncel, qui m'a accompagnée avec beaucoup de patience dans mes premières utilisations du logiciel Deformetrica et dans la mise en place du protocole d'étude qui est au cœur de mon travail de thèse. Jean, un immense merci pour ton aide, sans laquelle j'aurais été bien désemparée. J'espère que cette collaboration ne sera pas la dernière et je te suis reconnaissante d'avoir accepté de siéger dans mon jury de thèse en tant qu'invité. Je souhaite également remercier Frédéric Santos, qui a supporté sans broncher mes innombrables questions tout au long de la thèse. Fred, je te remercie pour toutes nos discussions et nos échanges de mails, qui m'ont permis d'avoir totalement confiance en la solidité de mes analyses. Sans compter que ton entrain donne envie de revenir inlassablement frapper à ta porte… tu ne chercherais pas à nous faire aimer les stats à notre insu, par hasard ? Je remercie également Thomas Colard, pour nos nombreux échanges depuis ceux, les premiers, de mon jury master, ainsi que Nicolas Vanderesse pour ses enseignements, conseils et soutien concernant les techniques d'imagerie. In addition, I would also like to give special thanks to Rudolph G. Venter, for his precious help in the acquisition of some of the data used in my doctoral research, but also for his kind encouragements during this whole project. Finally, many thanks to Viviana Toro-Ibacache and Maureen Devlin for our stimulating discussions on my research project.

During the past three years, I also had the pleasure to be involved in several research projects that have been the scene of enthusiastic and inspiring scientific discussions. I would therefore like to thank the members of the Bakeng se Afrika project, especially Mandi Alblas, Rudolph Venter, Chantelle Marais, Anna Beyers and Aimee Welmans for their friendly welcome in Stellenboch University in August 2022. I also address my special thanks to Ericka L'Abbé, Charlotte Theye, Alison Ridel, Okuhle Sapo, Meg-Kyla Erasmus, Miksha Harripershad and Marius Loots for their warm welcome at FARC, University of Pretoria, and for the great scientific exchanges. I would also like to thank the members of the CFD working group, namely Markus Bastir, Daniel Sanz Prieto, Manuel Burgos, Alejandro Pérez Ramos, Andrej Evteev, Viviana Toro-Ibacache and Yann Heuzé, for including me in the stimulating discussions we had around air conditioning and CFD simulations. Many thanks also to the members of the Jerome Lejeune project on sleep obstructive apnea and dementia in Down syndrome, and more specifically to Neus Martínez-Abadías, Yann Heuzé, Luis Miguel Echeverry Quiceno, Xavier Sevillano Domínguez, Helena Pardina Torner and Juan Fortea Ormaechea.

Je souhaiterais également adresser mes remerciements les plus chaleureux à toute l'équipe du programme de recherche PSPCA, à commencer par Jessie Cauliez, qui m'a accueillie à bras ouverts dans ce projet passionnant. Jessie, merci pour ta confiance, ton énergie et ta bienveillance, qui sont une véritable source d'inspiration. Merci également à Stéphane Hérouin, pour m'avoir accueillie sur le site d'Antakari de telle manière que je m'y suis d'emblée sentie à ma place. Stéphane, merci pour ton soutien dans les projets à venir. J'adresse également mes plus chaleureux remerciements à tous les autres membres du projet que j'ai eu la chance de rencontrer à travers ce projet : Xavier Gutherz, Benjamin Marquebielle, Jean-Baptiste Fourvel, Isabelle Crevecoeur, Mariam Abdoulkader, Ibrahim Osman Ali, Yasmine Mechadi, Nicolas Martin, Asma Youssouf, Carlo Mologni, Emmanuel Baudouin, Quentin Aubourg, Romain Mensan, Gwenaël Hervé, Jacques et Amel Jaillet, ainsi que tous nos collaborateurs du Gobaad. La diversité et la richesse de ce programme et les échanges que j'ai pu avoir avec chacun·e d'entre vous m'ont immensément inspirée, tant d'un point de vue professionnel que personnel. Un dernier mot pour Isa, car je ne te remercierai jamais assez de m'avoir demandé, un soir, autour d'un repas péruvien : « Tu veux venir fouiller à Djibouti ? ». Une bien heureuse proposition…

Je tiens également à remercier très sincèrement tou·te·s les membres de l'UMR PACEA que j'ai eu le privilège de côtoyer durant ces dernières années. Je remercie tout d'abord les deux

équipes de direction qui ont été en charge de l'UMR pendant ma période de thèse : Anne Delagnes et Christine Couture, puis William Banks et Priscilla Bayle. Je vous remercie pour nos échanges, votre soutien et votre volonté de dialogue. A tou·te·s les autres membres du laboratoire, bien trop nombreux·ses pour être cité·e·s, je souhaite adresser mes plus chaleureux remerciements. Durant ces quatre dernières années, j'ai fréquenté ce laboratoire avec beaucoup de joie et je suis très reconnaissante pour la bienveillance que vous m'avez témoignée. Au détour d'une réunion scientifique, de la machine à café du B8 ou d'un déjeuner (costumé) au B2, j'ai eu plaisir à échanger avec chacun·e d'entre vous. Nos discussions, scientifiques ou non, m'ont fait grandir au-delà du concevable. Je remercie également l'équipe pédagogique du laboratoire, et plus particulièrement Christine Couture, Priscilla Bayle et Christopher Knüsel, pour m'avoir permis de dispenser mes premiers enseignements universitaires dans le master BGS/ASA, ainsi que Christine Couture et Frédéric Santos pour m'avoir incluse dans l'organisation de la Graduate School en imagerie et morphométrie. Enfin, un mot pour mes deux binômes d'organisation/coordination des réunions scientifiques, Maïté Rivollat et Antony Colombo : merci de faire partie des gardien·ne·s de la flamme du collectif.

Je réserve ici une place particulière à mes collègues doctorant·e·s, post-doctorant·e·s et jeunes chercheur·se·s de PACEA. Comment vous exprimer ma gratitude en quelques lignes, à vous qui avez cheminé à mes côtés pendant ces dernières années ? Collègues souvent devenu·e·s ami·e·s, vous avez grandement participé à rendre cette expérience tantôt apaisée, tantôt drôle, tantôt simplement surmontable (ce qui, certains jours, est déjà beaucoup). Un immense merci, en particulier à Mathilde Augoyard, Maïté Rivollat, Eliza Orellana-Gonzalez, Ana Arzelier, Nicolas Martin, Alexandra Schuh, Kate McGrath, Floriane Rémy, Juliette Henrion, Quentin Villeneuve, Anaïs Vignoles, Anna Rufa, Patricia Santos, Kim Genuite, Marion Holleville, Monica Gala, Lila Geis, Diego Lopez-Onandia, Fanny Mendisco, Manon Bocquel, Elle Liagre, Sierra Blunt, Laura Cassard, Guilhem Mauran, Luc Doyon, Corentin Gibert, Dany Coutinho-Nogueira, Flora Chauvet-Dumur, Pauline Kirgis, Lisa Richelmi, Pierre Justeau, Pierre-Hadrien Decaup et Anaïs Du Fayet de la Tour. Nos chemins ne se sont parfois que brièvement croisés, mais ces rencontres, nos échanges, nos apéros et autres aventures resteront longtemps gravés dans ma mémoire. Merci.

Il paraîtra évident à la lecture de cette thèse que j'aime tenter de comprendre les chemins tortueux qu'emprunte le cours des choses. Mon intérêt dans l'exploration des

événements du passé et dans l'imagination des scénarios possibles s'applique aussi à mon propre parcours. Il me plaît, à l'occasion, de me retourner et d'apprécier chaque étape et chaque choix, eussent-ils été agréables ou pénibles, qui m'ont menée où je suis aujourd'hui. Je souhaiterais donc profiter des quelques lignes qui vont suivre pour remercier quelques personnes ayant eu une influence significative ($p<0.001$) sur ma micro-évolution personnelle. Je souhaiterais commencer par remercier ceux et celles qui ont été les premier·ère·s à me parler d'archéologie. Certaines m'ont même permis de la pratiquer : mon premier chantier de fouilles, il y a 10 ans, gardera ainsi toujours une place particulière dans ma mémoire. Je remercie également les membres du CReA-Patrimoine de l'Université Libre de Bruxelles que j'ai eu le plaisir de côtoyer, notamment (et surtout) sur le terrain. De mes années bruxelloises, je souhaite également adresser un remerciement tout particulier à Caroline Polet, pour m'avoir un jour, au détour d'une conversation, conseillé de postuler au master de Bordeaux. Enfin, à toutes les personnes dont j'ai croisé la route et qui ont influencé mon parcours : bien que je ne puisse citer tous vos noms, sachez que je suis riche de tous les apprentissages que vous m'avez apportés et que pour cela, je vous suis infiniment reconnaissante.

A tou·te·s mes ami·e·s, et tout particulièrement à P-ALM, Manon, Maïté, Mathilde, Manue, Eliza, Antony, Alexandra, Nico, Arthur, Adrien, Manon, Alice, Précillia, Yasmine, Céline, Tati, Ben… vous faites de ma vie une aventure follement joyeuse et joyeusement folle. Malgré la distance et les turbulences de l'existence, malgré les chemins qui, parfois, divergent, vous savoir dans ma vie a quelque chose d'immensément apaisant. Merci de me soutenir dans tout ce que j'entreprends. Merci d'être là, tout simplement.

Merci également aux professeur·e·s et aux élèves de l'Art et Fact Studio, particulièrement à Charlotte et aux merveilleuses chasseuses-cueilleuses du contempole. Merci à Amandine de faire vivre ce lieu, qui a été l'une de mes soupapes de décompression privilégiées depuis mon arrivée à Bordeaux, et notamment au cours de cette thèse.

Quelques mots également pour celles et ceux qui m'ont accompagnée, épaulée, secouée et rassurée avec acharnement durant le sprint final. La fin de la thèse est un moment empli de doutes, que vous avez apaisés avec patience et bienveillance. Vous avez été nombreux·ses à me témoigner des marques de soutien à travers de longues discussions existentielles, des messages d'encouragement, du joli courrier dans ma boîte aux lettres, des

massages de bureau, des dessins, des olas et de nombreuses autres petites attentions. A vous tou·te·s : merci du fond du cœur. Ces attentions, je les ai toutes reçues. Et je n'y serai pas arrivée sans vous. Merci également à mes relecteur·rice·s pour leur chasse à la coquille, ainsi qu'à Louis Lamour, Hans Zimmer et David Castello-Lopes pour leur inestimable soutien psychologique.

Enfin, je remercie toute ma famille, et plus particulièrement les quatre autres Maréchaux. Papa, maman, je vous dois une grande partie de ce que je suis. Vous n'avez cessé de m'encourager à poursuivre ma route, quels que puissent être les chemins tortueux et escarpés que j'ai parfois empruntés. Avec une patience et un amour intarissables, toujours un pas derrière moi pour me relever en cas de chute, mais à bonne distance pour me laisser joyeusement gambader vers l'avenir, vous avez ainsi créé un environnement dans lequel rien n'est impossible. A mes grandes sœurs, Justine et Noémie, qui ont toujours été là pour me faire rire, me protéger ou me rassurer quand, parfois, je me cogne contre la vie : merci d'être mon ancrage dans ce monde de fou. Merci également à mes deux super beaux-frères, Mathieu et Eric, d'avoir rejoint notre famille et de supporter nos extravagances.

Je conclurai ces remerciements par une pensée pour mes grands-parents binchous, Victor et Paulette, qui font partie intégrante de la personne que je suis devenue, et n'auront pourtant vu qu'une partie trop courte du chemin que j'ai suivi. J'aime à penser qu'il leur aurait plu de voir l'aboutissement de ce travail ; il leur est également dédié.

TABLE OF CONTENTS
TABLE DES MATIÈRES

LIST OF FIGURES
LISTE DES FIGURES

LIST OF TABLES
LISTE DES TABLEAUX

LIST OF APPENDICES
LISTE DES ANNEXES

• Chapter 1 •

INTRODUCTION

« There is nothing like looking, if you want to find something. You certainly usually find something, if you look, but it is not always quite the something you were after »

— J.R.R. Tolkien

1.1. Background of the research project

Climate is a fundamental and ubiquitous component of the natural environment, evolving slowly over geological time and acting, through its fluctuations, as a force of natural selection on living organisms. The diversity of climatic conditions on a global scale has notably shaped the evolution of human populations, whose biological differences can be explained to some extent by their ecological interactions with their physical landscape (James, 2010; Beall et al., 2012; Winder et al., 2015; Degroot et al., 2022). Since the emergence of the genus *Homo*, populations have moved into niches encompassing all habitable climatic regions including some extreme environments (e.g. Potts & Faith 2015). *Homo sapiens*, whose emergence in Africa is currently estimated around 300-200 ky ago (e.g. Schlebusch et al., 2017; Lipson et al., 2020) evolved from equatorial populations descending from ancestors well adapted to tropical environments (e.g. Hanna & Brown 1983). After dispersing throughout the globe, humans now occupy environments that are far from the prime tropical forests of our oldest ancestors, and can instead be characterized by low temperatures, a drop in barometric pressure at high altitudes and/or variation in ultraviolet (UV) radiation. We can consider that all these conditions are relatively new to us in an evolutionary perspective (James, 2010).

In biological anthropology, interest in human morphological variation resulting from natural selective processes dates from the 1950s (e.g. Washburn 1951). Starting from these early works, researchers have attempted to understand how and why specific phenotypic features, but also some genotypic variation (e.g. Hancock et al. 2011; Kalyakulina et al. 2020), have emerged within some human groups and how they might be partially explainable by environmental adaptability. Human adaptation to climate has involved a complex intermingling of biological and cultural evolution, to the point that today, the result of this long process inextricably links these two factors. This is true to such an extent that a plausible hypothesis is that biological adaptations to climate are no longer functionally essential for extant humans to survive in a wide range of climatic environments (Beall et al., 2012). Beyond the purely scientific interest of these questions, the study of the climatic adaptation of human populations in the past also gives us an overview of how the human body and human societies, all mixed in their biological and cultural aspects, react to changing and/or extreme environments. This topic of research thus provides essential information to be applied in our

modern world, in order to protect ourselves from the extreme climatic conditions that the future holds (IPCC, 2023).

In the present work, we focus specifically on morphological adaptation to cold temperature. In a cold environment, the body core temperature must be maintained at a sufficient level to ensure the functioning of cerebral and physiological processes. Human populations have therefore developed biological protections to cold through acclimatization, even though the cultural and behavioral adaptation to cold, which can vary widely across human groups and might have attenuated the extent of genetic selection in cold-climate populations, must not be neglected (Katzmarzyk & Leonard, 1998; James, 2010; Beall et al., 2012).

Several eco-geographic rules have been explored to explain the climate-related adaptation of morphology. In the nineteenth century, Bergmann (1847, translated in James, 1970) and Allen (1877) observed relationships between climate, adult body size and morphology in homoeothermic species (see Chapter 2.1.). Physical anthropologists have then confirmed that these rules can also apply to humans, for they partially explain morphological variation in human populations inhabiting different ecosystems (e.g. Ruff 1994; Katzmarzyk & Leonard, 1998). Another eco-geographic rule also formulated then (Thomson, 1913) involves the human nose, which displays a relatively narrower morphology when climate is cooler and dryer (see also Thomson & Buxton 1923). Previous research has also demonstrated a high inverse correlation between the nasal index (nose width/nose height) and vapor pressure, suggesting that humidity is a driving adaptive force (Weiner, 1954). Later studies, based on various archaeological and anatomical collections and focusing on the nasal morphology, have confirmed its association with environmental factors. These studies have shown that in colder and drier environments, humans tend to display a longer, taller and narrower nasal cavity (Franciscus, 1995; Churchill et al., 2004; Doorly et al., 2008; Yokley, 2009; Holton et al., 2011a, 2013; Evteev & Grosheva, 2019). This morphology would improve two physiological functions ensured by the nose: air conditioning, *i.e.*, the process by which the inspired air reaches body core temperature and a full saturation with water vapor (e.g. Wolf et al., 2004; Elad et al., 2008) and respiratory energetics, *i.e.*, the regulation of the amount of inhaled air to ensure the release of a substantial amount of energy for metabolic work (e.g. Churchill et al., 2004; Hall, 2005; Froehle et al., 2013). As both these physiological functions can be influenced by climatic factors

(see Chapter 2.2.), internal nasal structures are key anatomical areas for understanding the climatic adaptation of human species.

1.2. Research objectives

In this context, we have decided to join the collective research endeavor to understand how climatic factors have impacted nasal morphology in the human species. This doctoral project focuses more specifically on two research axes, each based on a different sample.

The first axis seeks to quantify modern variability for the nasal airway in extant *Homo sapiens* populations. While nasal cavity (*i.e.,* the negative volume defined by bone) has been extensively studied, biological anthropologists have to date paid little attention to the nasal airway (*i.e.,* the negative volume inside the nasal cavity, delimited by the nasal mucosa). Yet, nasal mucosa is the main tissue involved in the physiological functions thought to underlie climate-related variation of the nasal morphology. Furthermore, no study has yet demonstrated a strict covariation between hard and soft tissues in the nasal region. In our opinion, this should encourage caution in applying functional explanations to climate-related variation of the upper airway morphology, while studying solely the morphology of the bony nasal cavity.

With this in mind, we have set up a protocol based on medical CT scans collected in Cambodia, Chile, France, Russia and South Africa. The study of these data was achieved via 3D imaging and morphometric techniques. Considering the genetic diversity of these five populations, we do not seek to isolate the climate adaptation signal, which would be an unattainable goal with such a sample. However, we investigate the hypothesis that the genetic and geographic diversity of modern-day populations are responsible for a variation of the nasal airway morphology. Our approach also aims at exploring the intra-population variation of nasal airway morphology in relation to seasonality, sex and/or age.

The second axis aims at understanding the mechanisms connecting climatic and morphological variation. It has been showed that the relation between climate and human body morphology is driven by genetic mechanisms (Katzmarzyk & Leonard, 1998; Serrat et al., 2008), involving for example a natural selection for cold-adapted phenotypes over successive generations. Under this hypothesis, climatic stresses may have led to adaptations that are no longer essential for modern human survival. However, an increasing amount of evidence

suggests that adaptation to climate can also go through an acclimatization, or phenotypic plasticity (also referred to as developmental plasticity), *i.e.,* the physiological and morphological variation that results from an environmental stress and occurs between the conception and the maturity of an organism (Rae et al., 2006; Serrat et al., 2008). By definition, these epigenetic mechanisms only last during the lifetime of the organism. However, they may still have great biological significance (e.g. Gluckman & Hanson 2006). To date, little is known about such phenotypic plasticity of the nasal region.

The use of experimental approaches in controlled environments can provide a wealth of information to distinguish genetic from climatic causes of phenotypic variation. To address our second axis of research, we chose to work on microtomographic images of mice (*Mus musculus*) that were reared in different temperature conditions (these mice were reared either at 26˚C (thermoneutrality), 22˚C (control), or 10˚C (cold)). Since the studied mice are inbred, this sample allows us to artificially get rid of the natural selection signal. Our approach also aims to test the effect of masticatory forces on nasal morphology, as we fed the two groups of cold-reared mice with pellets of different hardness. This factor may be of importance since animals living in cold conditions tend to increase their food consumption in order to meet the higher energetic demands required in their extreme environment.

1.3. Organization of the manuscript

This work cannot be devoid of a chapter providing a detailed state of the art about climate influence on the morphology of the human craniofacial skeleton (Chapter 2). In this chapter, previously published as a book chapter (Maréchal & Heuzé, 2022), we provide a detailed description of upper airway anatomy and physiology and review the current knowledge on climate-related morphological variation in this area. In addition, we discuss the temperature-sensitive developmental pathways that might play a role in this morphological variation. In the scope of thermoregulation mechanisms, we explore how temperature can both directly and indirectly affect bone formation.

In the next chapter, we provide more information on the research methodology implemented to study our data (Chapter 3). More specifically, we develop the main theoretical concepts related to the shape comparison by surface registration. While some methodological

aspects relevant to the composition and treatment of each sample are described in the dedicated chapters (Chapters 4 and 5), the purpose of chapter 3 is also to provide more details on the methodological choices made during the different stages of data pre-processing and analysis.

Hence, the following chapters are intended to describe the results we obtained on each of our two samples, after presenting more specific details about the methodology applied to each of them. In chapter 4, we present the outcomes of the analysis of nasal airway morphology in five modern human groups, which was published as an article in Journal of Anatomy (Maréchal et al., 2023). We detail shape and volume variation both on an inter- and an intra-population scale. We then develop some potential explanations of such variation. In chapter 5, we present our findings on the inbred mice groups reared under different temperature conditions. We primarily focus our analyses on external craniofacial morphology, morphological variation of the nasal cavity, as well as volume variation of the nasal turbinates. This study is still in preparation and will be submitted for publication in the following weeks.

At the end of this work, we provide an extended discussion of all these results. We begin by placing them into the big picture of human adaptation to climate and discuss the relevance of using modern and experimental data to bring a fresh perspective to these long-standing research questions. Finally, we offer suggestions for further paths of research that we believe should be explored in the future.

• Chapter 2 •

CLIMATE INFLUENCE ON HUMAN CRANIOFACIAL MORPHOLOGY

INFLUENCE DU CLIMAT SUR LA MORPHOLOGIE CRANIOFACIALE HUMAINE

Chapter 2 was published as a book chapter:

> Maréchal L. and Heuzé Y. 2022. Interaction Between Environmental Temperature and Craniofacial Morphology in Human Evolution: A Focus on Upper Airways. In *Evolutionary Cell Processes in Primates: Genes, Skin, Energetics, Breathing, and Feeding*, Volume II, eds. M. K. Pitirri and J. T. Richtsmeier, CRC Press: Boca Raton and London.

Submitted 10 April 2020; Accepted 15 December 2020; eBook available 14 September 2021

Author contributions: LM: results interpretation, manuscript drafting and revision. YH: project conception, data collection, results interpretation, critical revision of the manuscript.

2.1. Introduction

The variation and evolution of craniofacial skeletal morphology in hominids is the result of a complex interplay between genetic factors (e.g. Adhikari et al. 2016; Pickrell et al. 2016; Shaffer et al. 2016; Zaidi et al. 2017; Claes et al. 2018) and biomechanical pressures related to brain growth, mastication, and respiration (Moss & Young, 1960; Enlow, 1990; Richtsmeier et al., 2006; Lieberman, 2011; Bastir & Rosas, 2013), as well as multiple environmental factors including diet, activity level, and ecogeographic variables such as temperature (e.g. Steegmann & Platner, 1968; Roseman, 2004; Rae et al., 2006; Evteev et al., 2014; Menéndez et al., 2014; Sardi, 2018; Wroe et al., 2018; Martin et al., 2021). Although developmental shifts in brain ontogeny and selective pressures in response to the biomechanical forces related to mastication and respiration appear to be predominant in human skull evolution (for a recent comprehensive review, see Lesciotto & Richtsmeier, 2019), environmental factors might still have a significant influence, though possibly more challenging to disentangle from other processes.

The influence of these environmental factors, particularly temperature, has been addressed in prior research, mainly focusing on their impact on infra- or post-crania morphology and body proportions (e.g. Holliday, 1997; Ruff, 2002; Holliday & Hilton, 2009). The pioneering work of Bergmann (1847, translated in James, 1970) states that homoeothermic organisms maintain stable internal body temperature by balancing the production of warmth within the volume of their body and the loss of warmth from its surface. In this thermoregulation process, the surface area-to-volume ratio of the body is therefore a predominant factor. According to Bergmann's rule, within a broadly distributed genus, species of larger size are found in colder environments, while species of smaller size are found in warmer environments. This rule, though still debated (e.g. Scholander, 1955; Mayr, 1963; McNab, 1971, 2010, 2012; Crognier, 1981a; Ruff, 1994; Katzmarzyk & Leonard, 1998; Ashton et al., 2000; Meiri & Dayan, 2003; Ochocińska & Taylor, 2003; Blackburn & Hawkins, 2004; Meiri et al., 2004; Rodríguez et al., 2006; Clauss et al., 2013; Foster & Collard, 2013; Alhajeri & Steppan, 2016; Gohli & Voje, 2016; Brown et al., 2017; Nunes et al., 2017; Sargis et al., 2018), also applies to the genus *Homo*. Allen's rule, based on another foundational work concerning the influence of environmental temperature on the morphology of homoeothermic organisms (Allen, 1877), states that in colder climates individuals tend to possess shorter limbs and extremities, thus reducing the surface area-to-volume ratio and the associated heat dissipation. In warm climates, the

opposite phenomenon is observed. However, Bergmann's and Allen's rules were based on observed variation of the postcranial skeleton and may not apply to the craniofacial skeleton. The impact of environmental temperature on the variation and evolution of skull phenotypes remains less clear, for example, in Neanderthals (e.g. Steegmann et al., 2002, but see Weaver, 2009). Moreover, attempts to provide mechanistic hypotheses to explain craniofacial morphological variation attributed to environmental temperature remain scarce. Hence, in the present chapter, we will review research relevant to two critical questions, which, from our perspective, are related and need to be addressed together to increase our comprehension of the role of climate in the evolution of craniofacial morphology: 1) what anatomical and functional units of the skull exhibit temperature-associated patterns of morphological variation? and 2) what developmental processes (genetic, molecular, and cellular) involved in craniofacial growth and development are sensitive to temperature, and could contribute to the explanation of such variation?

Among the different anatomical and functional units of the skull, the facial skeleton shows clear signs of morphological variation related to environmental temperature. In particular, temperature-related variation of the shape and size of the nasal cavity has been a focus of research in paleoanthropology and physical anthropology for many years. The nasal cavity forms the gateway to the respiratory system (Enlow, 1990). As such, the morphology of this interface region has long been considered a reliable proxy for studying the link between hominins and their environment (e.g. Davies, 1932; Weiner, 1954; Carey & Steegmann, 1981; Yokley, 2009; Noback et al., 2011). Two main hypotheses have been put forward to interpret how adaptive pressures impact nasal cavity morphology. These hypotheses are not mutually exclusive and relate to two factors that might simultaneously influence nasal morphology. The first hypothesis considers the morphology of the nasal cavity in relation to its air conditioning function and climatic adaptation (Shea, 1977; Cole, 1982a; Churchill et al., 2004; Yokley, 2009; Butaric et al., 2010; de Azevedo et al., 2017; Butaric & Klocke, 2018; Evteev & Grosheva, 2019; Heuzé, 2019). The air conditioning function of the nasal cavity is the process by which the inspired air reaches body core temperature and a full saturation with water vapor to protect the alveolar lining in the lower airway (Wolf et al., 2004; Elad et al., 2008). The second hypothesis emphasizes the role of the nasal cavity as the upper part of the respiratory system regulating

the amount of air inhaled and is thus closely related to the energetic demands of the body (Hall, 2005; Froehle et al., 2013; Holton et al., 2014, 2016; Wroe et al., 2018).

Neanderthals, who lived in Eurasia until about 28 kya ago (Finlayson et al., 2006), have received much attention on these matters. The morphology of the Neanderthal appendicular and facial skeletons has often been interpreted as cold adapted (e.g. Steegmann et al., 2002) and/or as the result of genetic drift (Weaver, 2009). In the facial region, this variation includes a larger nasal cavity in Neanderthal relative to anatomically modern Homo. This larger nasal cavity would allow an increased incoming airflow, associated with a larger volume of the ribcage to meet the high energetic demands of large-brained and heavy-bodied Neanderthals (Franciscus & Churchill, 2002; García-Martínez et al., 2018; Wroe et al., 2018) while providing an efficient way to condition air in cold climates (de Azevedo et al. 2017; but see Bastir 2019). Using computational fluid dynamics methods, one can quantify several airflow features characterizing respiration, as well as air conditioning efficiency in extant normal and pathological samples (Burgos et al., 2017; Kim et al., 2017). These methods have recently been used to study Neanderthals (de Azevedo et al., 2017; Wroe et al., 2018), though the virtual reconstruction of nasal mucosa of fossil specimens, achieved by morphing the modern human airway to fossil nasal cavities (see also Bourke et al. 2014), might be problematic (Evteev & Heuzé, 2018). Indeed, based on a relatively small sample (N = 30), Heuzé (2019) reported a rather low correlation between the volume of the bony nasal cavity and the negative volume defined by the nasal mucosa, that is, the functioning nasal airway, thus preventing robust direct interpolation of nasal airway volume on the basis of nasal cavity volume.

In this chapter, we take a step back and address the question of the interaction between environmental temperature and facial skeletal morphology from a new perspective. Our purpose is to provide an overview of the current knowledge of the temperature-related morphological variation of nasal and paranasal structures and to explore the temperature-sensitive pathways that might have a role in this variation. Genes sensitive to temperature are obviously of importance in temperature-related morphological variation, and examples are provided in this chapter. However, genes do not directly produce phenotypes (Cohen & MacLean, 2000; Richtsmeier & Lesciotto, 2020). Rather, phenotypes are the products of complex interactions between the genome and the internal and external environment. A concept central to these interactions is developmental plasticity, which is the response of cells, tissues, organs,

and/or an individual organism to environmental variation that occurs within the lifespan of an individual with a single genotype and results in the formation of more than one phenotype (Hall & Eckhard Witten, 2018). Acknowledging the key role of cellular processes in the making of phenotypes, this review focuses on the cellular response to temperature changes. In doing so, our purpose is to pave the way to a better understanding of the mechanisms that explain the relationship between climate variation and the morphology of the structures involved in respiration. We believe that such an approach will shed a new light on the role of temperature in human evolution.

2.2. Upper airway morphology

As stated, the nasal cavity forms the gateway to the respiratory system (Enlow, 1990). The covariation of environmental air temperature and humidity with morphology of the nasal structure has consequently been extensively addressed and these ecogeographic factors are considered a driving force in the expression of phenotypic variation and adaptation (Thomson, 1913; Thomson & Buxton, 1923; Davies, 1932; Woo & Morant, 1934; Negus, 1952, 1960; Weiner, 1954; Cottle, 1955; Wolpoff, 1968; Hiernaux & Froment, 1976; Carey & Steegmann, 1981; Crognier, 1981a,b; Franciscus & Trinkaus, 1988; Franciscus & Long, 1991; Franciscus, 1995; Roseman, 2004; Roseman & Weaver, 2004; Harvati & Weaver, 2006a,b; Márquez & Laitman, 2008; Hubbe et al., 2009; Yokley, 2009; Butaric et al., 2010; Bastir et al., 2011; Noback et al., 2011; Evteev et al., 2014; Jaskulska, 2014; Butaric, 2015; Maddux et al., 2016b; Zaidi et al., 2017; Marks et al., 2019). In the following, we discuss nasal anatomy and physiology and summarize what is currently known about climate-related phenotypic variation. Finally, we focus on the paranasal sinuses, their role in respiratory energetics, and current hypotheses about their covariation with nasal morphology and environmental factors.

Nasal anatomy and physiology

The nasal cavity is the area of the craniofacial skeleton that contains the nasal airway, the first anatomical region of the respiratory system involved in respiratory energetics and air conditioning. Conditioning of the inspired air in the nasal airway is achieved through contact with the respiratory mucosa producing heat exchange via convection and moisture exchange via evaporation (Cole, 1982b; Naclerio et al., 2007; Yokley, 2009). Skeletally, the nasal cavity is

bounded and defined by maxillary, nasal, palatal, vomer, sphenoid, frontal, ethmoid, and lacrimal bones. The shape, size, and relative position of these bones affect the morphology of the nasal cavity that, at least indirectly, conditions the quantity of air that can be inhaled and the air conditioning performances. The dimensions of the entry (piriform aperture) and exit (choanae) points significantly influence respiratory energetics (Swift & Proctor, 1977; Bastir & Rosas, 2013). Maddux et al. (2016b) argued that nasal cavity height was more likely to be associated with energetics, while nasal cavity width and length play an important role in air conditioning (Noback et al., 2011).

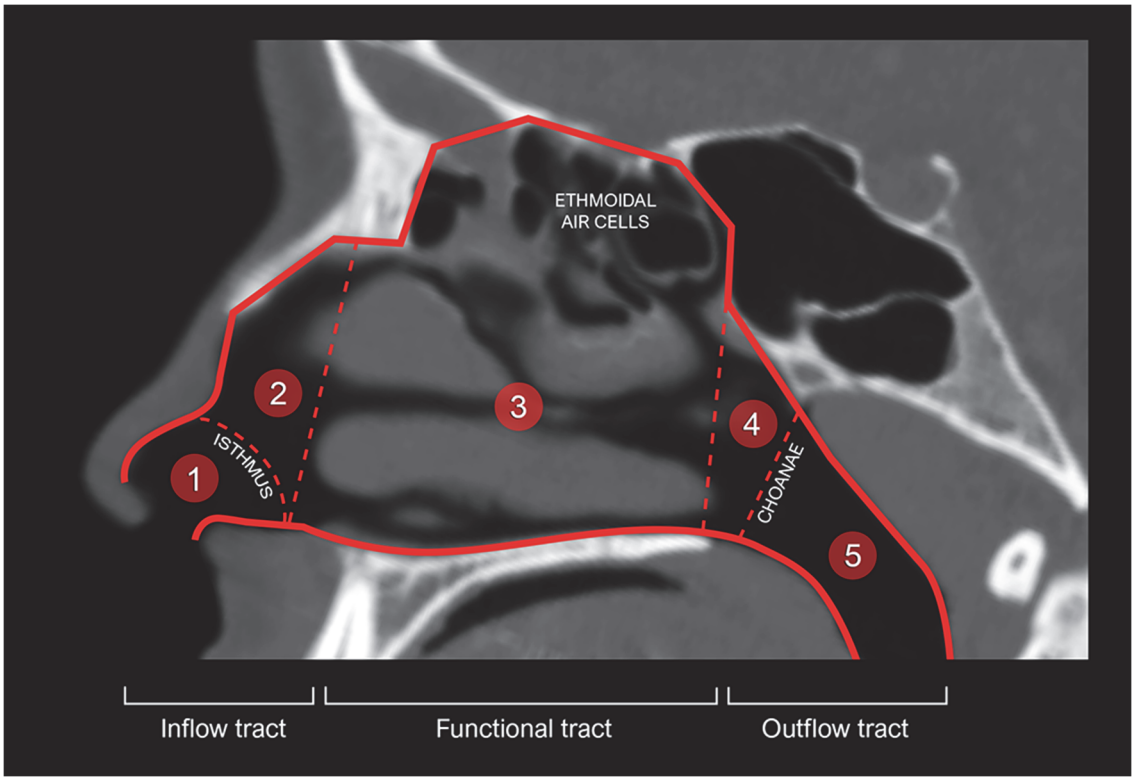

Figure 2.1. Sagittal cross-section from a CT scan showing the structural elements of the incoming nasal airflow pathway in lateral view. The inflow tract consists of the vestibulum (1) and the anterior cavum (2), which are separated by the isthmus. The functional tract is the area of the turbinates (3). The outflow tract is composed of the posterior cavum (4), choanae, and nasopharynx (5).

The mucous membrane lining the nasal cavity delimits the nasal airway that can be divided into three different units (Figure 2.1) (Mlynski et al., 2001; Bastir et al., 2020). The first part, the inflow tract, directs and diffuses the airflow, and contains the vestibulum, isthmus, and anterior cavum. The second part, the functional tract, includes the nasal turbinates. The third part, the outflow tract, directs warmed and humidified air toward the lower respiratory tract and is composed of the posterior cavum, choanae, and nasopharynx.

The thickness of the highly vascularized mucous membrane of the nasal airway fluctuates by contraction and expansion, depending on physiological factors such as blood pressure, nasal cycle, and nasal function (Cauna, 1982; Elad et al., 2008; Yokley, 2009; White et al., 2015). The variation in mucosa thickness causes congestion and decongestion of the nasal airway and affects its size and shape. Consequently, the speed, volume, and direction of airflow are also affected (Cauna, 1982), as well as the efficiency of air conditioning processes (Churchill et al., 2004; Naftali et al., 2005; Zhao & Jiang, 2014; Ma et al., 2018). Indeed, the nasal airway is the place where air conditioning takes place, which is necessary to optimize gas exchanges in the pulmonary alveoli and thus participate in global homeostatic thermoregulation (Havenith, 2005; White, 2006) while protecting the lungs from thermal damage, desiccation, and infection (Proetz, 1951, 1953; Walker & Wells, 1961; Cole, 1982a; Proctor, 1982; Keyhani et al., 1995; Williams, 1998; Keck et al., 2000; Eccles, 2002; Wolf et al., 2004; Yokley, 2006, 2009; Doorly et al., 2008; Elad et al., 2008; Hildebrandt et al., 2013). A large mucosal surface and a narrow channel generally facilitate heat and moisture exchange (Schmidt-Nielsen et al., 1970; Collins et al., 1971; Hanna & Scherer, 1986; Schroter & Watkins, 1989; Lindemann et al., 2009).

The nasal turbinates (or conchae) are complex, curled structures that extend from the side and upper walls of each nostril and play a major role in respiratory processes. These structures are divided into lower, intermediate, and upper turbinates (Moore, 1981; Smith et al., 2006; Maier & Ruf, 2014). They are covered with an epithelium that is olfactory for the upper turbinate (Zhao, 2004; Sahin-Yilmaz & Naclerio, 2011) and respiratory for the intermediate and lower turbinates (Doorly et al., 2008; Wen et al., 2008; Xiong et al., 2008; Sommer et al., 2012; Kim et al., 2017; Marks et al., 2019). Beneath the turbinates lie the superior, middle, and inferior meatuses that communicate posteriorly with the outflow tract; the middle meatus also holds the opening of the maxillary sinus (*ostium maxillare*). Ontogenetically, the turbinates and the associated meatuses develop from the six furrows, resembling ethmoturbinals, appearing on each lateral branch of the cartilaginous nasal capsule during weeks 9 to 10 of human fetal development (Jankowski, 2013). Postnatally, lower turbinates include numerous seromucous cells, providing a significant input of water vapor required in the air humidification process (Cole, 1982a; Tos, 1982; Keyhani et al., 1995; Naftali et al., 2005; Na et al., 2012). Studies using computational fluid dynamics methods have demonstrated the role of the two lower turbinates

in mediating the velocity and direction of airflow (Keyhani et al., 1995; Wang et al., 2005; Inthavong et al., 2007, 2018; Doorly et al., 2008; Zhu et al., 2011; Na et al., 2012; Li et al., 2017).

Climate-related variation of nasal structures

Numerous studies focusing on the nasal area have shown an association between its morphology and environmental factors (e.g., air temperature, humidity, altitude). Two main proxies for nasal morphology have been used to study this relationship: the negative volume defined by bone (*i.e.*, nasal cavity) and the negative volume defined by soft tissue (*i.e.*, nasal airway).

The first studies that accurately demonstrated a relationship between nasal morphology and eco-geographical factors were conducted using dry skulls and based on measurements of the facial skeleton and nasal aperture (Thomson, 1913; Thomson & Buxton, 1923; Davies, 1932; Weiner, 1954; Hoyme, 1965; Wolpoff, 1968; Hiernaux & Froment, 1976; Carey & Steegmann, 1981; Crognier, 1981b,a; St. Hoyme & Işcan, 1989; Franciscus & Long, 1991; Roseman, 2004; Hubbe et al., 2009; Leong & Eccles, 2009). Later studies addressed the morphology of the entire nasal cavity and confirmed this relationship (Yokley, 2009; Noback et al., 2011; Evteev et al., 2014; Fukase et al., 2016). Comparative inter-population studies have demonstrated that the only area of the nasal complex affected by variation related to eco-geographic factors is the internal nasal cavity (Maddux et al., 2016a). This area is also the main site of heat and moisture exchange within the nasal complex (Ingelstedt, 1956; Cole, 1982a; Keck et al., 2000; Naftali et al., 2005; Elad et al., 2008).

The results of these studies show that, when humans live in cold environments, they appear to possess a nasal cavity that is reduced mediolaterally and increased anteroposteriorly and superoinferiorly (Churchill et al., 2004; Doorly et al., 2008; Yokley, 2009; Holton et al., 2011b, 2013; Maddux et al., 2016a). Narrow nasal passages facilitate heat and moisture exchange by increasing the mucosal surface area relative to air volume (SA/V) ratio. This configuration increases nasal resistance for conditioning incoming airflow but also increases the amount of heat and water recovered during exhalation, thereby improving the conditioning capacity of the inner nasal cavity (Schmidt-Nielsen et al., 1970; Collins et al., 1971; Hanna & Scherer, 1986; Schroter & Watkins, 1989; Lindemann et al., 2009). In addition, when the anteroposterior

dimension of the nasal cavity increases, so does the time that airflow occurs in the nasal cavity, which also contains a larger volume of mucous membrane along this dimension, increasing efficiency of air conditioning (Inthavong et al., 2007; Noback et al., 2011). Last, the variation in nasal cavity height might be related to another aspect of climatic adaptation: energy demands. Several studies have shown that individuals with higher metabolic demands for oxygen consumption, which is generally the case in colder and/or drier environments, tend to have taller nasal cavities (Froehle, 2008; Bastir & Rosas, 2013, 2016; Holton et al., 2016). Furthermore, the increase in nasal height of individuals living in cold climates might also compensate for the reduction of nasal breadth that is also observed in these environmental conditions, thus maintaining a sufficient volumetric intake capacity (Maddux et al., 2016a).

While the nasal cavity has often been studied, the nasal airway has only become the focus of studies in the last few years. An *in vivo* study (Yokley, 2009) measured the SA/V ratio of individuals from European and African ancestry and observed that this SA/V ratio was only higher in European individuals when the nasal airway was fully decongested (*i.e.*, nasal mucosa fully contracted). When the nasal mucosa was not fully contracted, the SA/V ratio showed no significant differences between the individuals from European and African ancestry. This study underlines the importance of focusing not only on the nasal cavity but also on the volume delimited by the mucosa (*i.e.*, nasal airway) and its morphology. An important issue when addressing nasal airway morphology is to take into consideration the nasal cycle, which consists of the alternative partial congestion and decongestion of the right and left sides of the nasal airway during breathing, thus optimizing respiratory air conditioning (Hasegawa & Kern, 1977; Cauna, 1982; Eccles, 1982, 1996; Watelet & Cauwenberge, 1999; White et al., 2015; Pendolino et al., 2018). The influence of the periodicity of these nasal cycles on airway morphology needs to be addressed by studying larger samples and measuring the right and left sides separately (Heuzé, 2019).

Function of the paranasal sinuses

The paranasal sinuses are mucous membrane-lined cavities within bones that surround the nasal area (Figure 2.2). These include: the frontal sinuses, communicating with the nasal region through the meatus; the maxillary sinuses, communicating with the nasal region through the semilunar hiatus; and the sphenoid sinus. Ethmoidal air cells, which are thin-walled cavities

located in and defined by the ethmoidal labyrinth, are also often considered paranasal sinuses. However, ethmoid bone development in humans starts during the first trimester of gestation, while the other paranasal sinuses develop entirely after birth in aerial conditions, which could ontogenetically grant them another status (Jankowski, 2013). Furthermore, the mechanisms of paranasal sinus formation differ from those of the ethmoidal complex. One theory explaining paranasal sinus development – the epithelial theory – states that the maxillary, frontal, and sphenoid sinuses are produced via epithelial diverticula overflowing from the ethmoid labyrinth and causing a pneumatization of the surrounding bones (Zuckerkandl, 1893; Zollikofer & Weissmann, 2008).

Several functions have been assigned to paranasal sinuses without real consensus. One theory is that these structures were involved in reducing the weight and increasing pneumatization of the skull (O'malley, 1923; Tillier, 1977). Another theory raised the hypothesis of a potential role in thermal insulation of the brain and the eyes or in voice resonance (Masuda, 1992). A third hypothesis, the mechanistic theory, sees the paranasal sinuses as simple residual cavities that result from morphological changes in the surrounding structures that are constrained by biomechanical forces during craniofacial development (Rae et al., 2003; Holton et al., 2013; Jankowski, 2013; Butaric, 2015; Butaric & Maddux, 2016; Noback et al., 2016; Maddux & Butaric, 2017; Buck et al., 2019; Evteev & Grosheva, 2019). An additional hypothesis focuses on the role of the paranasal sinuses in the warming and humidification of inspired air (Gannon et al., 1997).

Another function attributed to the paranasal sinuses is the production of nitric oxide by the inner membranes of the sinuses, under the action of the enzyme I-NOS (NOS-2) (Lundberg et al., 1995, 1996). Nitric oxide is a powerful vasodilator, particularly involved in the cellular functions of the respiratory, nervous, and immune systems (Lundberg, 2008; Keir, 2009; Márquez et al., 2014). It is produced by the endothelial cells of sinus blood vessels and relaxes the muscle fibers of the vascular nasal wall when pumped into incoming airflow, thus regulating the intranasal temperature (Lundberg et al., 1995; Holden et al., 1999). In addition, nitric oxide may help maintain a sterile environment in the respiratory tract through two mechanisms: (1) nitric oxide is toxic to many viruses and bacteria and may therefore play a role in protection against infections (Mancinelli & McKay, 1983; Croen, 1993), and (2) the level of nitric oxide affects

the beat frequency of the cilia of airway epithelial cells that propel mucus-trapped debris and particles out of the lungs (Jain et al., 1993).

The proximity of the paranasal sinuses to the nasal structures and their role in respiratory processes has led researchers to study the relationship between the paranasal sinuses and climatic factors (e.g. Rae et al. 2011; Butaric 2015; Evteev & Grosheva 2019). While the sinuses show a high level of within- and between-group variation (Evteev & Grosheva, 2019) and are strongly correlated with craniofacial size (Rae et al., 2011; Butaric, 2015), a covariation has been measured between the maxillary sinus and nasal structures (Butaric, 2015). Indeed, individuals from cold-dry climates tend to have a larger maxillary sinus volume associated with a medial displacement of the lateral nasal walls, thus causing a reduction of the internal nasal breadth (Holton et al., 2013; Butaric, 2015; Butaric & Maddux, 2016; Evteev & Grosheva, 2019). Nevertheless, some confusion remains about the exact function of each of these sinuses, their relationship with neighboring structures, and how variation in paranasal sinuses relates to skeletal morphology of the entire face, not just the nasal aperture, and environmental factors.

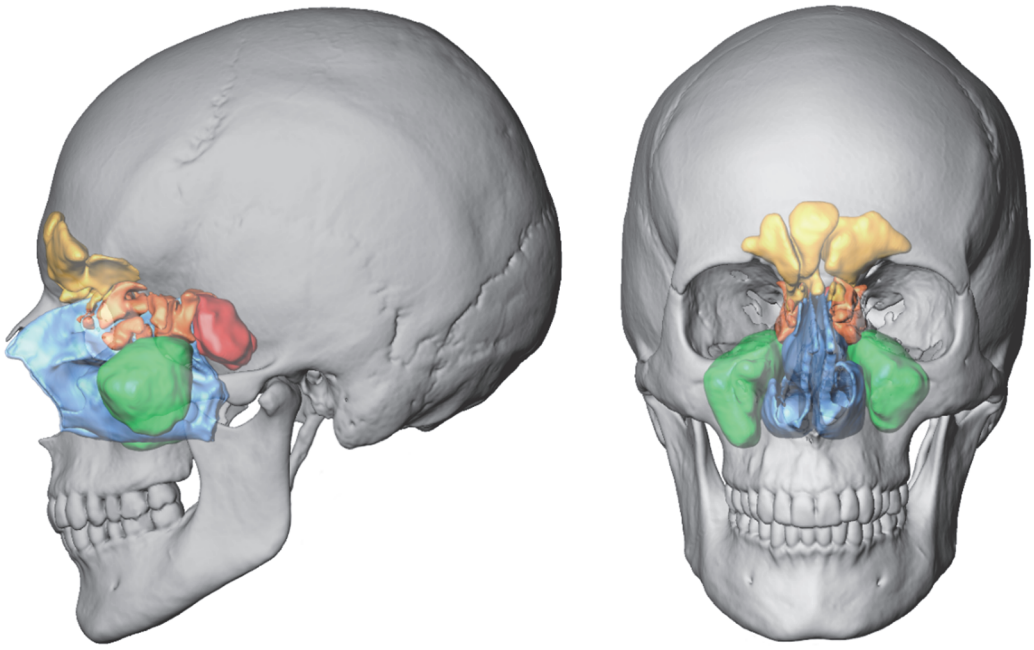

Figure 2.2. 3D reconstruction of a human adult skull allowing the visualization and localization of nasal and paranasal structures: nasal airway (blue), ethmoidal air cells (orange), frontal sinuses (yellow), sphenoid sinus (red), and maxillary sinuses (green).

2.3. Effects of environmental temperature on bone formation

The studies summarized previously focus on the correlation or covariation between ecogeographic factors (mainly temperature) and morphology of the nasal region and the hypothesized advantages of these phenotypes in cold or warm environments. Though it is widely acknowledged that the morphology of the nasal region depends in large part on the articulation of bones that surround it, the processes that contribute to bone formation that underlie this variation and generate its expression are rarely addressed. For instance, we do not yet understand the relative roles of heredity and developmental plasticity in the production of craniofacial phenotypes (Lovejoy et al., 2003). Here we present an overview of the manifestation of thermoregulation in extreme climatic environments and propose hypotheses on how stress caused by extreme temperature could modify bone formation processes and the resulting morphology of the nasal region. We then address the interaction between genes and the environment in the production of a phenotype through the identification of pathways or temperature-sensitive genes that could have an effect on the nasal and paranasal structures via cellular processes involved in bone and cartilage development.

We emphasize that trying to explain a phenotype as the direct result of temperature influence is unrealistic, as many other factors must be considered to explain craniofacial skeletal morphology. Diet, nutrition, and activity levels are examples of environmental inputs that can influence bone metabolism (e.g. Kiliaridis et al. 1985; Paschetta et al. 2010; Menéndez et al. 2014). Furthermore, temperature is not the only parameter defining ambient air, which also depends on the less acknowledged factor of humidity. Another major consideration is the integration among structures constituting the craniofacial skeleton that can induce a secondary variation in some specific area that is a response to the variation of its surrounding bony environment (Sardi et al., 2018; Scott et al., 2018). Age can also affect craniofacial morphology. Tooth loss and subsequent bone resorption in the maxillary area would induce a modification of palate morphology that could also affect the nasal and paranasal structures (Albert et al., 2007; Joganic & Heuzé, 2019). Though not meant to be exhaustive, we present some temperature-sensitive genes, pathways, and cellular processes involved in bone and cartilage formation and that could influence aspects of craniofacial morphology.

Thermoregulation in extreme climatic environments

Thermoregulation includes all the mechanisms used by an organism to control its body temperature and ensure optimal regulation of all metabolic processes (Iwen et al., 2018; Romanovsky, 2018). In homoeothermic species, the production of internal body heat must always be balanced with body surface heat loss in order to maintain homeostasis. To this end, various mechanisms have evolved, including skin vasodilatation, sweating, behavioral adaptations, insulation of the body by fur, clothing, and/ or intradermal fat accumulation (Cannon & Nedergaard, 2004; Kasza et al., 2014, 2016; Alexander et al., 2015; Fischer et al., 2016). Biological responses such as vasoconstriction and vasodilatation also allow heat to be retained or lost by the extremities. For instance, cold temperature leads to vasoconstriction that directs the blood flow towards the trunk and vital organs to reduce the dispersion of blood heat in the extremities (Tansey & Johnson, 2015). Indeed, the extremities of homoeothermic species are characterized by their regional heterothermy, that is, the ability to drop temperature of the limbs while maintaining that of the trunk (Harrison & Clegg, 1969; Ponganis et al., 2003; Serrat et al., 2008).

Experimental studies have measured an interaction between temperature, cell proliferation, and bone matrix production, which may affect cartilage growth and thus modify the morphology of endochondral bone (Serrat et al., 2008, 2010, 2015; Serrat, 2014). Hence, temperature can affect vertebral number in ectothermic and homoeothermic vertebrates (Hall, 2015), as well as limb and extremity length, which tend to shorten in response to a decrease in temperature (Allen, 1877; Feldhamer, 2020). One of the explanations of limb shortening proposed by Serrat (2014) is that the vasoconstriction induced by cold stress leads to a decreased blood flow in the extremities, altering the transport of important nutrients, oxygen, and hormones, and ultimately affecting endochondral ossification. Indeed, growth plates, though avascular, benefit from the nutritional support of the surrounding vasculature that transports solutes diffusing through the extracellular matrix to reach the cartilaginous cells (Brookes & Revell, 1998). An alteration in blood flow might therefore affect this nutrient supply, thus affecting normal growth. Interestingly, the effects of temperature on limb length can be observed within a single generation of outbred mice reared at warm and cold temperatures during the postnatal growth period (Serrat et al., 2008). These observations underscore the potential role of phenotypic plasticity. When driven by environmental factors, phenotypic

plasticity is considered a greater evolutionary force than random mutation (West-Eberhard, 2005), but few studies have addressed the potential effect of phenotypic plasticity on morphological variation of the upper airway. Rae et al. (2006) contributed to this question in their study of the dry crania of cold- and warm-reared rats. Their results show that cold stress causes subtle but significant changes in facial shape as well as maxillary sinus and nasal cavity volumes, suggesting developmental plasticity of the craniofacial skeleton in response to climatic variation.

Mechanisms of temperature influence on upper airway bone and cartilage

Potential responses of the craniofacial skeleton to cold stress are not well understood, but some authors have proposed hypotheses that might explain how temperature influences craniofacial variation. For example, a recent study on nasal turbinate morphology (Marks et al., 2019) hypothesized that the modification of cartilage development in cold environments could also apply to nasal turbinate cartilage and all cartilages of the nasal capsule of the forming chondrocranium. If this change occurred, the morphology of the surrounding non-cartilaginous skeletal structures developed through intramembranous ossification (e.g., the maxillary, premaxillary and nasal bones) would also likely be affected (Chae et al., 2003; Egeli et al., 2004; Opperman et al., 2005; Wealthall & Herring, 2006; Al Dayeh et al., 2013; Hall & Precious, 2013; Hartman et al., 2016; Holton et al., 2018). By altering the expression of genes and pathways that affect cellular processes involved in cartilage metabolism, temperature could then have an indirect effect on growth of the facial bones.

Selective brain cooling (SBC) is the mechanism that keeps the brain at a cooler temperature than the rest of the body through the precooling of the blood supplying the brain and provides an example of complex interaction between blood f ow intensity and morphological variation. This mechanism is achieved by dilation or constriction of the veins. For example, constriction of the veins returning blood from the nose and face precools that blood that will then be supplied arteriorly to the brain (Caputa, 2004). Regulation of the evaporation of water at the mucosal surfaces of nasal turbinates also contributes to SBC (Irmak et al., 2004). Furthermore, ethmoidal air cells and the sphenoid sinus could potentially help cool the adjacent brain lobes and vessels by thermal conduction. Part of the morphological variation of craniofacial structures might reflect adaptive changes in growth patterns that produce

morphology ensuring a more effective SBC specific to the environment. Finally, we know that cold stress implies greater oxygen consumption, due to the sympathetic activity associated with brown adipose tissue production and muscle activation during nonshivering thermogenesis (Lowell & Spiegelman, 2000). The increase of incoming airflow, which is closely related to the energetic demands of the body, could also play a role in the variation of nasal morphology (see also Maddux et al. 2016a).

Temperature-sensitive developmental pathways

Temperature not only affects the skeleton but almost every system in the body, causing many interactions among tissues that may experience different consequences of thermal stress (Tattersall et al., 2012). Although the number of genome-wide studies on the molecular basis of craniofacial morphology have been expanding in the last few years (e.g. Adhikari et al. 2016; Weinberg et al. 2018; Xiong et al. 2019), our understanding of the genetic basis for craniofacial variation is incomplete. It is therefore not an easy task to identify the temperature-sensitive genes that might directly and/or indirectly affect craniofacial morphology. Here, we highlight a few of these genes and associated pathways that were identified through *in vivo* and *in vitro* studies and which may explain some of the temperature-related variation of nasal and paranasal morphology (Figure 2.3). We begin by noting that the production of a "cold phenotype" or a "warm phenotype" does not necessarily imply mechanisms that would be opposites. Note that variation is expected in the phenotypic response to temperature-sensitive genes and associated pathways. Some of these phenotypic responses might be continuous and proportional to the temperature variation, while others might be expressed when a threshold is reached. Additionally, temperature variation at certain developmental stages can have different phenotypic outcomes varying both in pattern and intensity (e.g. Hall 2015).

Some researchers have demonstrated that temperature can have a direct effect on bone formation and growth by altering the activity of bone-forming osteoblasts and bone-resorbing osteoclasts. An *in vitro* study using cells derived from rat trabecular bone (Patel et al., 2012) has shown that, after 14–16 days of culture, the activity of calvarial osteoblasts was reduced by 75% in mild hypothermia and by 95% in severe hypothermia. A reciprocal effect of hypothermia was also observed on osteoclastogenesis, that showed a 1.5- to 2-fold stimulation, thus increasing bone resorption.

Temperature was also shown to affect preosteoblast activity *in vitro*, including mesenchymal stem cell differentiation (Shui & Scutt, 2001; Chung & Rylander, 2012). When subject to heat stress, preosteoblast cells can promote expression of osteocalcin and osteopontin, two proteins involved in bone mineral density and metabolic regulation. However, the combination of heating and osteoinductive growth factors leads to the expression of heat shock proteins (HSPs), osteoprotegerin, and vascular endothelial growth factor (VEGF). Osteoprotegerin is involved in bone resorption through its role as a decoy receptor in the RANKL/RANK pathway (Aubin & Bonnelye, 2000), and VEGF stimulates angiogenesis and controls bone formation (Dai & Rabie, 2007). HSPs are multifunctional proteins that can be induced by heat stress or cold stress (Rylander, 2005; Barna et al., 2012; Patil & Paul, 2014; Hang et al., 2018). HSP70, for example, increases the proliferation and differentiation of osteoprogenitor cells, which are bone marrow-derived stromal cells (Shui & Scutt, 2001), and regulates both the resorption activity of osteoclasts via the RANKL/RANK pathway and the bone production activity within osteoblasts by activating the ERK and Wnt/β-catenin pathway (Hang et al., 2018). The temperature of the cell culture also influences HSP27, which is particularly involved in the regulation of bone cell physiology through upregulation of TGF-β (Hatakeyama et al., 2002), estrogen (Cooper & Uoshima, 1994), endothelin-1 (Tokuda et al., 2003), and prostaglandins (Kozawa & Tokuda, 2002). These results point to HSP27 as a potentially important factor in the modulation of cellular events in bone and cartilage.

Clock genes are also involved in cell proliferation in cartilage. Clock genes are transcriptional activators that play a central role in the regulation of circadian rhythms, the 24-hour cycles in physiology that precisely regulate organ function (Reppert & Weaver, 2001). The expression of clock genes is directly dependent on temperature, and their mutation can lead to an altered regulation of bone volume or deficiencies in long bone growth because of their control of chondrocyte differentiation (Gossan et al., 2013; Marks, 2018; Steindal & Whitmore, 2019). Circadian clocks might also have a potentially important role in bone growth and maintenance and the production of morphology (Takarada et al., 2012).

Temperature can also affect global human DNA methylation and RNA editing (Garrett & Rosenthal, 2012; Shi et al., 2021), as well as telomere length (e.g., Romano et al. 2013). Genes with methylation status have been shown to be affected by temperature changes. For example, low temperature induces the hypermethylation of ZKSCAN4, expressed by an increase of blood

pressure (Xu et al., 2020), an indirect pathway that could affect bone growth. Another study addressed the contribution of cold-inducible RNA-binding protein (CIRP) to tissue remodeling in chronic rhinosinusitis (Shi et al., 2021). This cold shock protein is a chaperone that is upregulated under mild hypothermia and facilitates mRNA translation. CIRP seems to be involved in cold-induced suppression of cell proliferation, but its precise role is still poorly understood.

Finally, temperature can alter the endocrine system, which has a fundamental role in homeostasis. By affecting extracellular matrix proteins, cold stress can modify the diffusion rates of endocrine and paracrine growth regulators affecting the diffusion and transport of hormones and ultimately skeletal morphology. Among the hormones that could affect the skeleton (Massaro & Rogers, 2004), thyroid hormones and leptin are probably the best studied.

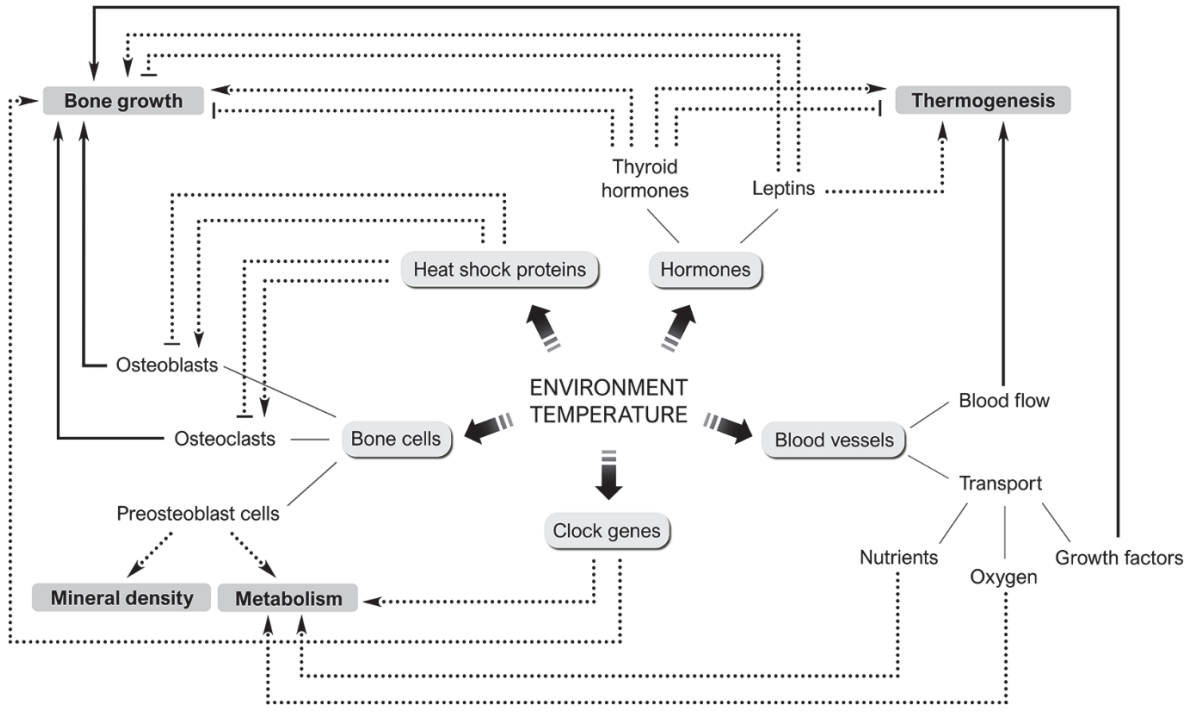

Figure 2.3. Diagram summarizing the major physiological pathways through which environmental temperature could influence nasal and paranasal morphology. Solid lines show direct temperature influences on bone growth and metabolism. Dashed lines indicate indirect ways through which temperature can alter bone cells. Indirect pathways include the endocrine system (e.g., thyroid hormones and leptin play a role in thermogenesis and bone growth), the circulatory system (temperature variation can induce a vasoconstriction or a vasodilatation, thus affecting blood flow and the transport of nutrients, oxygen, and hormones involved in bone metabolism), and other temperature-sensitive proteins and genes (e.g., HSP and clock genes both influence bone growth and metabolism).

It has been shown that thyroid hormones play a very important role in the regulation of homeostasis (Iwen et al., 2018). These hormones modify the transcription rate of uncoupling protein 1, localized in brown adipose tissue and involved in nonshivering thermogenesis (Enerbäck et al., 1997; Golozoubova et al., 2001; Devlin, 2022), increase metabolic rate, and can directly influence the sodium/potassium and calcium pumps in skeletal muscle (Silva, 2006), as well as the vasoconstriction and vasodilatation of blood vessels (Warner et al., 2013). Thyroid hormone levels also influence intramembranous and endochondral ossification and, consequently, craniofacial development (Bassett & Williams, 2016). Indeed, skeletal hypothyroidism is expressed in a delayed ossification of the skull, which can cause defects such as wider and/or persistent cranial sutures and fontanelles. Conversely, skeletal hyperthyroidism causes advanced ossification that can manifest as malformations including craniosynostosis. Interestingly, the phenotypes produced by an altered thyroid status display similarities with loss-of-function or gain-of-function mutations affecting FGF (fibroblast growth factor), IGF (insulin-like growth factor) and WNT (Wingless-related integration site) signaling pathways, which are key pathways in craniofacial development. Since thyroid hormone T3 induces FGF, FGFR, IGF1, and IGF1R expression and enhances MAPK signaling in chondrocytes and osteoblasts but also enhances WNT signaling and RUNX2 (runt related transcription factor 2) expression in chondrocytes and inhibits WNT signaling in osteoblasts, it is possible that these signaling pathways interact in the regulation of craniofacial development together with thyroid hormones (see for review Leitch et al. 2020).

Leptin, a pleiotropic adipocyte derived hormone, is also known to increase with cold exposure and plays an important role in cold acclimatization and thermogenesis (Korhonen et al., 2008; Zhao, 2011; Robbins et al., 2018). For example, studies have identified leptin target neurons that are involved in the sympathetic control of brown adipose tissue (e.g., Cannon & Nedergaard 2004). Brown adipose tissue is prevalent in newborns and hibernating mammals but is also metabolically active in human adults for nonshivering thermogenesis (Shum et al., 1991; Nedergaard et al., 2007; Saito et al., 2009; Devlin, 2015; Oreskovich et al., 2019). Leptin is also involved in the regulation of bone growth (Kishida et al., 2005) and can regulate angiogenesis (new vessel formation) (Rezai-Zadeh & Münzberg, 2013), which would permanently modify the blood flow and directly affect intramembranous ossification (Percival & Richtsmeier, 2013).

2.4. Implications for human craniofacial evolution

To improve our understanding of climate-related patterns of craniofacial morphological variation in human evolution and the developmental processes underlying this variation, several paths could be explored.

First, to refine our understanding of the phenotypic expression of climate-related craniofacial variation, additional quantitative studies are needed to evaluate morphological differences between populations living in regions with recorded differences in temperature and/or humidity. Medical images of modern individuals living in different climates would enable measures of bone and nasal mucosa morphology that are crucial to obtain valid estimates used in the evaluation of the covariation between these two anatomical structures (Heuzé, 2019). Studying the covariation between nasal cavity and nasal airway will help with the interpretation of the results obtained on dry skulls in terms of respiratory energetics and air conditioning.

Second, studies of the influence of ambient temperature on growth and development of rodents (e.g. Rae et al. 2006; Serrat 2014) have shown that experimental studies of animals could be used to better understand the effects of temperature on the morphology of nasal structures. The use of laboratory animals can help sort genetic causes from other variables, like temperature, that potentially affect morphology. Experiments on inbred mice could enable quantitative comparison of the volume and morphology of upper airway structures between groups of animals exposed to either cold or warm environments. These studies could help determine the extent to which morphological variation can be explained by a genetically driven adaptation and/or by a physiological response to environmental factors, that is, by phenotypic plasticity. Animal models would also allow exploration of the cellular processes involved in the morphological response to temperature. An *in vitro* study on hyperthermia effects on the proliferation of bone and cartilage cells (Flour et al., 1992) showed that chondrocytes might be thermoresistant and osteogenic cells thermosensitive. To our knowledge, such results still need to be tested *in vivo*. Future studies based on animal models could investigate the effects of temperature (both hypo- and hyperthermia) on the differentiation of osteochondroprogenic cells into osteoblasts and chondrocytes (Hall, 2015) and on the proliferation of bone and cartilage cells. Laboratory mice could serve as a useful model system for this purpose, which

would then help us discuss the effects of temperature on nasal morphology for other mammals such as primates.

Finally, the use of computational fluid dynamics offers great opportunities to achieve a better understanding of respiratory energetics. The complex structures of the nasal airway tend to restrict *in vivo* studies of nasal airflow, but computational fluid dynamics enables a valid and accurate numerical simulation of airflow patterns within the nasal cavity (e.g., Inthavong et al. 2007; Chen et al. 2010; Keck & Lindemann 2010; de Gabory et al. 2020). Thoughtful use of this technique applied on modern samples of healthy or pathological individuals could contribute greatly to the discussion about how thermoregulation, respiratory energetics, and climate interact to produce differential phenotypes in humans.

Integrating these three approaches would allow a more precise definition of the anatomical and functional units of the craniofacial skeleton showing climate-related patterns of morphological variation, which would in turn expand our knowledge of developmental processes that are sensitive to temperature, providing potential explanations at the cellular, organ, and organismal levels of this observed morphological variation.

2.5. Conclusion

Previous research has shown that human morphological variation can correspond with differences in climate. We provided a review of the temperature-related morphological variation of nasal and paranasal structures and a discussion of genetic, cellular, and systemic temperature-sensitive pathways that might have a role in the production of morphological variation of the nasal cavity. We observe that temperature both directly and indirectly affect bone formation, either by altering the activity of preosteoblast cells, bone-forming osteoblasts, and bone-resorbing osteoclasts or by affecting proteins or hormones (e.g., heat shock proteins, clock genes, thyroid hormones, leptin) involved in the activity of bone cells. Beyond providing a review on ecogeographic patterns of morphological variation in upper airway and cellular processes that potentially influence this morphology, our purpose in this chapter is to highlight the need for studies integrating these two areas of research. Such research could ultimately improve our understanding of the role of climate in the evolution of craniofacial morphology.

Synthèse

Le développement du squelette cranio-facial humain résulte de l'interaction complexe d'influences génétiques, physiologiques, biomécaniques et environnementales. Parmi ces dernières, la température a été identifiée comme un facteur ayant un impact sur la morphologie cranio-faciale, et en particulier sur les voies respiratoires supérieures. En fonction de l'environnement dans lequel ils vivent, les humains ont tendance à présenter des morphologies différentes : par exemple, dans les environnements froids, la cavité nasale a tendance à être plus étroite, plus profonde et plus haute. Nous présentons ici un état de l'art sur la variation morphologique des structures nasales et paranasales en lien avec la température.

Nous développons ensuite les voies biologiques sensibles à la température et susceptibles d'avoir joué un rôle dans cette variation. La température peut affecter directement et indirectement la formation osseuse : directement, en modifiant l'activité des préostéoblastes, ostéoblastes et ostéoclastes ; indirectement, par le biais de protéines ou d'hormones (e.g. protéines de choc thermique, gènes Clock, hormones thyroïdiennes, leptine) impliquées dans l'activité des cellules osseuses.

Summary

The development of the human craniofacial skeleton results from the complex interaction of genetic, physiological, biomechanical, and environmental influences. Among environmental influences, air temperature has been identified as a factor impacting craniofacial morphology, particularly the upper airway. According to whether they live in warm or cold environments, humans tend to display different morphological features in this anatomical region: e.g. in colder environments, the nasal cavity tends to be narrower, longer and higher. Here, we provide an overview of the current knowledge of temperature-related morphological variation of nasal and paranasal structures.

We then develop the temperature-sensitive developmental pathways that might have played a role in this morphological variation. Temperature can indeed both directly and indirectly affects bone formation. Directly, by altering the activity of preosteoblast cells, bone-forming osteoblasts, and bone-resorbing osteoclasts. Indirectly, by inducing proteins or hormones (e.g. heat shock proteins, clock genes, thyroid hormones, leptin) involved in the activity of bone cells.

• Chapter 3 •

RESEARCH METHODOLOGY

MÉTHODOLOGIE DE RECHERCHE

« Scientists do not seek to impose their needs and wants on Nature, but instead humbly interrogate Nature and take seriously what they find. (…) We insist on independent and quantitative verification of proposed tenets of belief. We are constantly prodding, challenging, seeking contradictions or small, persistent residual errors, proposing alternative explanations, encouraging heresy »

— C. Sagan

In this doctoral thesis, the studied samples are virtual data obtained through tomographic (human sample) and microtomographic (murine sample) acquisition (Figure 3.1). Computed tomography is a medical imaging technique that generates volumes composed of a set of slices (*i.e.,* images), resulting from the tomographic reconstruction of multiple X-ray measurements (Hounsfield, 1980). Our sample composition choices, *i.e.,* which individuals we chose to include in our human sample and how was set up the experimental protocol to constitute our groups of mice, is described in chapters 4 and 5 respectively. The statistical analyses, softwares and packages used to study the data are also detailed in the following chapters and will not be addressed here. The purpose of the present chapter is to provide more details on the methodological choices made during the different stages of data pre-processing and analysis.

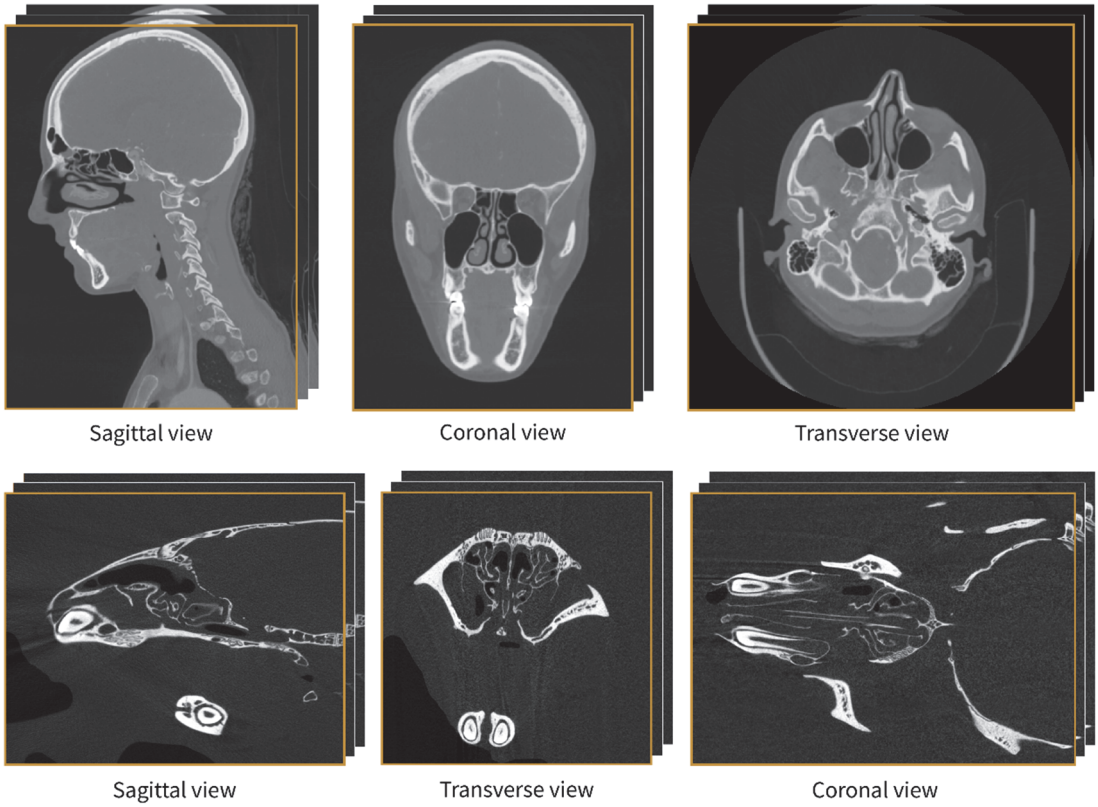

Figure 3.1. Illustration of the tomographic images used in this study. Tomographic acquisition of the human sample (above) and microtomographic images acquired for the murine sample (below).

In this work, all our research questions revolve around the quantification of the morphological variation of the nasal anatomical structures, both in size and shape. Several tools can be used to achieve this purpose. Quantitative study of size can be easily achieved through the statistical analysis of the data obtained after segmentation of the tomographic

images, *i.e.,* by delimiting the area of interest on all the slices, either manually or from automated processing (e.g. Balanoff et al. 2016; Buzi et al. 2023). Statistical analyses can then be performed on the extracted volumes after reconstruction of the segmented areas to study their variation.

To study the shape of anatomical structures, geometric morphometrics is one of the most appropriate tool (Bookstein, 1991; Rohlf & Marcus, 1993). Geometric morphometrics include methods of acquisition, processing, statistical analysis, and visualization for the study of shapes. It is based on the acquisition of shape descriptors (landmarks) that simplifies the shape and allows an objective, reproducible and statistically robust study of the morphological variation (Slice, 2005).

While the use of geometric morphometrics was obvious in the framework of this work, we faced a major issue: the lack of reproducible anatomical landmarks in the internal nasal region, which prevents us from accurately and reliably quantifying the morphology of these structures using landmark-based morphometrics. In addition, the complexity of the shapes studied would have been poorly represented by such a reduced set of shape descriptors. In order to study these specific anatomical structures, we have thus decided to use a surface registration-based method. In this following section, we will present the main concepts of this procedure, its different steps, and the methodological choices we made in data pre-processing to ensure the highest accuracy for the study of each of our samples.

3.1. Shape analysis by surface registration

Surface registration

Surface registration is a geometric transformation that computes the correspondence between two surfaces. Comparing surfaces allows to study a dataset without any preconceptions and is currently an actively growing field of shape analysis (e.g. Palmer et al., 2015; Wang et al., 2021; Klatzow et al., 2022). The registration between two individuals A and B requires to determine the geometric transformation (Φ) that verifies the following equation: $X_B = \Phi (X_A)$, where X_A and X_B are the coordinates of the points composing the objects A and B, corresponding to the same anatomical positions. Optimization systems can be employed to minimize local and global errors in the surface registration, especially when the morphologies

are substantially different. The quantitative results of the surface registration provide a measure of the similarity between two surfaces, *i.e.*, between two shapes, and can be extended to the comparison of individuals or specimens of entire datasets (Dumoncel, 2017).

Surface registration can be achieved with different parameters, starting with the very way the transformation should occur, *i.e.*, how one surface should project onto another. The rigid transformation method, for example, is the alignment of a surface X_A to a shape X_B only through translation, rotation and scaling (when the size effect must be minimized). This transformation is appropriate to compare two shapes displaying small anatomical differences, for example when studying longitudinal data for the same specimen (Dumoncel, 2017). But in most cases, this type of transformation is not sufficient to capture the complexity of the shapes under study.

Diffeomorphism-based registration

The variation of biological shapes can also be modeled with non-rigid transformations based on mathematical diffeomorphisms, which describes the continuous evolution of a shape from a discrete set of observations (e.g. Grenander, 1996; Durrleman et al., 2014; Zhang & Golland, 2016). This method is based on a diffeomorphic flow, which means that the result of the registration is a set of successive deformations between 0 and 1 (where 0 represents the reference surface and 1 the reference surface deformed to the target surface). The result is a continuum of deformation field that continuously moves from one shape to another: the diffeomorphism-based registration is therefore regular and has a regular reverse. The use of diffeomorphisms has been extended to many structures including landmarks, point clouds, or surfaces (e.g. Vaillant et al., 2007; Durrleman, 2010; Fishbaugh et al., 2017). The application of this method in paleoanthropology, while expanding these last few years (e.g. Beaudet et al., 2016, 2020; Dumoncel et al., 2016; Urciuoli et al., 2020; Zanolli et al., 2023), still remains scarce, mainly because of the complexity of its implementation. Yet, increasing the studies and diversifying the investigated anatomical structures would allow the expansion of this method in the upcoming years. Another prospect of interest would be to develop more studies comparing the results of morphometric analyses with and without landmarks, as was done for example by Braga and colleagues (2019).

The mechanism of the diffeormophism-based registration is illustrated in Figure 3.2. The purpose is to deform a template surface mesh on a target surface mesh, each of them being a set of points forming edges that are bound in a connectivity table. In order to find the non-rigid registration that transforms the reference to the target, we need to compute a deformation without modifying these connectivity tables, *i.e.,* to maintain the original topology of the template (Dumoncel, 2017). The first step of this procedure is to rigidly align the target on the template, in order to minimize the differences in position, orientation and scale. The algorithm generally used to rigidly align two surfaces is the *Iterative Closest Point* (ICP) algorithm (Besl & McKay, 1992). This preliminary rigid alignment is crucial to avoid false inferences linked to misregistration artefacts when comparing the groups or populations further in the analysis (Gee & Treece, 2014).

Once this standardization step is completed, the non-rigid diffeomorphic transformation is computed on a set of points called control points, automatically distributed around the studied structures. The result of the computation includes the optimized momentum vectors for each individual or specimen, estimated at the control points and representing the velocity field associated with each control point (Durrleman et al., 2014). These vectors will allow a visualization of the registration flow.

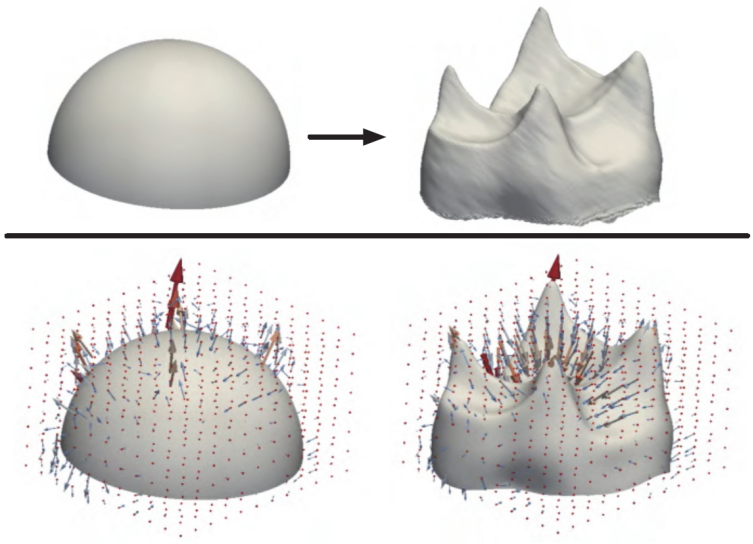

Figure 3.2. Illustration of the diffeomorphism-based surface registration. The template (above, left) and the target shape (above, right) and the results of the surface registration (below) represented by the vectors associated to the control points, projected both on the template and the target shape (left and right respectively) (from Dumoncel, 2017).

Atlas creation

Applying the concepts of diffeomorphism-based surface registration to the scale of complete samples is grounded in the definition of a reference surface from which we want to evaluate the morphometric variation to various target surfaces. This definition is based on the computation of a global mean shape for a given set of shapes (*i.e.*, the target shapes). The global mean shape and the target shapes constitute what is called an atlas (Figure 3.3), which represents the global deformations observed in a sample, by summarizing the deformation of the global mean shape to each individual (Durrleman et al., 2012; Beaudet, 2015). This global mean shape is generated in order to explore the variability of a set of shapes and can be used for statistical analyses (Durrleman et al., 2013).

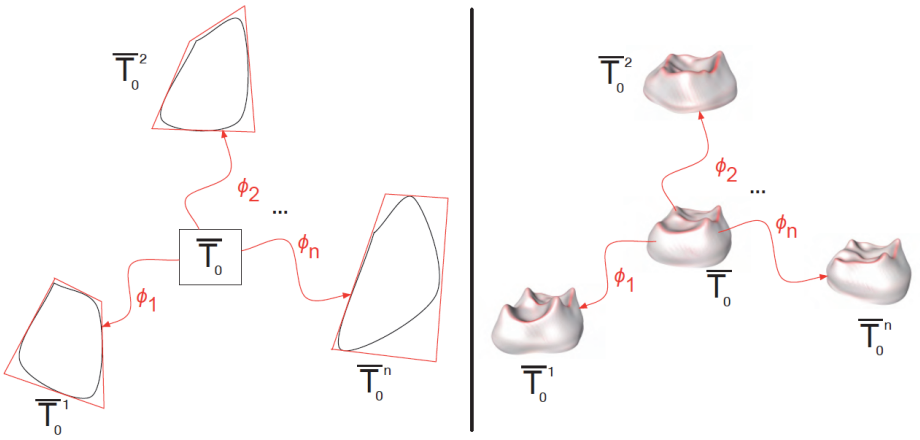

Figure 3.3. Illustration of an atlas. Deformation of the global mean shape T_0 to each target shape of the sample (from 1 to n). Schematic illustration (left) and illustration with enamel-dentine junctions (right) (from Dumoncel, 2017).

3.2. Method implementation

Pre-processing of the data

The main anatomical structures of interest studied in this work are cavities, *i.e.*, negative air-filled volumes. A preliminary segmentation of the structures is thus necessary to extract the meshes that are needed to proceed to the analysis of their shape by surface registration. For this work, we performed semi-automatic (human sample) and manual (murine sample) segmentations. The major challenge regarding these structures is that they are in direct

continuity with the external air. However, this can be solved easily by setting some boundaries to “close” their extremities. More details on the implementation of the appropriate boundaries for each of the studied structures are provided in Chapters 4 and 5 (for the human and murine samples respectively). Beyond these considerations, other practical aspects, more specific to the application of the surface registration method itself, required some particular attention. We illustrate these aspects in Figure 3.4 with an example from the human nasal airway analysis.

To study this structure, we set an anterior limit at the piriform aperture and a posterior limit at the choanae. After performing a threshold-based segmentation of the air between these two limits, we decided to exclude the ethmoidal air cells, for they are more related to olfaction than respiration and are thus less relevant regarding our research questions (Jankowski, 2013). In order to do that, we manually excluded each ethmoidal air cell from our segmentation label. Furthermore, the threshold-based segmentation of the air constituting the nasal airway failed to include some of the thinnest sections and areas of the structure. Yet, an important prerequisite of the surface registration is that the surface meshes of the individuals do not contain holes or missing parts with respect to the template shape. Otherwise, these areas will be perceived as actual morphological variation that will be taken into account in the deformation. Our final step was then to manually correct these missing parts on each individual segmentation.

This whole segmentation process was, as it always tends to be, highly time-consuming. We faced a magnified version of these issues and constraints with the murine sample, for which we had to perform the segmentation almost completely manually, slice by slice. Besides the time-consuming aspect (once the protocols were set up, we spent about 2 hours per individual for the human sample and 4-5 hours per specimen for the mice sample), this can also lead to some errors in the segmentation, which could be avoided by more automatic methods. In the study of the two samples presented here, we took particular care in this segmentation work to make it as accurate and reliable as possible. We systematically verified the process along the way with intra-observer tests, so as not to include biases in our data sets. But we must keep in mind that some human errors can subsist against our will. In this context, the recent development of automatic segmentation of cranial cavities (Buzi et al., 2023) is a very promising prospect for reducing data processing times.

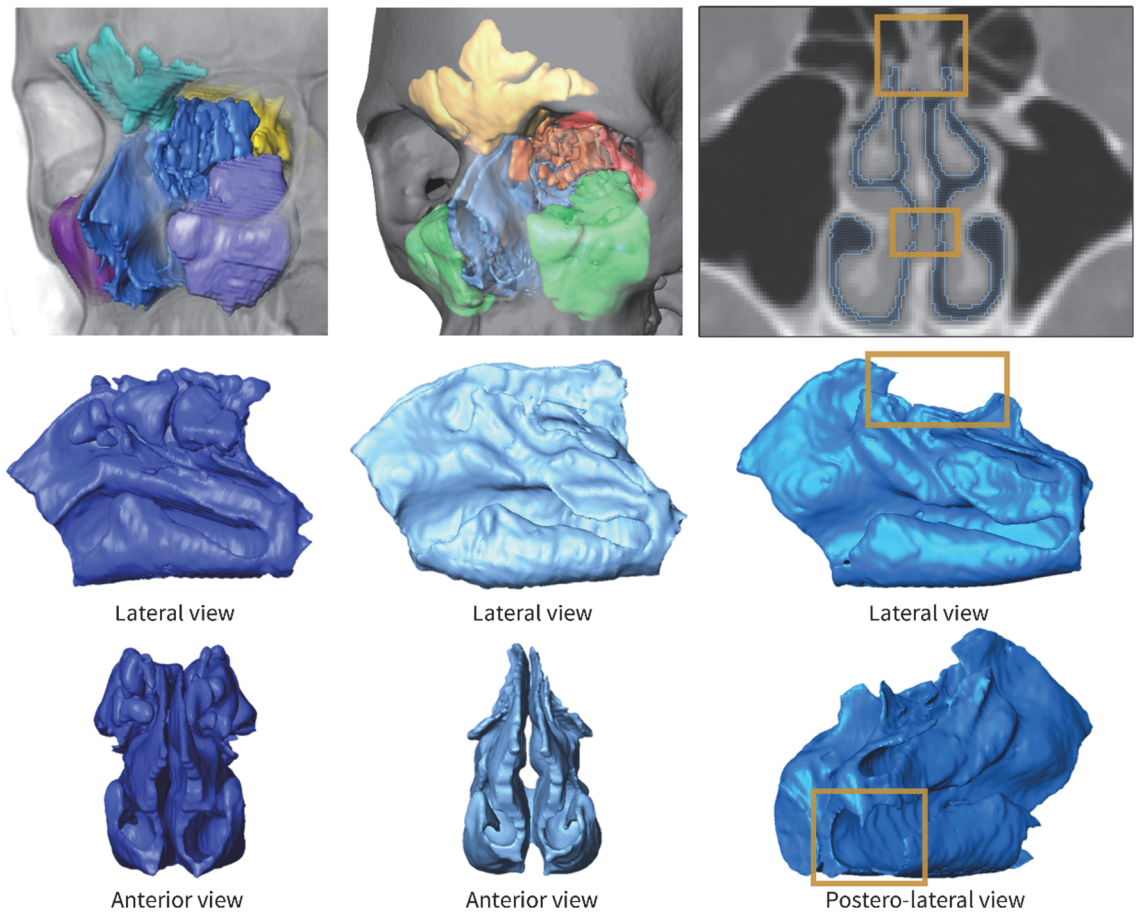

Figure 3.4. Segmentation of human nasal airway. Protocol of segmentation including the ethmoidal air cells (protocol from Heuzé 2019) (left), exclusion of the ethmoidal air cells (middle), examples of areas that were not filled during threshold-based segmentation and need to be manually corrected (right).

Template choice

Before building the atlas, the question arises of the choice of the template shape, which will be used to generate the global mean shape when computing the atlas. This choice is critical, because the use of a shape that is too different from the specimens could have an impact on the final result of the registration. We can highlight several approaches in the selection of this template shape, the most straightforward being to use a simple geometric shape such as a cube, sphere or cylinder. This strategy works well for anatomical structures that are not too complex (e.g. the use a semi-sphere is perfectly relevant to establish the global mean shape of a tooth sample), but is not applicable to more complex shapes. It is then possible to use as the template shape either a specimen of the sample (e.g. Joshi et al., 2016), or a geometric shape constructed from a set of individuals. In the second option, it is strongly recommended to smooth the shape

extensively so as not to introduce elements that could influence the computation of the global mean shape (Dumoncel, 2017).

Considering the complexity of the anatomical structures studied in this work, it was not possible to use simple geometrical shapes as templates and we therefore had to adopt different strategies (Figure 3.5). For the human sample, we decided to use a template based on a simplified nasal airway shape created by Keustermans and colleagues (2018). This model included the anatomical areas anterior to the piriform aperture and posterior to the choanae. Using Autodesk Meshmixer v.3.5, we cut these two parts to fit the segmented anatomical area in our protocol. For the murine sample, as we did not find a suitable preexisting model, we decided to use one of the specimens. To identify the specimen having the most "average" morphology, we performed four preliminary surface registrations, using as templates four different specimens, randomly selected one in each experimental group. We then performed, for each computed atlas, a principal component analysis (PCA) on the results of the deformations. We selected as the final template a specimen located as close as possible from the origin of the PCA in each of the four preliminary registrations, which was one of the mice from the control goup.

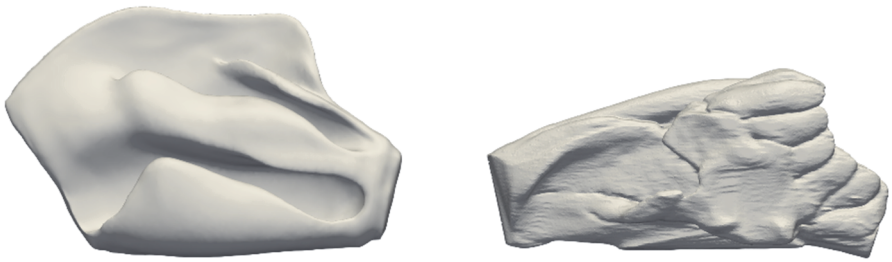

Figure 3.5. Template shapes used for each sample of this project. The template used for the human sample is a simplified, smoothed and symmetrical nasal airway and the template used for the murine sample is the segmented nasal cavity of the specimen 15614_1553 (control group).

Registration parameters

The final step of the methodology, *i.e.,* the diffeomorphism-based surface registration itself, was performed using the software Deformetrica (Durrleman et al., 2014), through remote access to the computing center of the National institute of nuclear and particle physics. In this

software, the registration is computed based on several parameters configurable in the files (.xml) that will be read by the executables. Among these parameters, the most important one to configure the deformation is the kernel width (Figure 3.6), whose value conditions the size of the variation to be taken into account, as well as the rigidity of the deformation (Dumoncel, 2017). After testing for different kernel width values in both samples, we set up this value at 2 for the human nasal airway analysis and at 0.3 for the murine nasal cavity analysis, for these were the values that performed the best fit in the deformation.

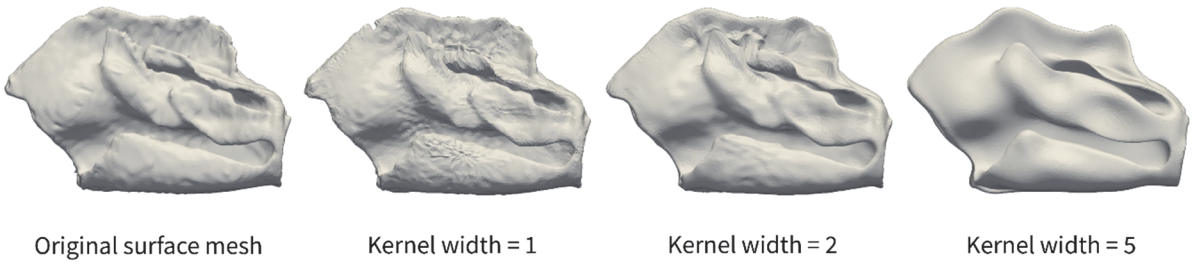

Figure 3.6. Kernel width configuration. Results of the deformation of a human nasal airway surface mesh (FR005) with a kernel width value set respectively on 1, 2 and 5.

• Chapter 4 •

VARIABILITY OF UPPER AIRWAY MORPHOLOGY IN MODERN HUMANS

VARIABILITÉ DE LA MORPHOLOGIE DE LA VOIE AÉRIENNE CHEZ LES HUMAINS MODERNES

Chapter 4 was published as an article:

> Maréchal L., Dumoncel J., Santos F., Astudillo Encina W., Evteev A., Prevost A., Toro-Ibacache V., Venter R.G., Heuzé Y. 2023. New insights into the variability of upper airway morphology in modern humans. *Journal of Anatomy* 242(5), 781-795.

Submitted 1 September 2022; Accepted 12 December 2022

The Supplementary Information is presented in Appendix A

Author contributions: LM: study design, data processing and analysis, results interpretation, manuscript drafting and revision. JD, FS: data analysis, manuscript revision. WAE, RGV, AE, VTI, AP: data collection, manuscript revision. YH: project conception, data collection, results interpretation, critical revision of the manuscript.

4.1. Introduction

Since its appearance between 2.4 and 1.8 million years ago in Africa, the genus *Homo* has undergone significant climatic fluctuations that have influenced its evolution (Potts & Faith, 2015; Winder et al., 2015). How these environmental changes shaped hominins morphology has been a recurring question in paleoanthropology research for decades. The exact nature of the influence of ecogeographic factors, their interaction with other processes causing morphological variation (*i.e.*, genetic and biomechanical factors), and the extent of their respective influence on the phenotype are highly debated questions.

One of the anatomical areas that has received particular attention regarding environmental adaptation is the craniofacial skeleton. Specifically, many authors have demonstrated the influence of climate on the morphology of the internal nasal region (Thomson & Buxton, 1923; Davies, 1932; Weiner, 1954; Cottle, 1955; Negus, 1960; Wolpoff, 1968; Carey & Steegmann, 1981; Crognier, 1981a,b; Franciscus & Long, 1991; Roseman & Weaver, 2004; Harvati & Weaver, 2006a; Yokley, 2009; Butaric et al., 2010; Bastir et al., 2011; Noback et al., 2011; Evteev et al., 2014; Jaskulska, 2014; Maddux & Butaric, 2017; Zaidi et al., 2017; Marks et al., 2019), which is in direct contact with the external environment. The influence of some climatic factors (e.g. environmental temperature and humidity) on nasal morphology are generally interpreted in relation to two physiological functions: air conditioning (Charles, 1930; Shea, 1977; Keck et al., 2000; Churchill et al., 2004; Naftali et al., 2005; Elad et al., 2008; Yokley, 2009; Butaric et al., 2010; Maddux et al., 2016a; de Azevedo et al., 2017; Butaric & Klocke, 2018; Evteev & Grosheva, 2019; Heuzé, 2019) and respiratory energetics (Hall, 2005; Froehle et al., 2013; Wroe et al., 2018).

Air conditioning is the process by which the inspired air is warmed to body core temperature and fully saturated in water vapor to protect the lower airways from thermal injuries (Proetz, 1951; Walker & Wells, 1961; Williams, 1998; Wolf et al., 2004; Elad et al., 2008; Hildebrandt et al., 2013). This function is ensured by the highly vascularized respiratory mucosa lining the bony nasal cavity (Froehle, 2008; Holton et al., 2013). In addition to climatic conditions, several physiological factors such as blood pressure or nasal cycle can modify the thickness of the nasal mucosa (Elad et al., 2008; White et al., 2015). This also affects the morphology of the soft tissue nasal passageway through which the air flows and which is called

the nasal airway. The second physiological function that can be linked to a response to environmental variation is respiratory energetics. The nasal cavity is involved in meeting the energetic demands of the body in that it is the upper part of the respiratory system that regulates the amount of air inhaled (Hall, 2005; Froehle et al., 2013; Wroe et al., 2018). An increase in the energetic demands of the body, which are needed for example in colder and/or drier environments, would therefore imply a more voluminous nasal airway (Hall, 2005).

Both air conditioning and respiratory energetics functions can therefore lead to variation in the size and shape of the nasal airway, which will directly affect the velocity, volume and direction of inspired airflow. Because these physiological functions are dependent on climatic factors, nasal morphological variation is an important indicator for understanding the climatic adaptation of modern and extinct human species. This has been demonstrated in numerous studies on dry skulls investigating the link between environmental factors and nasal cavity morphology. The results of these studies have shown that in colder and drier environments, humans display a longer, taller and narrower nasal cavity (Franciscus, 1995; Churchill et al., 2004; Doorly et al., 2008; Yokley, 2009; Holton et al., 2011a, 2013; Evteev & Grosheva, 2019). This morphology would improve the air conditioning capacity by increasing the ratio of mucosal surface area relative to air volume (SA/V) (Schroter & Watkins, 1989; Lindemann et al., 2009), but also the occurrence time and the turbulence of the airflow in the nasal cavity (Inthavong et al., 2007; Noback et al., 2011). Such a morphology could also benefit respiratory energetics, in that higher nasal cavities have been observed in populations with higher metabolic oxygen demands. These higher demands could be linked to a larger lean body mass or a higher level of physical activity in these populations, but also to more demanding climatic conditions (Froehle, 2008; Bastir et al., 2011; Bastir & Rosas, 2016; Holton et al., 2016). Additionally, the shape of the nasal turbinates, which are curled structures that extend from the lateral and upper walls of each side of the nasal cavity, also seems to be affected by climatic factors (Marks et al., 2019). However, the morphology of these structures have been very scarcely studied in humans.

While nasal cavity morphology and its environmental fitness has been extensively discussed, our knowledge on nasal airway morphological variation is still incomplete. A study on *in vivo* data showed non-significant differences in the SA/V ratio between individuals from

European and African descent, unless the nasal airway was completely decongested, which is more indicative of the morphology of the nasal cavity rather than of the nasal airway (Yokley, 2009). This raises the question of the covariation between the volumes and the shapes of nasal cavity and nasal airway. The study of a small sample from France addressed this question by studying the correlation between nasal airway and nasal cavity volumes. When including the ethmoidal air cells, which are olfactory anatomical structures closely connected to the respiratory nasal airway, Heuzé reported a non-significant correlation between nasal cavity and nasal airway volumes. When excluding the ethmoidal air cells, this correlation was significant but rather low (Heuzé, 2019). These findings call for caution when interpolating climatic explanations of nasal airway morphology based on nasal cavity morphology. A quantification of the climate-related nasal airway variation and of the covariation between the nasal airway and the nasal cavity are therefore crucial steps to be able to discuss the climatic adaptation of this anatomical area.

The study of archaeological series or anatomical collections does not allow to solve these questions entirely, because soft tissues are absent. However, medical computed tomography (CT) of living individuals, whose age and sex are reliably known, allows us to study both hard and soft tissues. In this research study, we use CT data to quantify the extent of nasal airway morphological variation in five samples from different modern human populations. Our goal is not to investigate climatic adaptation *per se*, as the populations we study are genetically different and geographically widely dispersed. However, we expect that the genetic and geographic diversity of our sample will impact the morphological variation of the nasal airway. On an intra-population scale, we expect a morphological variation of the nasal airway related to seasonality and characterized by an increase of the nasal resistance and a reduction of nasal patency in cold or dry conditions (Salman et al., 1971; Olsson & Bende, 1985; Fontanari et al., 1996). We also anticipate morphological variation related to size that could be associated with different energetics demands. On this matter, we expect for instance to observe sexual dimorphism in nasal airway morphology (Holton et al., 2014, 2016; Bastir et al., 2020). Finally, we will explore the potential influence of aging on nasal airway morphology, that could be linked to the atrophy of nasal mucosa throughout life (Schrödter et al. 2003).

4.2. Methods

Materials

The present study is based on 195 *in-vivo* CT scans of adult individuals aged between 20 and 95 years old. These CT images were collected in five different geographic areas: Santiago, Chile (N = 35), Bordeaux, France (N = 40), Phnom Penh, Cambodia (N = 40), Moscow, Russia (N = 40) and Cape Town, South Africa (N = 40). The data were collected after institutional review board (IRB) approval (ethical agreements references: DC 2015/172 (CHU Bordeaux); 090 (Hospital of the University of Chile); N19/12/158 (Tygerberg Hospital); National Scientific and Practical Center of Children's Health of Moscow (see Evteev et al., 2018); no ethical clearance was required for a retrospective and anonymized study on data from Phnom Penh Central Hospital). The CT images were anonymized and the only information collected were the age and sex of the individuals. Additionally, the month at which the scans were performed were used to determine the local average temperature and humidity (The World Bank Group, 2021). We excluded the patients displaying nose and sinus disorders such as nasal fractures, rhinitis or choanal atresia causing an obstruction of the nasal airway, or sinusitis. We also excluded patients under respiratory assistance or scanned with their mouths open, to ensure a functional nasal breathing. The application of these criteria led to the exclusion of 56% of the data collected. Among the remaining individuals, we selected males (N = 99) and females (N = 96) over the age of 20 and divided them into three age categories based on those commonly used in biological anthropology (Buikstra & Ubelaker, 1994): 20-35 years (N = 66), 36-50 years (N = 64) and 51+ years (N = 65) (see Figure A1 for detailed composition of the selected sample). The voxel size of the CT-scans ranges from 0.42 to 0.52 mm perpendicular to the axial scan direction and from 0.63 to 1.25 mm in the axial direction.

Segmentation of the nasal airway

Nasal airway surfaces were produced through semi-automatic segmentation and 3D mesh reconstruction in the software Avizo v.9.0.1 (Figure 4.1). First, a threshold-based segmentation was used for filling the air in the negative space delimited by the nasal mucosa. Depending on the acquisition parameters of the original CT scans, the threshold values set on the basis of the histogram were slightly adjusted visually to find the best fit to the segmented

structures. As a next step, volumes were inspected and corrections were manually made to include areas that were not initially selected to the final volumes corresponding to the nasal airway. We excluded all ducts connecting the nasal airway with paranasal sinuses. The nasal airway was delimited anteriorly by the piriform aperture and posteriorly by the choanae. The ethmoidal air cells, located in the ethmoid labyrinth (also known as the olfactory labyrinth), were not included in this model, as they are covered with olfactory mucosa rather than respiratory mucosa (Jankowski, 2013). In the case of a connection between the ethmoidal air cells and the common and/or upper nasal meati, the ethmoidal air cells and the ducts connecting these structures were manually excluded. All the segmentation process was performed by one observer (LM) and an intra-observer test (Figure A2) confirmed the repeatability of the procedure.

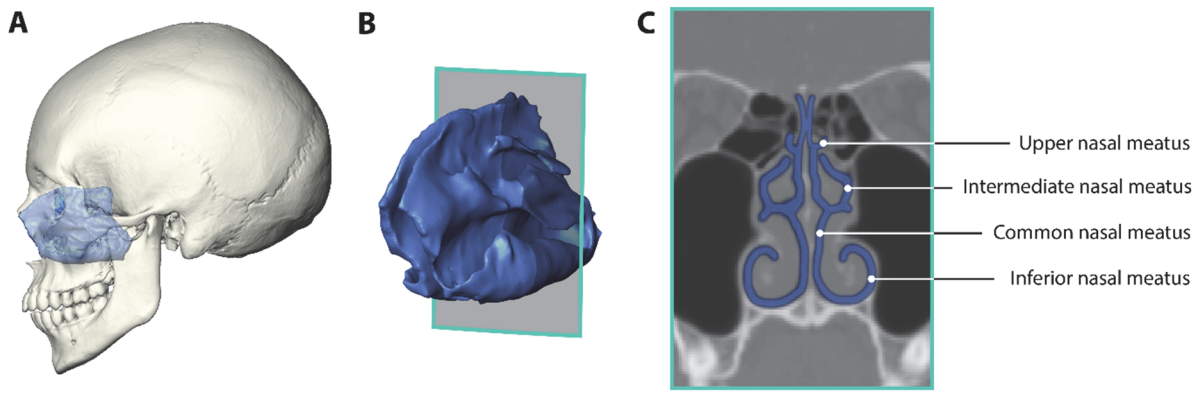

Figure 4.1. Anatomy of the nasal airway. Localization of the nasal airway inside the craniofacial skeleton (left lateral view) (A). Note that the nasal airway is delimited by the nasal mucosa visible on the *in vivo* CT images. The anterior limit is defined by the piriform aperture and the posterior limit by the choanae. 3D reconstruction after segmentation of the nasal airway (B). Coronal slice (C) of the nasal airway along the plane figured in B.

In order to observe the morphological variation of the nasal airway in real physiological conditions, we did not decongest or average it to exclude the potential effect of the nasal cycle, as it has been done in several studies (Yokley, 2009; Patel et al., 2015). The labels resulting from the segmentation were used to build a surface mesh by applying the marching cubes algorithm (Lorensen & Cline, 1987) ("Generate Surface" module in Avizo v.9.0.1). The number of triangles was set to 75.000 faces for each individual's nasal airway to reduce computation time while maintaining sufficient morphological accuracy. These surface models were smoothed using a smoothing algorithm allowing minimal surface shrinkage (Taubin, 1995) ("Smooth Surface"

module in Avizo v.9.0.1). As a pre-processing step, all surfaces were rigidly aligned in position, orientation, and scale with respect to a reference surface (randomly selected) using an Iterative Closest Point algorithm ("Align Surface" module in Avizo v.9.0.1). We then exported each simplified, scaled and aligned surface in PLY file format and converted them into VTK files on Paraview v.5.7.0.

Surface-based morphological comparison

The nasal airway shape was analyzed with a landmark-free method based on the construction of a surface representing the mean shape of a sample and its deformation to each individual surface (Durrleman et al., 2012, 2014; Beaudet et al., 2016). This deformation is modelled as a diffeomorphism: it is not based on a point-to-point correspondence between shapes but on a smooth and invertible deformation of the entire 3D surface (Durrleman, 2010). This method was shown to increase the statistical power of shape comparison and to increase its precision by allowing the observation of non-homologous features of shapes (Vaillant et al., 2007; Braga et al., 2019). The mean shape is computed with the software Deformetrica from a set of surfaces, based on a set of control points located near the most variable parts and a set of momenta (or vector fields) representing the deformation from the global mean shape (GMS) to each individual. We also calculated population mean shapes (PMS) for each geographic group, based on the mean of the momenta within each population.

Exploratory multivariate analysis

To test the effects of geographic origin, demographic factors (sex and age), and environmental factors (mean temperature and humidity) on nasal airway morphology, statistical analyses were carried out using R v.4.0.5 (R Core Team, 2021) and the packages RToolsForDeformetrica (Dumoncel, 2020), ade4 (Chessel et al., 2004; Dray & Dufour, 2007; Dray et al., 2007; Bougeard & Dray, 2018; Thioulouse et al., 2018), vegan (Oksanen et al., 2020) and pairwiseAdonis (Martinez Arbizu, 2020). We quantified inter-population variation by performing a principal component analysis (PCA) on the GMS-to-individuals nasal airway deformations of the whole sample. Intra-population variation was explored by performing a PCA on the deformation fields from PMS to the individuals. Deformated shapes along the PCs illustrate how the GMS (inter-population) or the PMS (intra-population) varies from the mean to one time the

standard deviation. Color maps onto the nasal airway surfaces rendered the magnitude of the displacements caused by the deformation. To represent an accurate vision of our data and make it accessible to people with color-vision deficiencies (Moreland, 2016; Crameri et al., 2020) we use the viridis color map (van der Walt & Smith, s. d.) for our data vizualisation. Permutational multivariate analyses of variance (PERMANOVAs) were used to explore the variables influencing the distribution of the individuals on the main principal components (*i.e.*, geographic group, sex, age, temperature, humidity). The effect of allometry on the shape variation was tested via bivariate regressions (Pearson correlation) between PC scores and the log-transformed volume of the nasal airway (Urciuoli et al., 2020). We also explored nasal airway volume variation among and within populations with ANOVAs. To be able to normalize these volumes by the size of the facial skeleton, we measured 11 landmarks on the facial skeleton of each individual and used centroid size as a proxy for size (Figure A3). Centroid size is defined as the square root of the sum of squared distances of all the landmarks of an object from their centroid. These landmarks were measured by one observer (LM) and their repeatability was assessed by an intra-observer test (Figure A2).

4.3. Results

Nasal airway shape variation among geographic groups

The PCA analysis of nasal airway shapes performed among all the geographical groups shows a strong overlap of the five populations. Nevertheless, we can observe differences in the distribution of these groups on several principal components, including PC1, PC2 and PC3 accounting for 18.59%, 6.91%, and 5.26% of total shape variance respectively (Figure 4.2). Due to the high overlap of the groups on the PCA scatterplot, we also represented the distribution of the individuals with boxplots showing their scores on the first three principal components. In addition to quantitative comparisons, we also computed the mean shapes for each geographic group (Figure 4.3) to provide a qualitative comparison of these shapes with the corresponding GMS-to-PMS deformations. These comparisons can be visualized with colormaps and vectors showing the magnitude and orientation of the variation.

PC1 highlights major variation in nasal airway length, width, and height as well as the degree of protrusion of the anterosuperior part of the common nasal meatus (Figure 4.2). The

Cambodian and South African samples have the highest scores on PC1 (Figure 4.2) because of the anteroposteriorly contracted and mediolaterally extended morphology of their nasal airways (Figure 4.3). The reduction in the anteroposterior axis is due to an anterior displacement of the choanae and a posterior displacement of the piriform aperture. The mediolateral elongation is related to a lateral displacement of the inferior and intermediate meati, while the common meati approximately remain in the same position. The French and Russian samples are found rather in the negative values (Figure 4.2) because their nasal airways have a longer and narrower shape and show significant protrusion of the anterosuperior part of the common meati (Figure 4.3). The lower part of the common meati is displaced downward, contributing to a slight overall increase in height. Individuals from Chile spread out all along PC1 with a median centered at 0 (Figure 4.2). The Chilean PMS shows the lowest rate of variation compared to the GMS (Figure 4.3).

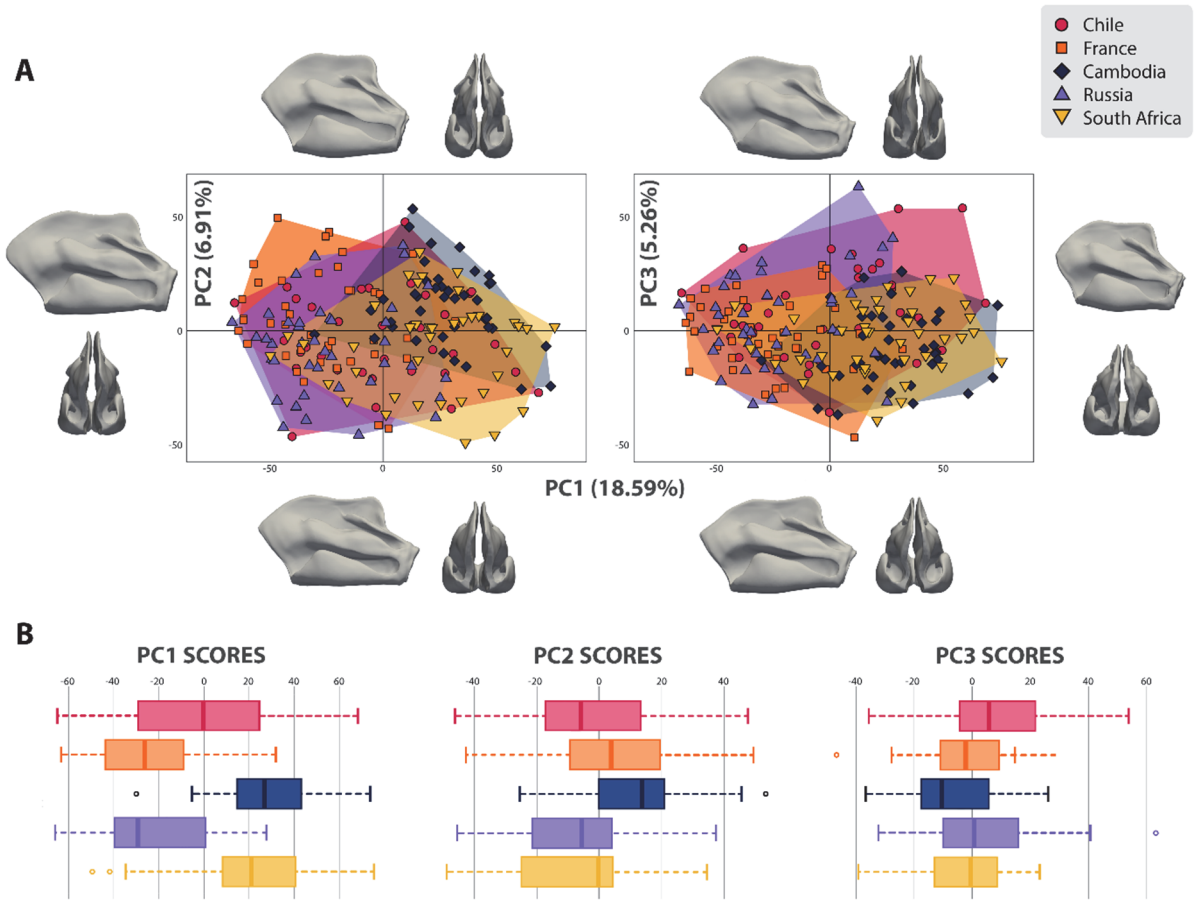

Figure 4.2. Shape differences between groups. Principal Component Analysis of the deformation-based shape comparison made on the nasal airway of the five populations (Chile, France, Cambodia, Russia, South Africa) (A) and boxplots showing the distribution on PC1, PC2 and PC3 (B).

PC2 captures variation in nasal airway height, length and width, but also in the morphology and relative position of the meati. Individuals from Cambodia are mainly found in the positive values on PC2 (Figure 4.2) because of their morphology being relatively larger in the superior-inferior dimension, shorter in the anterior-posterior dimension and wider in the medial-lateral dimension. The elongation in the superior-inferior plane is due to an upward displacement of the superoposterior portion of the common meati, which are proportionally much higher than in the negative values (Figure 4.3). This part of the common meati also shifts significantly forward. PC2 discriminates the Cambodian and South African samples because the latter, although wider and shorter than the GMS, is found rather in the negative values (with a median centered at 0) because of its contraction in the superior-inferior plane. Individuals from Russia are also predominantly found in the negative values (Figure 4.2) because their PMS shows an increase in overall nasal airway length and a reduction in nasal airway width. Their shape is also defined by a displacement of the intermediate meati floor, implying a relative position that is closer to the inferior meati. The curvature of the intermediate meati is also more curled toward the common meati, especially at their posterior part.

PC3 accounts for the asymmetry in the shape of the nasal airway. On this PC, all populations are more equally distributed (Figure 4.2). Negative values characterize wider inferior meati and narrower intermediate and upper meati. The upper and anterior part of the common meati is displaced to the left while the middle part is displaced to the right. This creates a torsion of the overall shape. The choanae are displaced upward and the anterior part of all meati is displaced downward. In positive values, there is a mirror-like variation.

The PERMANOVAs performed on all the PC scores (Table A1) of the morphospace confirm what we observe on the PCA by revealing statistically significant differences between geographic groups ($R^2 = 0.12$, $p = 0.001$) and, to a lesser extent, between sexes ($R^2 = 0.01$, $p = 0.04$). These PERMANOVAs also show that the temperature at the time of scanning significantly influences the distribution of individuals in the morphospace ($R^2 = 0.08$, $p = 0.001$). However, this last factor is strongly correlated with the geographical groups. Individuals scanned at the highest temperatures (over 25°C) are only found in the Cambodian sample and the individuals scanned below 0°C all belong to the Russian sample. Finally, the PERMANOVAs on all the PC scores do not highlight an influence of age or mean humidity at the time of scanning on the distribution in the morphospace.

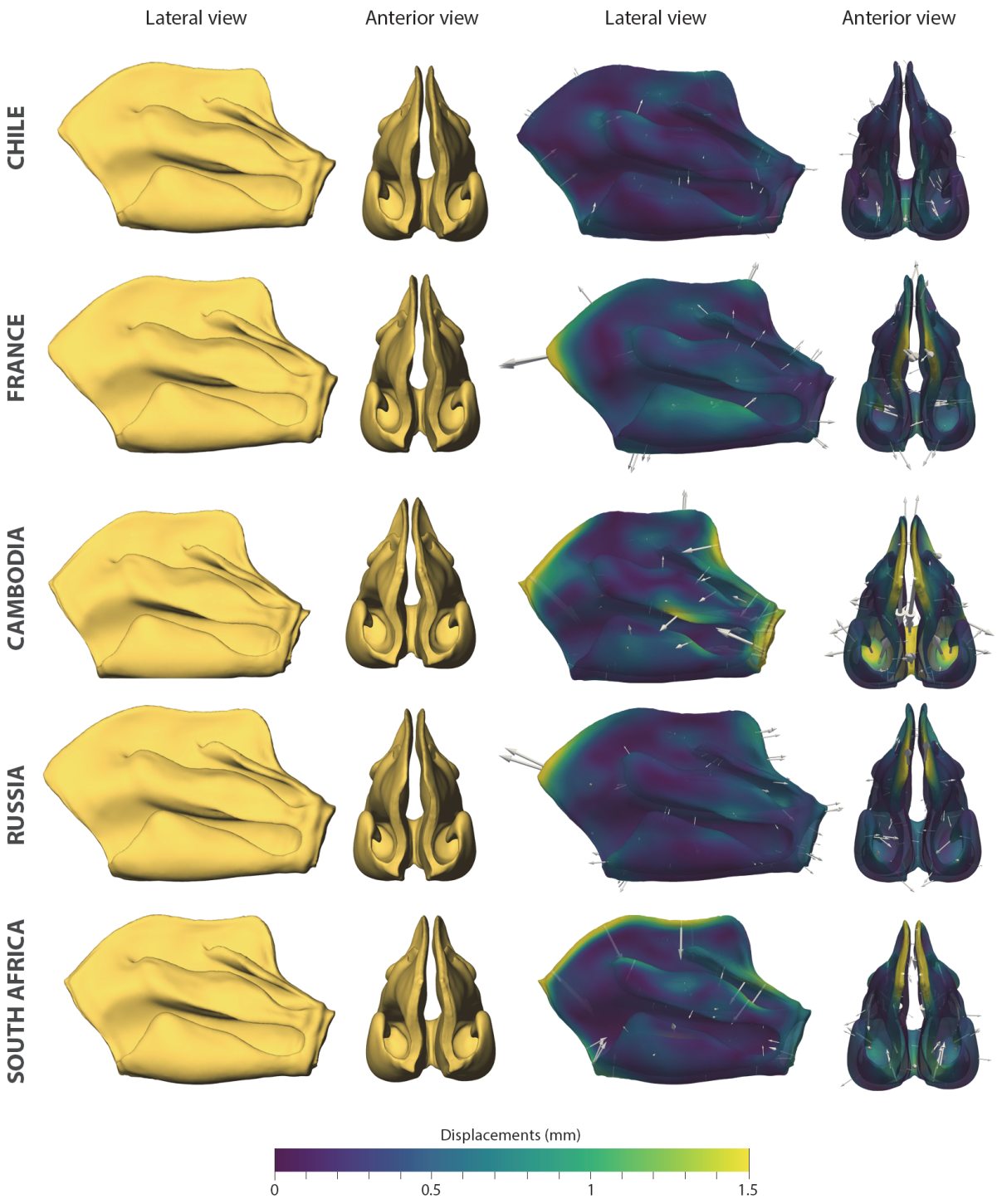

Figure 4.3. Population mean shapes. Mean shapes computed for each population (PMS) (left) and comparative maps of morphological deformations from the global mean shape (GMS) computed for the total sample to the PMS (right). Deformation from the GMS is rendered by a colormap ranging from dark blue (lowest values) to yellow (highest values) at the surfaces of each PMS. The magnitude and orientation of the deformation from the GMS to the PMS is represented by the white vectors (scale factor set to 5 for a better vizualisation). The range of the color bar (from 0 to 1.5 mm) has been homogenized to best represent global and local deformation, even if some recorded deformations exceeded this value.

Table 4.1. Between-groups morphological distances. Pairwise distances represented by: the regularity values (sorted from highest to lowest) associated with the between-groups shape comparison; and the results of the pairwise PERMANOVAs performed on all the PCs.

Pairs of geographic groups		Regularity	F	R^2	p
Cambodia	Russia	850.90	12.303	0.136	0.002*
Cambodia	France	825.20	13.425	0.147	0.002*
South Africa	France	677.40	10.046	0.114	0.002*
South Africa	Russia	585.80	8.241	0.096	0.002*
Chile	Cambodia	404.50	5.770	0.073	0.002*
Chile	France	354.20	4.306	0.056	0.002*
Chile	South Africa	254.20	3.312	0.043	0.002*
Cambodia	South Africa	238.10	3.520	0.043	0.002*
Chile	Russia	223.30	2.664	0.035	0.002*
Russia	France	133.40	1.872	0.023	0.005*

The morphological distances between the geographic groups can be represented by the F value of the pairwise PERMANOVAs between group levels and by the regularity value associated with the deformation-based shape comparison and representing the amount of deformation from GMS to each PMS (Table 4.1). The groups that are the closest in the morphospace and thus show greatest morphological similarities are Russia and France. The pairs of groups that are the most distant in the morphospace are Cambodia-Russia (cf. regularity value) and Cambodia-France (cf. F value). When performing post-hoc tests between the temperature categories (Table A1), we find redundancy in this information: the pairs of groups that are significantly the most distant are patients scanned between 0-9°C (*i.e.*, almost exclusively French and Russian individuals) and patients scanned above 25°C (all the Cambodian individuals). The two significantly closest groups are patients scanned between 0-9°C and between 20-25°C (mainly individuals from Chile, but also from France and Russia).

When performing PERMANOVAs on each PC (Table A2) from PC1 to PC8 (which all account for more the 3% of the overall variation), we observe that the geographical groups influence the distribution of the individuals on all the PCs, except PC5. On PC1 (18.59% of the overall variance), the affiliation to a geographical group explains 42% of the distribution of the individuals. PC3 (5.26% of overall variance) is the only PC to be moderately but significantly correlated with sex (R^2 = 0.02, p = 0.03). To quantify the effect of allometry on the sample distribution in the morphospace, we also performed bivariate regressions between each PC and

the log-transformed volume of the nasal airway (Table A3). Of the first three PCs, only PC2 (R^2 = 0.057, p <0.001) and PC3 (R^2 = 0.069, p <0.001) show a significant correlation between these two factors and, therefore, an influence of allometry.

Factors of volume variation in the total sample

The ANOVAs performed on nasal airway volume (Table A4) highlighted that it is not influenced by geographic groups affiliation. However, nasal airway volume varies significantly according both to sex (F = 26.57, p <0.001) and age (F = 9.16, p = 0.003). Nasal airway volume is overall higher in males than in females and tends to increase with age (Figure 4.4). When we normalize nasal airway volume by the centroid size of the facial skeleton, we obtain the same results, *i.e.*, no influence of geographic group on normalized nasal airway volume, but a significant influence of sex (F = 10.10, p = 0.002) and age (F = 12.99, p <0.001).

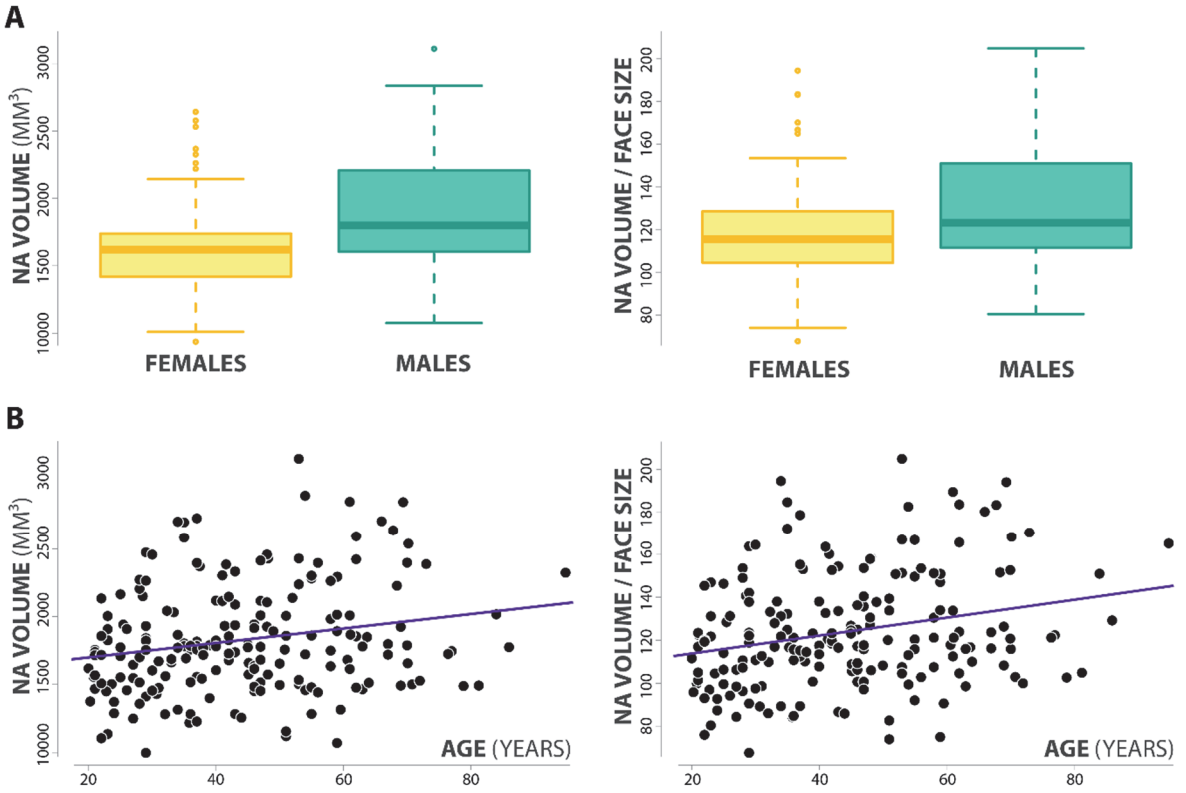

Figure 4.4. Factors of volume variation. Box-whisker plots (A) representing sexual dimorphism in nasal airway (NA) volume (left) and in nasal airway volume normalized by the centroid size of the facial skeleton (right) of the 5 populations. Regressions between nasal airway volume and age (left) and nasal airway volume normalized by the centroid size of the facial skeleton and age (right) among the 5 populations (B).

Factors of shape variation within geographic groups

After analyzing variation between geographic groups, we quantified the influence of sex, age and temperature and humidity at the time of scanning on morphological variation within each population. Temperature and humidity factors were not observable on the South African individuals, as the scans were all acquired during the same month. Similarly, we could not observe the correlation between temperature and nasal airway morphology in the Cambodian population, as there was only one temperature category represented. According to the PERMANOVAs (Table A5), the only sample subject to the influence of one of these factors is the Russian population, whose morphology is significantly correlated with temperature at the time of scanning (R^2 = 0.10, p = 0.03). PCA analysis performed on the nasal airway shapes of this sample (Figure 4.5) shows the clear distinction of the group containing individuals scanned during months with temperature above 20°C from the other three groups scanned during colder months. This is confirmed by a post-hoc test on the results of the PERMANOVA (Table A5), showing that individuals scanned at more than 20°C are significantly different from the groups scanned at < 0°C (R^2 = 0.08, p = 0.04) and 10-19°C (R^2 = 0.12, p = 0.04). On the PCA, this group (>20°C) is localized in negative values on PC1, which can be illustrated by a nasal airway shape that is more contracted antero-posteriorly and that shows an asymmetry in the width of the two sides of the nasal airway. The same group is located in positive values on PC3, in which we observe an even greater asymmetry in nasal airway width.

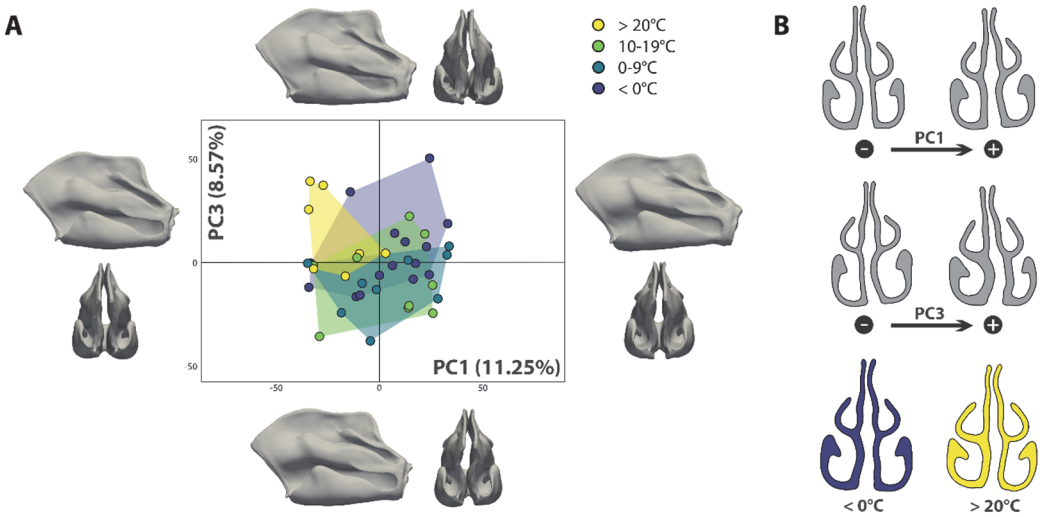

Figure 4.5. Seasonality. PCA of the deformation-based shape comparison made on the nasal airway of the sample from Russia (A). Colors represent the temperature at the time of the scan. Nasal airway cross-section at the extreme values on PC1 and PC3 and of the groups scanned below 0°C and above 20°C (B).

Factors of volume variation within geographic groups

Within each population, nasal airway volume varies significantly with sex, age, or both (Table A4). In contrast, we observe no effect of temperature or humidity on nasal airway volume. We record sexual dimorphism in nasal airway volume for populations from France ($F = 8.98$, $p = 0.005$), Cambodia ($F = 4.70$, $p = 0.037$), Russia ($F = 7.61$, $p = 0.009$) and South Africa ($F = 4.03$, $p = 0.052$). Age influences nasal airway volume in samples from Chile ($F = 4.12$, $R^2 = 0.11$, $p = 0.05$) and Russia ($F = 10.21$, $R^2 = 0.21$, $p = 0.003$). We observe the same pattern of variation to that observed for the total sample, with greater nasal airway volume in males than in females (Figure A4) and a nasal airway volume increasing with age (Figure A5). When we normalize nasal airway volume by the centroid size of the facial skeleton, we obtain slightly different results. We still record significant sexual dimorphism in normalized nasal airway volume for the population from France ($F = 4.31$, $p = 0.045$) but no longer for the populations from Cambodia, Russia and South Africa. Age still influences normalized nasal airway volume in samples from Chile ($F = 5.26$, $R^2 = 0.14$, $p = 0.03$) and Russia ($F = 8.85$, $R^2 = 0.19$, $p = 0.005$), but also the population from France ($F = 5.08$, $R^2 = 0.12$, $p = 0.03$).

4.4. Discussion

Inter-population variation of the nasal airway

To our knowledge, no study had investigated the extent of nasal airway morphological variation in large samples (N>100) from different modern human populations. Our results highlight subtle but significant morphological differences between the five geographical groups we studied. We can observe two groups showing strong morphological similarities, which are France and Russia. These two samples are broadly overlapping in the PCA and the distance between them is the smallest of all pairwise distances. Their PMS are anteroposteriorly larger and mediolaterally smaller compared to the GMS. They both show an important protrusion of the superior-anterior part of the common meati, which can be reasonably linked to the relative position of the nasal bones and the shape of the external nose. The sample that diverges the most from the French and Russian groups is the Cambodian sample, which is the most distant in the morphospace. The Cambodian PMS is anteroposteriorly contracted and superoinferiorly and mediolaterally extended compared to the GMS. Cambodian population is also the most clustered group on the PCA, indicating that it is the sample with the least shape variation, *i.e.*,

the most homogenous population. In contrast, Chile individuals spread all along each PC and form a very scattered cluster. When we look at Chile PMS, which is very close to the GMS, we get the impression that the morphological variation within this sample is very low. On the contrary, the PCA rather indicates a great deal of morphological diversity that averages in a shape that is very close to the GMS. Finally, the South African PMS is morphologically close to the Cambodian PMS, although more contracted in the superoinferior dimension. On the PCA, South African sample tends to overlap greatly with the Cambodian sample, with a shift of some individuals towards the negative values on PC1, *i.e.*, towards French and Russian morphology.

Obviously, morphological variation among these five modern populations cannot be explained in a unifactorial manner. As stated in our introduction, we are aware of the limitations of our sample composition: first, the location where the patients were scanned does not provide information about their geographic and genetic background. We therefore have to consider that our samples can be more or less heterogeneous. Furthermore, other data that could influence the morphology of the nasal airway, such as lifestyle (e.g. diet, smoking habits…), medical history or air quality are out of our reach. Other environmental factors can also influence nasal airway morphology, such as altitude, which we were unable to observe either. Indeed, the locations from which the data were obtained are coastal or valley environments, which limits the elevation variation between 19 m (Phnom Penh, Cambodia) and 561 m (Santiago, Chile) (OpenStreetMap, 2022). However, keeping in mind all these limitations and the fact that the observed variation has a multiple etiology, we discuss two factors that could partially explain this variation and that are difficult to disentangle from each other: genetic and climatic factors.

Genome-wide association studies have found significant association for multiple facial traits including nose-related traits and have identified several genes involved in craniofacial development (Adhikari et al., 2016; Shaffer et al., 2016). This implicates a genetic basis for craniofacial morphology, which makes us hypothesize that the genetic traits of individuals will condition in part the morphology of their nasal airway. From this point of view, one could expect that the populations of this study which are genetically the closest will also be the closest morphologically. This hypothesis seems to be verified in the morphological proximity of the populations from France and Russia, which also share a lot of similar ancestry components (Cavalli-Sforza & Piazza, 1993) despite the genetic differences between Western Europeans and Balto-Slavic populations (Kushniarevich et al., 2015). The three other populations have very different ancestral histories linked to historical migration patterns. The Chilean population has

a genetic structure defined by 40.43% of European ancestries, 57.11% of Native-American ancestry and 2.46% of African ancestry (Eyheramendy et al., 2015). It is thus rather coherent to find this population so widely distributed in our morphospace. As for the South African population, it includes 79.2% of black southeastern Bantu-speakers, 8.9% of an admixed population (with major ancestral components that are predominantly Khoesan (32–43%), Bantu-speaking Africans (20–36%), European (21–28%) and Asian (9–11%) (de Wit et al., 2010)), 8.9% of whites of European origin, and 2.5% of a population originating from the Indian sub-continent (Choudhury et al., 2017). As for all our geographical groups, we have no information on the composition of this sample. We can therefore only suppose that it is heterogeneous, and that the distribution we observe in the morphospace reflects this diversity. Finally, the Cambodian population is morphologically the most distant from the European populations and the least variable for nasal airway shape, which reflects the fact that there is no recent admixture with European populations. The homogeneity observed in between and within different Cambodian ethnic groups (Kloss-Brandstätter et al., 2021), indicating early genetic isolation of the whole population, can also be observed morphologically in this study.

Even if the distribution of our individuals in the morphospace reflects to a certain extant these genetic affinities, we can still raise the question of the part played by climate adaptation in the phenotypes. This question is relevant, especially in view of the results of a study on the external nose, having demonstrated with Qst-Fst comparisons that nares width is more differentiated across populations than expected under genetic drift alone (Zaidi et al., 2017). This study also proved that the width of the nares is correlated with temperature and absolute humidity. It appears that some aspects of nose shape may indeed have been driven by local adaptation to climate, in addition to other non-neutral forces such as sexual selection.

As stated above, we do not have the right sample to address climatic adaptation. For that purpose, we would need to constitute a comparative sample of genetically close groups living in more variable environments (Evteev & Grosheva, 2019). However, two of our samples, that are genetically and geographically rather close, could raise such discussion: France and Russia. According to Köppen-Geiger climate classification, Bordeaux (France) benefits from a warm temperate climate and Moscow (Russia) from a continental, colder climate (Dfb) (Table 4.2). Yet, their morphology is very close and the volume of their nasal airway is not significantly different. As expected, the link between nasal airway morphology and climate is not

straightforward and we may consider that the part of the variation resulting from climatic adaptation lies is the subtle morphological differences between these two populations.

We can raise this question of climatic adaptation for all the samples in our study and ask what aspect of the morphology of each population can be explained by this factor and in which proportion. The antero-posteriorly contracted and mediolaterally extended Cambodian mean shape could be linked to a reduction of nasal resistance and time occurrence of the airflow in order to improve air conditioning in a tropical climate. This interpretation would be coherent with the observations made on bone nasal cavity in previous studies (Franciscus & Long, 1991; Maddux et al., 2016a). However, our data also highlights the fact that morphological variation is not limited to these three main dimensions. It also lies in the overall curves, protrusions and retrusions of the different parts of the nasal airway, as well as in the relative position and the curvature of the meati. Concerning the latter, our results do not allow us to make a straightforward connection with the observations made on the nasal turbinates, which define, to a certain extent, the morphology of the meati. Marks et al. (2019) showed that individuals from the Arctic Circle possessed superoinferiorly and mediolaterally larger inferior turbinates compared to Equatorial individuals, which reflects climate-mediated evolutionary demands on heat and moisture exchange. An interesting avenue of research would be to study the covariation between soft tissues meati and bony nasal turbinates, to further confirm the functional expectations in this area of the nasal cavity.

Interestingly, we record no correlation between nasal airway volume and geographical groups. This implies that the modification of nasal airway shape between the studied populations does not impact the volume of air that can pass through the nasal airway. As higher metabolic demands for oxygen requirements (e.g. linked to higher body mass or colder and/or drier environments) may place constraints on the size of the nasal cavity (Bastir et al., 2011; Froehle et al., 2013; Holton et al., 2014, 2016), we expected to observe nasal airway volume variation due to the climatic and ancestry diversity of our samples. However, the populations constituting those samples are not subject to strong constraints, whether environmental (e.g. extreme climatic conditions), genetic (e.g. low degree of genetic admixture) or biomechanical (e.g. mechanically challenging diet, see Brachetta-Aporta & Toro-Ibacache, 2021). The absence of volume variation and high level of stress lead us to hypothesize that the nasal airway shape variation between modern human populations may not be primarily driven by a functional role. As proposed by Eyquem et al. (2019), the reduction of functional constraints might actually be

a key to greater degree of shape variation in modern populations. Our findings suggest that volume might be more of a conserved trait constrainted by a sex and age effect, whereas the shape associated with this volume would be the element that varies among populations. This hypothesis could be verified by comparing our results with body mass index variation, but also by conducting population-scale airflow simulations to understand how airflow is distributed in this morphology (e.g. Keck & Lindemann, 2010; de Gabory et al., 2020).

Table 4.2. Climatic data. Annual mean temperature (The World Bank Group, 2021), Köppen-Geiger classification (Cls) (Kottek et al., 2006; Rubel et al., 2017) and corresponding climate for the five regions of origin of the populations studied.

Location	Mean T° (°C)	Cls	Main climate	Precipitation	Temperature
Santiago (CL)	10.5	Cfa	Warm temperate	Fully humid	Hot summer
Bordeaux (FR)	14.2	Cfb	Warm temperate	Fully humid	Warm summer
Phnom Penh (KHM)	28.8	Am	Equatorial	Moonsoonal	
Moscow (RUS)	6.2	Dfb	Snow	Fully humid	Warm summer
Cape Town (SA)	17.3	Csb	Warm temperate	Summer dry	Warm summer

Seasonal reactivity of the nasal mucosa

In this study, one important aspect to explore was the way environmental temperature can, in a very short time period, affect the morphology of nasal mucosa and, subsequently, the morphology of the nasal airway. The only sample that allowed us to do so was the Russian sample, as it is the only one that contains individuals that were scanned throughout the year and therefore in different seasons. Of course, we do not know at what temperature the individuals were scanned in the hospital and consider that this data must be controlled to study this question. However, we seeked to observe the potential volume or shape variation that could have been linked either to the temperature of the outside environment or, conversely, to the use of air conditioning or heating in the hospital during certain seasons.

We found that this population displayed a correlation between the average temperature at the time of the scan and the nasal airway shape and that individuals scanned above 20°C separate from the other groups in the morphospace. However, by observing the extreme shapes on PC1 and PC3, we saw that the morphology of this group is mainly characterized by an asymmetry in the sectional width of the meati. This asymmetry is related to the nasal cycle, which is an alternative partial congestion and decongestion of the right and left sides of the

nasal airway during breathing (Watelet & Cauwenberge, 1999; White et al., 2015). Yet, two of the three individuals in the > 20°C group that fall outside of the morphological variation and that drive the signal of this group towards negative values on PC1 and positive values on PC3 have been scanned at a strongly asymmetric moment of their nasal cycle. This signal could therefore highlight a sample composition bias or indicate a higher activity of the nasal cycle when the temperature is warmer. We can point out however that the volume of the nasal airway is not correlated with environmental temperature or humidity, as would have been expected knowing that cold-dry conditions tend to increase nasal resistance and to reduce nasal patency (Salman et al., 1971; Olsson & Bende, 1985; Fontanari et al., 1996).

Causes of intra-population variation of the nasal airway

Sex had no influence on nasal airway shape, but did influence their volume. Males have on average 17% larger nasal airways than females (10% when normalized by the size of the facial skeleton), which can be explained by the fact that they have higher energetic demands, requiring higher air volume intakes (Bastir et al., 2011, 2020; Holton et al., 2014, 2016). Previous studies (Keustermans et al., 2018; Bastir et al., 2020) demonstrated sexual dimorphism in the shape of the soft tissues of the upper respiratory tract. Nevertheless, they all included in their 3D analysis the inflow region (external nose) and the outflow region (behind the choanae) and stated in their results that these two regions showed stronger sexual dimorphism than the nasal airway itself (Bastir et al., 2020). Our results corroborate these observations, as we show no sexual dimorphism in nasal airway morphology.

Our results highlight that age has no effect on nasal airway shape but influences its volume. Nasal airway volume tends to increase by 11% between younger (20-35 years) and older (51+ years) individuals. This would indicate that nasal mucosa tends to shrink with age, thus increasing the negative volume that constitutes the nasal airway. This alteration of the nasal mucosa has been observed in previous histological and histochemical studies showing a significant atrophy of the epithelium in older individuals (Toppozada, 1988; Schrödter et al., 2003). This atrophy of the nasal epithelium can be linked to age-related differences in the molecular signature associated with ciliation and mucin biosynthesis (Balázs et al. 2022). This result underscores the importance of taking into account the infuence of age on nasal airway morphology in future studies.

Finally, in order to observe possible asymmetries related to deviations of the nasal septum, we did not symmetrize the two nasal hemi-cavities. On the PCA performed on the total sample, these assymetries are well reflected by PC3, accounting for 5.26% of the overall variance. This underlines their importance in nasal airway shape variation, even if it has been demonstrated that they do not affect the heating function of the nose (Keustermans et al., 2020). PC3 is moderately but significantly correlated with geographic group affiliation, which explains 9% of the distribution on this PC. This tenuous link between populations and asymmetries indicates that the latter are fairly randomly distributed in our five samples. We can note however that populations from France, Russia and South Africa tend to average around 0. The sample from Chile is slightly displaced towards the positive values, which tends to indicate a higher occurence for rightward torsions in this sample, while the Cambodian sample tends to be more towards negative values, which represents a leftward torsion of the nasal airway shape.

Perspectives

The results of our study show complex patterns of variation in nasal airway morphology. At the inter-population level, we quantify shape variation between our five samples that we could connect to genetic background and climate. This shape variation is surprisingly not associated with volume variation, which question the climate-related metabolic demands for oxygen consumption. At the intra-population level, sex and age have no influence on the nasal airway shape, but do influence nasal airway volume, which is higher in males than in females and tends to increase with age. These factors of variation, to which we can add temperature and asymmetries, do not have the same role and/or the same magnitude for all the samples. The quantification of these patterns of variation allows us to take a step towards a better understanding of the multiple factors driving the morphological variation and evolution of the upper airways. To take this a step further and link a phenotype to air conditioning and respiratory energetic capacities, we could use the population mean shapes we produced with our data in a computational fluid dynamics (CFD) study (Inthavong et al., 2007; Chen et al., 2010; Keck & Lindemann, 2010; de Gabory et al., 2020). This would allow us to numerically simulate airflow patterns in modern humans on a population scale. After taking this first step, we could consider transposing these research questions to the fossil record. A better knowledge of the etiologies and intricacies of modern nasal shape variation could lead to more accurate reconstructions of the functional nasal airway of fossil hominins. This could allow to apply CFD techniques on these reconstructions to get an insight into the breathing of fossil hominins.

Synthèse

Dans ce chapitre, nous présentons l'étude de 195 CT-scans réalisés *in vivo* sur des humains adultes provenant de cinq zones géographiques (Chili, France, Cambodge, Russie et Afrique du Sud). L'objectif est de quantifier la variation morphologique de la voie aérienne nasale, qui est l'espace négatif délimité par la muqueuse nasale. Après segmentation et reconstruction de maillages 3D de la voie aérienne nasale, nous l'analysons à l'aide d'une méthode de morphométrie par déformation de surface.

Nos résultats démontrent des différences de conformation subtiles mais significatives entre les voies aériennes nasales de nos cinq échantillons. Nous n'observons aucune différence de volume de la voie aérienne nasale en fonction des groupes, ce qui soulève la question de l'influence du climat sur les demandes métaboliques. Nous ne détectons aucun effet de l'âge ou du sexe sur la conformation de la voie aérienne, mais ces deux facteurs en influencent le volume. Les hommes présentent une voie aérienne nasale plus volumineuse que les femmes afin de répondre à des demandes énergétiques plus importantes. Le volume de la voie aérienne a tendance à augmenter avec l'âge, probablement en raison d'une rétraction de la muqueuse nasale.

Summary

In this chapter, we present the study of 195 *in vivo* CT scans of modern adult humans collected in five different geographic areas (Chile, France, Cambodia, Russia and South Africa). The objective is to quantify the morphological variation of the nasal airway, *i.e.*, the negative space delimited by the nasal mucosa. After segmentation of the nasal airway, we reconstruct 3D meshes that are analyzed with a landmark-free morphometrics method based on surface registration.

Our results highlight subtle but statistically significant shape differences between the nasal airways of our five samples. Interestingly, we record no correlation between nasal airway volume and geographical groups, which raises the question of climate-related metabolic demands for oxygen consumption. While we do not detect any effect of age or sex on the shape of the nasal airway in our samples, these factors are shown to influence nasal airway volume. Males display larger nasal airways than females, presumably to meet higher energetic demands. The nasal airway volume also tends to increase with age, which could be linked to an age-related shrinkage of the nasal mucosa.

• Chapter 5 •

PHENOTYPIC PLASTICITY IN MURINE CRANIOFACIAL MORPHOLOGY

PLASTICITÉ PHÉNOTYPIQUE DE LA MORPHOLOGIE CRANIOFACIALE MURINE

Chapter 5 is based on a publication in preparation:

> Maréchal L., Magne L., Santos F., Devlin M., Heuzé Y. Food hardness and cold stress influence on the craniofacial and nasal morphology of inbred mice.

Expected submission in June 2023

The Supplementary Information is presented in Appendix B

Author contributions: LMar: study design, data processing and analysis, results interpretation, manuscript drafting and revision. LMag, FS: data analysis, manuscript revision. MD, YH: project conception, data collection, results interpretation, manuscript revision.

5.1. Introduction

For decades, paleoanthropologists have interpreted the morphological evolution of hominins from the perspective of climatic adaptation (Trinkaus, 1981; Jelinek, 1994; Steegmann et al., 2002; Evteev et al., 2014). The craniofacial skeleton has been the subject of much attention in these considerations, and several authors have suggested that, in addition to natural selection, genetic drift could also explain some of the differences in cranial morphology between different hominin groups (Ackermann & Cheverud, 2004; Roseman, 2004; Weaver et al., 2007). Nevertheless, it is reasonable to assume that several intermingled factors and mechanisms are involved in phenotypic variation. The potential influence of selective pressures caused by extreme climatic environments on specific craniofacial regions is therefore still considered and debated (e.g. Roseman, 2004; Harvati & Weaver, 2006; Wroe et al., 2018).

Several studies on dry skulls of anatomically modern humans have demonstrated that the morphology of the nasal cavity covaries with eco-geographic factors (e.g. temperature, humidity, altitude) (Davies, 1932; Weiner, 1954; Carey & Steegmann, 1981; Franciscus & Long, 1991; Roseman, 2004; Hubbe et al., 2009; Yokley, 2009; Noback et al., 2011; Evteev et al., 2014; Fukase et al., 2016; Maddux et al., 2016b). The nasal cavity is indeed indirectly involved in the conditioning of the inspired air, for it houses the nasal mucosa that set the air to body temperature and saturate it in water vapor before it enters the lungs (Elad et al., 2008). Several mechanisms could explain the correlation between nasal cavity morphology and eco-geographic variables such as air temperature. It could be the result of natural selection, influencing nasal morphology over successive generations and finally leading to genetically-mediated climatic adaptations. But we can also consider the hypothesis that environmental factors may act on an individual scale, by causing a physiological response to temperature that is independent of genotype (*i.e.*, phenotypic plasticity) (Rae et al., 2006; Serrat et al., 2008).

These two evolutionary mechanisms can lead to identical morphological outcomes and are therefore difficult to disentagle in human samples. The use of experimental approaches in controlled environments can help to test hypotheses about the origin of the observed phenotypic variation by sorting out the genetic and environmental components. For this study, we chose to work on mice (*Mus musculus*) models (Figure 5.1), relying on the high degree of conservation of the different developmental phases and major physiological functions in

mammals. Furthermore, protein-coding regions of the mouse and human genomes are 85% identical (Mouse Genome Sequencing Consortium, 2002) which explains the extensive use of the mouse in biomedical and evolutionary research. To our knowledge, only one similar study has quantified the effects of a cold environment on the skull morphology of laboratory rats (Steegmann & Platner, 1968; Rae et al., 2006). The results of this study suggest that cold environments induce subtle but significant changes in the internal and external morphology of the facial skeleton.

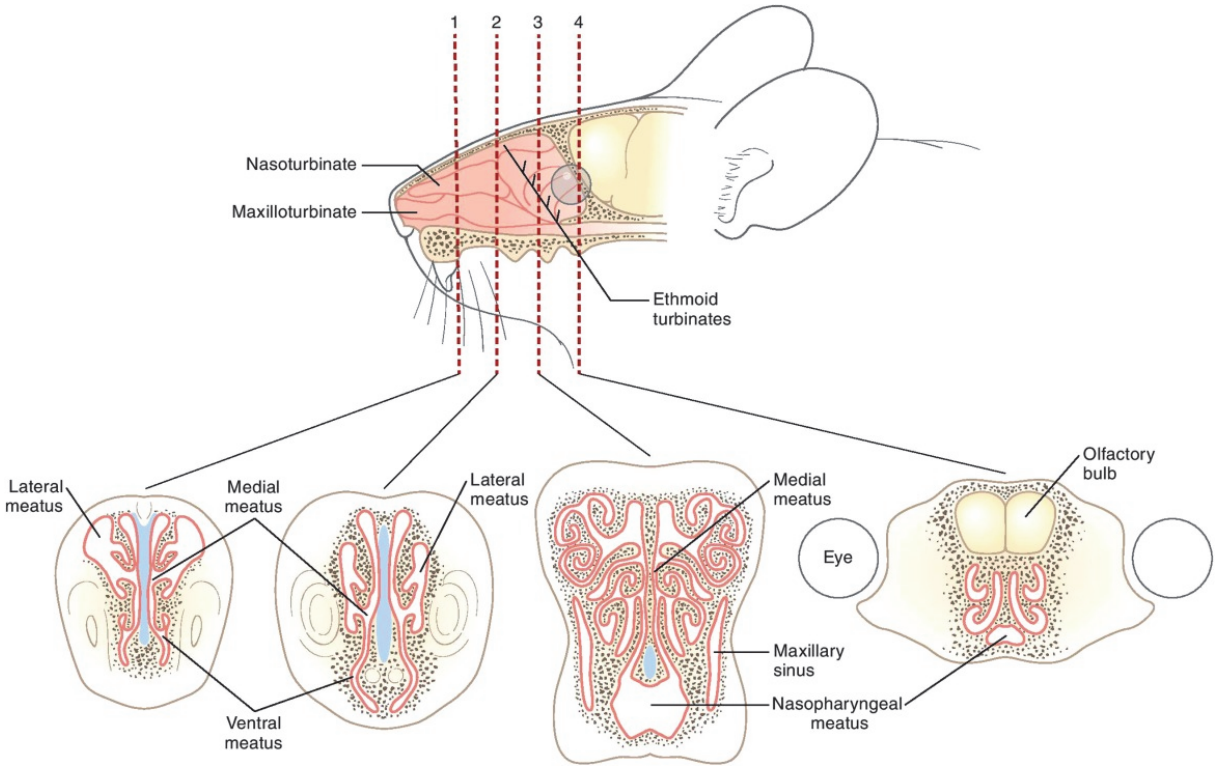

Figure 5.1. Murine nasal and paranasal anatomy. Sagittal section of the skull and corresponding coronal sections (from Al-Sayed et al., 2017)

The objective of our study is to replicate the study by Rae et al. (2006) by improving their experimental approach in several aspects. First, one of our concerns in setting up the protocol was to control the amount and hardness of food ingested by each group of mice. Knowing that food intake is generally higher in colder environments (Serrat et al., 2008), we hypothesize that this variable may influence craniofacial morphology through increased mastication-linked mechanical loading. Second, in addition to the anatomy of the external craniofacial skeleton and the nasal cavity, we also investigated the morphological variation of the nasal turbinates. These structures, covered by either respiratory or olfactory epithelium, are involved in the turbulence of the inspired air in the nasal cavity and are thus closely associated with the

processes of air warming (Inthavong et al., 2007; Doorly et al., 2008). Finally, we were able to quantify volume and shape variation in the craniofacial and nasal anatomy, using both anatomical landmarks and a landmark-free 3D morphometric method (surface registration).

The first objective of this study is to quantify the extent and location of craniofacial morphological variation that is correlated with external temperature and that could be interpreted as a signal for phenotypic plasticity in postnatal development. The second main objective is to quantify the morphological differences between the two groups of cold-reared mice, in order to determine the potential contribution of food (*i.e.*, hardness and quantity) to the phenotypic variation (Rae et al., 2006).

5.2. Methods

Material

The original sample for this study consists of 32 male inbred mice (C57BL/6J, Jackson Laboratory, Bar Harbor, ME), studied under an experimental protocol that received approval from the University of Michigan Institutional Animal Care and Use Committee. At 3 weeks of age, the mice were separated into 4 groups of 8 mice each and these groups were reared under different air temperature and food hardness conditions for 9 weeks. A control group was reared at 22°C and fed with dry pellets; a thermoneutrality1 group was reared at 26°C and fed with dry pellets; a cold-reared group was reared at 10°C and fed with dry pellets. To control for the effects of mastication and food hardness, a second cold-reared group (10°C) was fed pellets that were moistened for five minutes in water. The resulting pellets were softer but maintained their shape. All the pellets had the same composition, whether they were dry or moistened: 13% kcal/fat, 30% kcal/protein, 57% kcal/carbohydrate. The food intake was recorded two to three times a week for each pair of mice. Every three weeks, each mouse was weighed and bone mineral density and body tissue composition were measured via a DEXA system (Lunar PIXImus, GE Lunar Corp). At the age of 12 weeks, the mice were euthanized by CO2 inhalation. Skulls were

[1] Thermoneutrality corresponds to the equilibrium point of heat production and loss, point where the mouse can maintain its body temperature without additional energy expenditure (McDonald, 2009; Neff, 2020)

defleshed, placed in a 34 mm diameter specimen holder and scanned using a microCT system (µCT100, Scanco Medical, Bassersdorf, Switzerland). Scan settings were: voxel size 18 µm, 70 kVp, 114 µA, 0.5 mm AL filter, and integration time 500 ms.

Segmentation

Nasal cavity was segmented manually in the software Avizo v.9.0.1 by one observer (LM). After a resampling of the voxel size to 0.024 x 0.024 x 0.024mm, we defined the limits of the anatomical structure, which is open both anteriorly and posteriorly. We defined the anterior limit of the nasal cavity by the anterior extremity of the nasal bone (superiorly) and the anterior extremity of the premaxillary bone (inferiorly) (Figure 5.2). To define the posterior limit of the nasal cavity, we used a slice passing through three points on the skull: the intersections between frontal, parietal and temporal (bilateral) and a point on the zygomatic bone, between the first and second molar (left side). We then translated this slice to the most posterior part of the ethmoidal labyrinth and used this plane as the posterior limit of the nasal cavity.

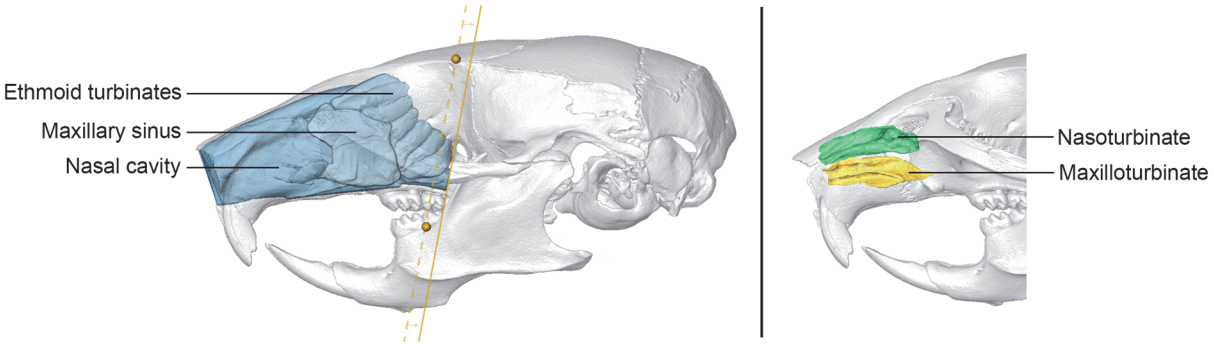

Figure 5.2. Segmentation of the nasal cavity and turbinates. *Left:* nasal cavity (blue) and slice (dashed yellow) that was translated (solid yellow) to set the posterior limit of the nasal cavity. The maxillary sinus and the ethmoidal turbinates were not segmented separately: they are highlighted here for illustration purpose. *Right:* left nasoturbinate (green) and left maxilloturbinate (yellow) in lateral view.

As mice were skeletonized, we could not separate the paranasal sinuses nor the olfactory area from the nasal cavity, as all these anatomical areas are only separated from each other by soft tissues. Rather than setting artificial limits that did not correspond to a biological reality, we decided to include all these soft-tissue-defined structures in our nasal cavity label. Despite the fact that we could not separate them in the segmentation, we include in Figure 5.2 an informative representation of these different anatomical regions, which will be useful when describing the morphology.

The label resulting from the segmentation was used to build a surface mesh by applying the marching cubes algorithm (Lorensen & Cline, 1987) ("Generate Surface" module in Avizo v.9.0.1). The number of triangles was set to 200,000 faces for each specimen's nasal cavity, to reduce computation time while maintaining sufficient morphological accuracy. All surface meshes were then rigidly aligned in position, orientation, and scale using an Iterative Closest Point algorithm ("Align Surface" module in Avizo v.9.0.1). We then exported each simplified, scaled and aligned surface in PLY file format and converted them into VTK files in Paraview v.5.7.0.

The left respiratory turbinates, including the nasoturbinate (superior) and the maxilloturbinate (inferior) (Figure 5.2), were segmented semi-automatically by one observer (YH) using Avizo v.9.0.1.

Craniofacial landmarking

To investigate the morphology of the external shape of the craniofacial skeleton, 57 anatomical landmarks (Table B1) were collected using the software Avizo v.9.0.1 by one observer (YH). The three-dimensional coordinates were analyzed with geometric morphometrics after being superimposed with generalized Procrustes analysis, using the package shapes (Dryden & Mardia, 2016) in R v.4.0.5 (R Core Team, 2021). Centroid sizes (*i.e.*, the square root of the sum of squared distances of each landmark to the centroid) were also computed to be used as a proxy for craniofacial skeleton size.

Surface-based morphological comparison

To study the nasal cavity shape, we used a landmark-free method based on the construction of the mean shape of a sample and its deformation to each individual (Durrleman et al., 2012, 2014; Beaudet et al., 2016). This deformation operates as a diffeomorphism: it is based on a smooth and invertible deformation of the entire 3D surface mesh, and not on a point-to-point correspondence between shapes (Durrleman, 2010). This method increases the statistical power of shape comparison and its precision by allowing the observation of non-homologous features of the studied shapes (Vaillant et al., 2007; Braga et al., 2019; Maréchal et al., 2023). The mean shape computation is based on a set of control points located near the

most variable parts of the structure and on a set of momenta representing the deformation from the global mean shape (GMS) of the sample to each individual. We also calculated the mean shape of each group, based on the mean of the momenta within each group of mice.

Multivariate statistical analyses

To test the effects of temperature and food hardness on craniofacial and nasal morphologies, statistical analyses were carried out and visualized using R v.4.0.5 (R Core Team, 2021) and the packages *RToolsForDeformetrica* (Dumoncel, 2020), *ade4* (Chessel et al., 2004; Dray & Dufour, 2007; Dray et al., 2007; Bougeard & Dray, 2018; Thioulouse et al., 2018), *vegan* (Oksanen et al., 2020), *pairwiseAdonis* (Martinez Arbizu, 2020), *onewaytests* (Dag et al., 2018) and the set of packages *tidyverse* (Wickham et al., 2019).

The craniofacial shape was studied by performing a principal component analysis (PCA) on the Procrustes coordinates of the 57 landmarks. For the nasal cavity, we quantified between-groups shape variation by performing a PCA on the 32 GMS-to-individual deformations. Additionally, PERMANOVAs were used to test for group differences on the 6 first principal components. The effect of size on shape variation (*i.e.*, allometry) was tested via bivariate regressions (Pearson correlation) between the PC scores and the nasal cavity volume.

Skull centroid size, nasal cavity volume and nasal turbinate volume variation were visualized with box-and-whisker plots and statistically explored with location tests. Due to the heteroscedasticity of some variables, we chose to avoid tests assuming equal variance among groups (Zimmerman, 2004) and rather used Welch's F-tests (Welch, 1951). In addition to these differences in variance, we also note the presence in our data of extreme specimens, which can behave as “biological outliers”. To control for the influence of these specimens on our overall signal, we also performed Kruskal-Wallis tests with no p-value adjustment (Rothman, 1990). We systematically performed both tests for each variable. In the *Results* section, we first present the results of the Welch’s F-test, which is more conservative. We then report the results of the Kruskal-Wallis test, which consistently validate the results of the Welch’s F-test, but detect more significantly different pairs of groups in the pairwise comparison. In the text, we specify which pairwise group differences were detected by Welch’s F-test and which were detected by Kruskal-Wallis test.

5.3. Results

The mean statistical data for each group of mice is summarized in Table 5.1. This includes mean body mass and lean mass, mean skull centroid size calculated with the craniofacial landmarks, and mean nasal cavity and nasal turbinates volumes based on the segmentation of these anatomical structures.

Table 5.1. Summary statistics of the raw and scaled measurements (mean (sd))

	Cold-reared	Cold-reared	Control	Thermoneutr.
Number of specimens	8	8	8	8
Temperature	10°C	10°C	22°C	26°C
Food type	Moist pellets	Dry pellets	Dry pellets	Dry pellets
Body mass (g)	30.73 (3.2)	28.24 (1.2)	27.69 (2.0)	26.26 (1.9)
Lean mass (g)	22.62 (1.3)	21.76 (0.8)	21.77 (1.3)	20.54 (1.4)
Fat mass (g)	7.68 (2.1)	6.05 (0.6)	5.46 (1.6)	5.30 (1.2)
% fat	24.7%	21.4%	19.6%	20%
Skull centroid size	52.03 (0.4)	52.08 (0.5)	52.15 (0.4)	51.45 (0.6)
Nasal cavity volume (mm^3)	97.32 (1.4)	90.95 (3.2)	95.07 (3.4)	92.99 (3.4)
Nasoturbinate volume (mm^3)	0.72 (0.1)	0.73 (0.1)	0.70 (0.1)	0.74 (0.2)
Maxilloturbinate volume (mm^3)	0.44 (0.1)	0.41 (0.1)	0.50 (0.1)	0.47 (0.1)

Body mass and lean mass

Cold-reared mice fed with moist food have the largest body masses (30.73 g on average), followed by cold-reared mice fed with dry food (28.24 g on average) (Table 5.1). The mice of the control and thermoneutrality groups are smaller (average body mass of 27.69 g and 26.26 g, respectively). These differences in body mass are consistent with the average food intake of each group of mice (Figure 5.3). Location tests (Table B2) show a statistically significant difference of body mass between the groups (Welch's F-test: F=3.91, p=0.031; Kruskal-Wallis test: χ^2=10.85, p=0.013) (Figure 5.3). The results of the pairwise comparison show a significant difference in body mass between the thermoneutrality group and the group of cold-reared mice fed with moist food (Welch's F-test), between the latter and the control group and between the thermoneutrality group and the group of cold-reared mice fed with dry food (Kruskal-Wallis test).

The lean mass follows the same pattern of variation (Welch's F-test: F=4.98, p=0.013; Kruskal-Wallis test: χ^2=8.18, p=0.042) (Table B3) although we observe a greater heterogeneity of

variance between the groups. The thermoneutrality group is statistically different from both the group of cold-reared mice fed with moist food (Welch's F-test) and the group of cold-reared mice fed with dry food (Kruskal-Wallis test).

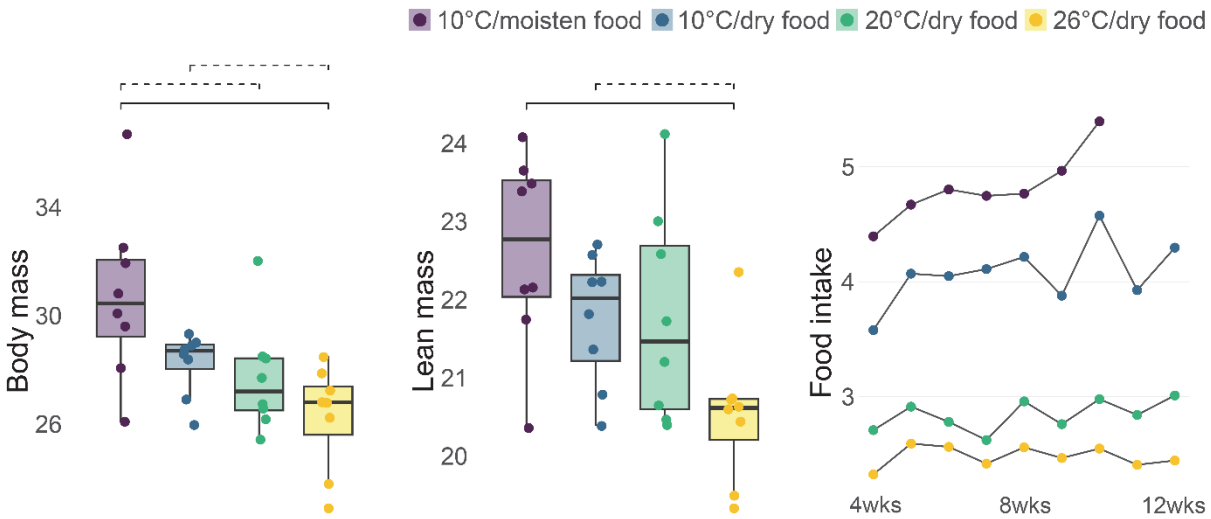

Figure 5.3. Body mass, lean mass and average food intake per group. Brackets represent significant differences ($p<0.05$) between groups in pairwise comparisons (both Welch's F-test and Kruskal-Wallis test: solid lines; Kruskal-Wallis test: dashed lines).

External craniofacial morphology

The PCA based on the 57 landmarks measured on the craniofacial skeleton shows no clear separation between groups (Figure B1). A PERMANOVA analysis did not support the hypothesis of a significant variation in shape between the 4 groups ($F=1.19$, $p=0.136$). Additionally, Welch's F-test results highlight no statistically significant difference in skull centroid size between groups ($F=2.20$, $p=0.129$) (Table B4).

Nasal cavity morphology

Shape variation

PCA analysis of the nasal cavity shape (Figure 5.4) shows a clear distinction between groups. This observation is confirmed by the results of the PERMANOVA testing for group differences ($F=2.61$, $p<0.001$) (Table 5.2), which shows that groups are all morphologically different from one another, except for the control and thermoneutrality groups.

Table 5.2. Pairwise morphological distances between groups resulting from the pairwise PERMANOVAs performed on all the principal components of the morphospace. The results are considered significant (*) when p<0.05.

			F	p	
PERMANOVA (testing for group differences)			2.606	<0.001	*
Pairwise comparison	Cold (dry food)	Cold (moist food)	4.133	0.002	*
	Cold (dry food)	Control	2.913	0.002	*
	Cold (dry food)	Thermoneutrality	2.901	0.002	*
	Cold (moist food)	Thermoneutrality	2.282	0.002	*
	Cold (moist food)	Control	2.278	0.002	*
	Control	Thermoneutrality	1.154	0.226	

On PC1 (15.58%), the cold-reared group fed with dry food is distributed in the negative values, almost strictly separated from the three other groups which are predominantly located in the positive values. These observations are confirmed by the pairwise PERMANOVA testing for shape differences between groups (F=20.45, p<0.001), which shows that the cold-reared group fed with dry food is significantly different from the other three groups (Table B5). The shape associated with negative values is overall relatively more elongated in the antero-posterior axis, especially in the area anterior to the maxillary sinus. The overall shape of the nasal cavity is narrower (in the medio-lateral plane) and lower (supero-inferiorly). The upper part of the nasal cavity appears flatter than in the positive values, but is also lower than the ethmoid turbinates, while these two anatomical areas are aligned with each other in the positive values of the PC. The maxillary sinus is square-shaped in the negative values and bean-shaped in the positive values. The ethmoid turbinates are more triangular in the negative values, while more rounded in the positive values. Proportionally, the ethmoid turbinates area is larger than the maxillary sinus area in the negative values, and conversely in the positive values.

PC2 (11.14%) separates the cold-reared group fed with moist food, mainly in the negative values, and the thermoneutrality group, predominantly in the positive values. The PERMANOVA testing for shape differences between groups (F=4.33, p=0.017) confirms the morphological differences between these two groups (Table B5). Overall, the shape associated with negative values on PC2 is longer, slightly lower, and narrower than the shape in the positive values. However, in the negative values on PC2, the anterior area of the nasal cavity is less elongated, higher and narrower than what we observe, for instance, on PC1. Furthermore, in the positive values on PC2, the upper part of the ethmoid turbinates area is more prominent than

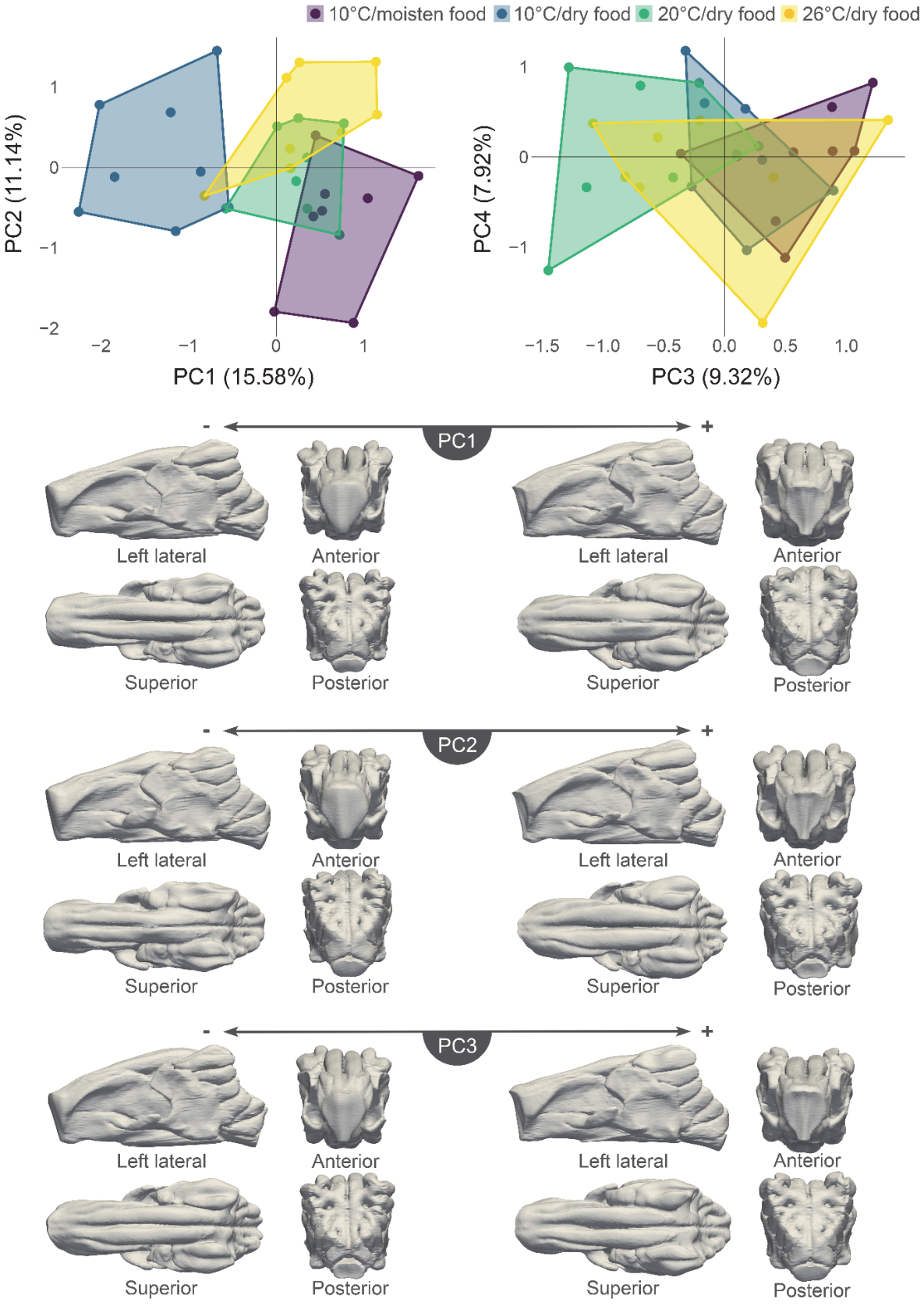

Figure 5.4. Principal Component Analysis (PCA) of the nasal cavity shape comparison between the 4 groups of mice. The surfaces represent shape changes associated with PC1, PC2 and PC3, with 4x magnification of the real shape variation.

on PC1 and the maxillary sinus is more supero-inferiorly elongated. Proportionally, the maxillary sinus area is even smaller than the ethmoid turbinates area in the positive values on PC2.

On PC3 (9.32%), the control group is distributed mainly in the negative values, while the two cold-reared groups are mostly found in the positive values. The PERMANOVA testing for shape differences between groups ($F=5.97$, $p=0.005$) corroborates these morphological differences (Table B5). The shape associated with positive values on PC3 is wider, longer and drastically lower than the shape in the negative values. In the positive values, the upper part of the nasal cavity is very flat, while rounded in the negative values. The maxillary sinus is square-shaped and more elongated in the antero-posterior axis in the positive values, while bean-shaped and more elongated in the supero-inferior axis in the negative values. Posteriorly, the ethmoid turbinates are more triangular in the positive values, while rounded in the negative values.

All the shape changes we observe on the first three principal components can, to a lesser degree since the variation is very subtle, be observed by comparing the mean shapes of the different groups (Figure B2). Overall, the mean shape of the cold-reared group fed with moist food is shorter, wider and higher than the mean shape of the cold-reared group fed with dry food. This explains why the cold-reared group fed with moist food is distributed near the thermoneutrality and control groups on PC1, as they are also higher and wider than the cold-reared group fed with dry food.

While there is no allometric effect when considering all principal components, *i.e.*, 100% of variation ($R^2=0.091$, $p=0.093$), we record a significant effect of allometry on PC1 ($R^2=0.242$, $p=0.004$) and on PC2 ($R^2=0.338$, $p<0.001$). No effect of allometry is recorded on PC3.

As we did not symmetrize the data, we can observe some asymmetry in the shapes associated with extreme negative and positive values on the three first PCs. On PC1, it is characterized by a shape that is higher on the left side and lower on the right side in the negative values, and inversely in the positive values. On PC2, the asymmetry is less strong and follows a reverse pattern than PC1. PC3 shows an asymmetry pattern similar but stronger than on PC1, the left side being substantially higher on the shape associated with negative values. The asymmetric signal is however minor compared to the overall shape variation of the nasal cavity.

The description of the shape changes for each PC therefore tends to overlook these asymmetries, which are not our main focus.

Volume variation

Mean nasal cavity volume values (Table 5.1) show that the group of cold-reared mice fed with moist food has on average the largest nasal cavities, while the group of cold-reared mice fed with dry food have the smallest ones. We record statistically significant group differences in nasal cavity volume (Welch's F-test: $F=10.03$, $p<0.001$; Kruskal-Wallis test: $\chi2=15.20$, $p=0.001$) (Figure 5.5). The pairwise comparisons show that the cold-reared group fed with moist food is different than the cold-reared group fed with dry food and the thermoneutrality group (Welch's F-test) and that the control group is different than the two cold-reared groups (Kruskal-Wallis test) (Table B6).

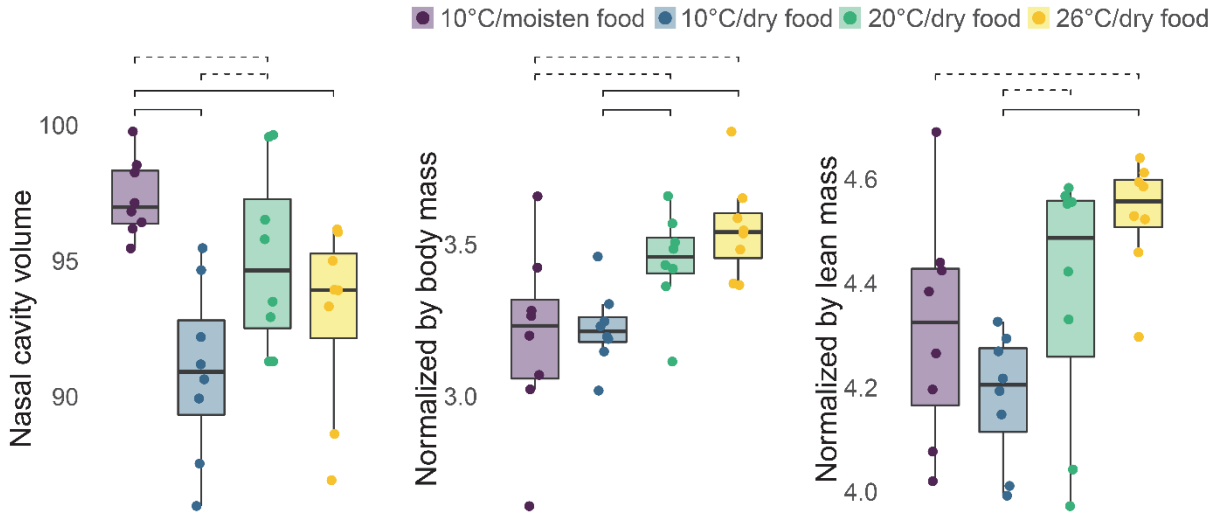

Figure 5.5. Volume of the nasal cavity per group (1) raw (2) normalized by body mass and (3) normalized by lean mass. Brackets represent significant differences ($p<0.05$) between groups in pairwise comparisons (both Welch's F-test and Kruskal-Wallis test: solid lines; Kruskal-Wallis test: dashed lines).

Knowing that cold-reared mice fed with moist food have larger mean body mass and mean lean mass and that both factors have an effect on nasal cavity volume (Table 5.3), we normalized the nasal cavity volume by body mass and by lean mass. At equivalent body mass, the two cold-reared groups are not statistically different (Table B7), neither are they at equivalent lean mass (Table B8). They are, however, both different from the two other groups when nasal cavity volume is normalized by body mass (Kruskal-Wallis test). When normalized

by lean mass, the nasal cavity volume of the cold-reared group fed with dry food is significantly different from the thermoneutrality and control groups. The cold-reared group fed with moist food is then only different from the thermoneutrality group.

Table 5.3. PERMANOVAs testing the factors influencing nasal cavity volume. The results are considered significant (*) when p<0.05.

	F	p	
Body mass effect on nasal cavity volume	16.756	<0.001	*
Lean mass effect on nasal cavity volume	13.187	0.001	*

To verify the potential effect of body mass and lean mass differences on nasal cavity shape, we performed a multivariate regression between the nasal cavity shape and (1) the residuals of a linear regression of nasal cavity volume on body mass and (2) the residuals of a linear regression of nasal cavity volume on lean mass. This analysis demonstrated that there is no significant correlation between nasal cavity shape and the share of the nasal cavity volume variable that is not explained by body mass variation (R^2=0.06, p=0.098) nor with the share of the nasal cavity volume variable that is not explained by lean mass variation (R^2=0.05, p=0.11).

Nasal turbinates morphology

Statistical analysis of the nasoturbinate and the maxilloturbinate volumes demonstrated no significant difference between the four groups of mice (Table B9 and Table B10). When normalized by the nasal cavity volume to control for scale effect, the results remain non-significant for the nasoturbinate (Table B12). Concerning the normalized maxilloturbinate volume (Figure 5.6), the Welch's F-test is not significant but the Kruskal-Wallis test is (χ2=7.87, p=0.049) (Table B11). Pairwise comparison shows that the cold-reared group fed with dry food is statistically different from the thermoneutrality group and the other cold-reared group, which are both characterized by smaller normalized maxiloturbinate volumes.

We record no statistically significant between-group differences for the maxilloturbinate surface area (Table B13), nor for the nasoturbinate surface area (Table B14). We performed other tests on the ratio of the surface area of the turbinates to the volume of the nasal cavity, which gave significant results both for the maxilloturbinate (Welch's F-test: F=6.38, p=0.006; Kruskal-Wallis test: χ2=9.87, p=0.019) (Table B15) and for the nasoturbinate (Welch's F-test:

F=10.81, p=0<0.001; Kruskal-Wallis test: χ2=12.41, p=0.006) (Table B16). Overall, the ratio of the surface area of the turbinates to the volume of the nasal cavity for both respiratory turbinates of the cold-reared group fed with moist food is lower than the three other groups (Figure 5.6). Pairwise comparison for the maxilloturbinate shows that the cold-reared group fed with moist food is significantly different from the other cold-reared group (Welch's F-test) and from the two other groups (Kruskal-Wallis test). Regarding the nasoturbinate, the cold-reared group fed with moist food is significantly different from the thermoneutrality group (Welch's F-test) and from the two other groups (Kruskal-Wallis test).

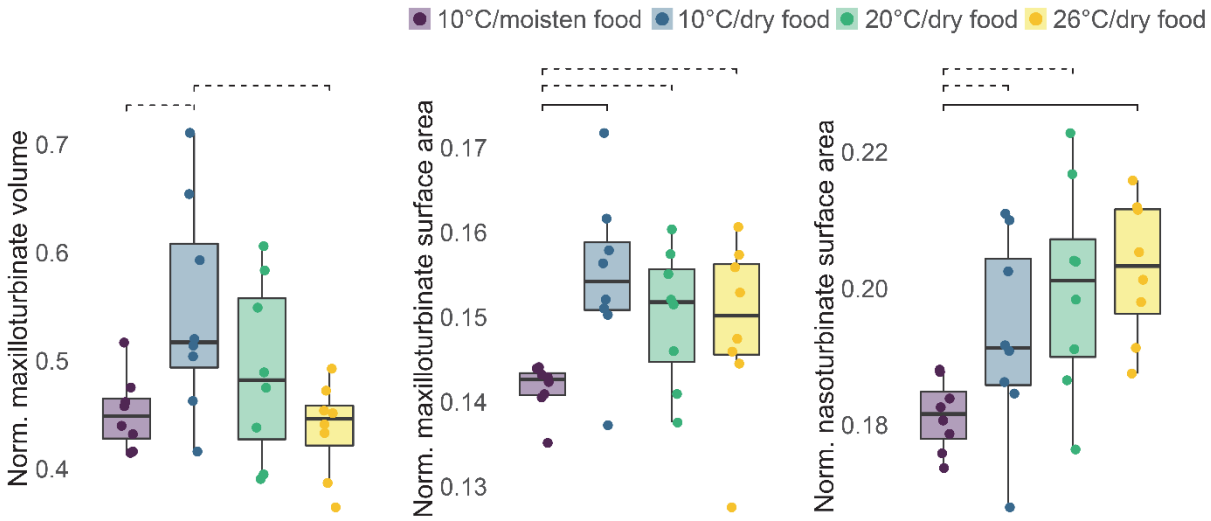

Figure 5.6. Normalized volume and surface area of the respiratory turbinates per group (normalization by nasal cavity volume). Brackets represent significant differences (p<0.05) between groups in pairwise comparisons (both Welch's F-test and Kruskal-Wallis test: solid lines; Kruskal-Wallis test: dashed lines).

5.4. Discussion

Food intake and mass in cold-reared mice

Both cold-reared groups consumed more food than the thermoneutrality and control groups, which was expected given long acknowledged higher energetic demands to maintain homeothermy in the cold (Campbell, 1945; Barnett, 1965; Serrat et al., 2008). As a consequence, the two groups of cold-reared mice have larger body masses and overall, a higher fat mass. This is especially true for the group fed with moist food, which is significantly different in fat mass from the 3 other groups (Kruskal-Wallis test). But these groups are not only fatter: they also have higher lean mass than the thermoneutrality group.

Moreover, we observe differences in food intake within the two cold-reared groups: the group fed with moist food ate more than the other cold-reared group. This could be explained by the increase in food waste due to the greater friability of pellets. But this group of mice also has greater mean body mass, lean mass and fat mass, which excludes the hypothesis that this pattern reflects only food waste. One possible explanation for these differences in food consumption could be that this group of mice might need to masticate more, in order to wear their teeth equally to mice fed with dry food. Or maybe another mechanism is at play: moist food may be more appetizing and/or easier to eat, which could lead the mice to consume more food. The fact that the cold-reared group fed with moist food has a significantly higher mean fat rate (24.7% fat) than the other cold-reared group (21.4% fat) may reinforce the hypothesis that the former ate more than than was necessary to fulfill their energetic needs, which could point towards another mechanism than the maintenance of homeothermy whether related to eating behavior or to a biomechanical purpose.

Overall craniofacial variation

We observe no difference between the groups in craniofacial morphology, either in terms of shape or size. Based on our sample, we can conclude that neither temperature nor food hardness have an effect on the overall shape or size of the craniofacial skeleton. These results are surprising given that they contradict previous observations on Sprague-Dawley rats (Rae et al., 2006), which highlighted significant differences in craniofacial size and shape. The morphology of the cold-reared rats in the study by Rae and colleagues is characterized by an anterior displacement of the maxillozygomatic suture, a posterioinferior positioning of the infraorbital fissure, and a shift of the entire nasal-premaxillary complex in a relatively more antero-superior position. The authors conclude that these results are the consequence of the variation in ambient temperature. The differences between these results and our own may be explained by several factors. First, the cold-reared group in the Rae et al. study was reared at 5°C, which may indicate a response to more extreme temperatures than we used in our study. Second, the species difference may also imply a different plastic response, perhaps more pronounced in Sprague-Dawley rats than in C57BL/6J inbred mice. This could for example be due a size effect, knowing that male rats are over 10x the body mass of mice (400-500g vs. 30g at 12 weeks of age). Finally, the sample used in the Rae et al. study originally comes from an experiment (Steegmann & Platner, 1968) that did not control for food intake. Both the cold-

reared rats (5°C) and the control group (22°C) were fed *ad libitum*. We do not have information on the amount of food ingested by each group, but we can expect, based on our own observations, that the cold-reared group ate more, and thus masticated more than the other group. We can hypothesize that, in rats, increased masticatory forces may be more likely to affect the overall shape of the craniofacial skeleton.

The effects of food hardness on nasal cavity shape

Regarding nasal cavity shape, all groups are morphologically different from each other, except for the pair of control and thermoneutrality groups. We can summarize the main shape variation we observed as follows: the mean nasal cavity shape of the cold-reared group fed with moist food is shorter, wider and higher than the cold-reared group fed with dry food. The mean nasal cavity shapes of the thermoneutrality and control groups are higher and shorter than the two cold-reared groups. They are wider than the cold-reared group fed with dry food but narrower than the cold-reared group fed with moist food. More specifically, we observe an elongation of the anterior part of the nasal cavity in the cold-reared groups, which is accentuated in the cold-reared group fed with dry food. As we explained in the Methods section, we were not able to segment and then measure precisely the volume of the maxillary sinus and the ethmoid turbinates (olfactory) region. However, we can observe on our shape differences that relatively, the olfactory area of the cold-reared group fed with dry food seems more developed than the maxillary sinus area, and conversely for the other groups.

How can we explain this shape variation? First, we can point out that the cold-reared group fed with dry food is probably the group that masticated the most. Indeed, the mice of this group ate more food than the mice of the control and thermoneutrality groups, which were also fed with dry pellets. Moreover, they ate harder food than the other cold-reared group, which could imply that the required masticatory forces were higher. However, we have to keep in mind that the amount of food ingested by the cold-reared group fed with moist pellets is higher, which complicates our perception of the masticatory loads in these two groups of mice. The anterior loading applied during gnawing with the incisors might be one explanation of the lengthening of the shape of the nasal cavity. However, the results of a study by Myers et al. (1996) on prairie deer mice, rather point towards an anterior shift of the incisors of animals fed a soft diet.

Based on our sample, we can conclude that the shape variation we observe on the nasal cavity is mainly driven by masticatory forces. We obtain similar results to previous studies when we consider only the groups of mice fed with dry food, which could then be interpreted as a response to temperature. Indeed, the PC1 of our shape analysis clearly shows that the cold-reared group fed with dry food is different from the control and thermoneutrality groups. However, adding the cold-reared group fed with moist food to the equation changes our results completely. This group does not tend to cluster with the other cold-reared group but rather with the control and thermoneutrality groups. If there is an adaptative response to temperature, it is therefore completely blurred by the effect of the masticatory forces related to the quantity and consistency of the food ingested.

Temperature-related phenotypic plasticity and craniofacial integration

The volume of the nasal cavity might be one variable that, in our sample, shows a clear plastic response to temperature. Cold-reared mice fed with moist food have the largest mean nasal cavities and cold-reared mice fed with dry food have the smallest mean nasal cavities. But at equal body mass and at equivalent lean mass, the two cold-reared groups both have significantly smaller nasal cavity volumes thant the two other groups. In their study, Rae et al. (2006) obtained the same result, with cold-reared rats displaying significantly smaller nasal cavity volume for a same skull size. Interestingly, this variation in nasal cavity volume is not correlated with a variation of the size of the skull.

We have no clear signal of nasoturbinate or maxilloturbinate volume variation between groups, even when they are normalized by the nasal cavity volume to control for scale effect. We do not record any between-group differences in either maxilloturbinate or nasoturbinate surface area. However, when we normalize the turbinates surface area by nasal cavity volume, we obtain significant differences between groups. For the cold-reared group fed with moist food, the surface area of both respiratory turbinates normalized by nasal cavity volume is lower than the three other groups. This means that for a given nasal cavity size, the cold-reared group fed with moist food display respiratory turbinates that are the same size as the other groups, but have a less complex shape. In terms of thermoregulation processes, a more complex shape of the turbinates allows more air turbulence and, therefore, a better warming of the inspired air (Inthavong et al., 2007; Na et al., 2012), which would typically be required in a cold environment.

These findings perhaps highlight the part of the shape complexity of the respiratory turbinates that is not determined by thermoregulation purposes, but by the overall integration of the craniofacial skeleton.

Conclusions and perspectives

As previous studies on experimental samples showed, we observed several morphological differences in the nasal anatomy of mice reared at different temperatures. Cold-reared mice stand out from control and thermoneutrality groups in several ways, the most noticeable being the volume variation of the nasal cavity, with cold-reared mice displaying significantly smaller nasal cavities than the two other groups. We emphasize that these results demonstrate a clear effect of phenotypic plasticity in response to temperature. However, we also note that the pattern of morphological variation, and notably the shape of the nasal cavity, is also depending on food consistency. Several factors related to feeding behavior and masticatory forces might therefore also be involved in the morphological variation that has previously been attributed to a response to temperature. One prospect that could be explored in future studies would be to conduct the same kind of study but also trying to quantify the masticatory load for each of these groups, for example with Finite Element Analysis (FEA).

Synthèse

Nous évaluons ici les rôles potentiels de la plasticité phénotypique en lien avec la température ainsi que de la consistance de la nourriture sur la variation cranio-faciale de 4 groupes de souris consanguines élevées à des températures différentes. Grâce à la morphométrie et à une analyse statistique des volumes et des surfaces, nous analysons la morphologie de leur crâne, cavité nasale et turbines nasales.

Nos résultats démontrent un effet de plasticité phénotypique en réponse à la température : le volume de la cavité nasale des deux groupes de souris élevées au froid est significativement plus petit que celui des groupes contrôle et thermoneutralité. Nous soulignons que la dureté de la nourriture a un effet majeur sur la conformation de la cavité nasale, ce qui brouille sensiblement le signal d'une réponse potentielle à la température. Cela peut être lié à une variation des forces masticatrices, due à la fois à la consistance de la nourriture et à sa quantité. En effet, les souris élevées au froid ont consommé plus de nourriture, en particulier lorsque la nourriture est ramollie (possiblement pour assurer l'usure dentaire). Enfin, nous n'observons aucune différence significative pour la morphologie externe du squelette cranio-facial.

Summary

Here, we try to evaluate the potential role of temperature-related phenotypic plasticity and food hardness on the craniofacial variation of inbred mice reared under different temperature conditions. We study the morphology of the skull, the nasal cavity and the respiratory turbinates of 4 groups of mice, using geometric morphometrics, surface registration and statistical analysis of volumes and surface areas.

Our results demonstrate an effect of developmental plasticity in response to temperature: the nasal cavity volume of the two groups of cold-reared mice is significantly smaller than the control and thermoneutrality groups. We also highlight that food hardness has a major effect on the shape of the nasal cavity, critically blurring the signal of a potential response to temperature. These observations can be linked to differences in masticatory forces, due to both food hardness and food intake. Indeed, we observe a higher food intake in the two groups of cold-reared mice. In the group of cold-reared mice fed with moist food, the intake is even higher, which may be related to tooth wearing considerations. Finally, no significant between-group difference is observed in the morphology of the overall craniofacial skeleton.

• Chapter 6 •

OVERVIEW AND PERSPECTIVES

SYNTHÈSE ET PERSPECTIVES

« When we try to pick out anything by itself, we find it hitched to everything else in the Universe »

— J. Muir

The main objective of this work was to quantify the morphological variation of the internal nasal anatomy, in order to provide new reflections on the evolutionary mechanisms likely to explain, at least partially, this morphological variation. The focal point around which we have made our thinking revolve is the climatic adaptation of this anatomical region, which has been the subject of heated debate for several decades. The research question to which this work aims to contribute can be stated quite simply: how do specific nasal phenotypes emerge and develop during human evolution? By which evolutionary paths and detours have we reached the nasal morphology of current humans? If formulating the question is simple, answering it is much more complex, given that the only available information to answer it are: 1) the results of this evolution, *i.e.*, the extant human phenotypes, and 2) some precious milestones, *i.e.*, the fossil record, which are however relatively few compared to the time scale of the evolution of a species, not to mention the very poor preservation of this anatomical region in fossils.

But before even trying to answer these questions, it is essential to quantify this variation. For reasons already mentioned in this manuscript, we are convinced that, in order to have a complete picture, the upper airway must be studied as a whole, considering all its components, bone and mucosa, and trying to understand their interactions. From this point of view, a considerable amount of work has already been done by many authors over the years and our work only constitutes a humble, yet hopefully original, interesting and useful, contribution.

Through this step of variation quantification, we hold several pieces of our large evolutionary puzzle. The final goal is to try to put these pieces together, to understand how they relate to each other. Some will remain isolated, unexplained, while others will begin to constitute a portion of the big picture. Through them, we will attempt to understand the mechanisms and the role of the different factors at the origin of the quantified phenotypic variation: which traits are inherited? Which are related to phenotypic plasticity? What role did climate, masticatory forces, covariation with other craniofacial structures or any other factor of variation, play in this phenotypic variation? In this final chapter, we present some thoughts on all these questions, based on the data provided by previous works and our own. Finally, we suggest some research perspectives to continue adding new pieces to this vast and thrilling puzzle.

6.1. The internal nasal morphology: patterns of variation

In the study of nasal morphology, three closely interconnected features of the anatomical structures are commonly studied: their volume, their surface area-to-volume ratio (SA/V), and their shape. In this section, we will briefly summarize what is known about the variation of the nasal cavity and the nasal airway for each of these characteristics in extant human populations. This will allow us to discuss, in the following section, features pointing towards a functional adaptation to climate and/or other variation factors.

Nasal volume variation

Nasal cavity volume has been shown to be larger in human groups living in colder climates (Butaric & Klocke, 2018; Evteev & Grosheva, 2019). Furthermore, Evteev and Grosheva (2019) demonstrated that across populations of Asian ancestry inhabiting different climatic environments, there was a strong negative and highly significant association between nasal cavity volume and mean temperature of the coldest month. This is consistent with the predictions of Shea (1977) arguing that, for purposes of respiratory needs, the internal nasal structures and specifically the inferior meatus and turbinate, should be larger in individuals inhabiting colder climates. This hypothesis is based on the assumption that a larger nasal cavity volume increases the surface area where the respiratory mucous membrane may extend, which therefore implies a better humidification and warming of the inspired air.

Regarding the nasal airway, the results of our study do not show significant variation in volume between our five studied populations. These results confirm those of Yokley (2009), who similarly observed no variation in volume between two US populations (one European-American group and one African-American group) for the congested nasal cavity, *i.e.*, the nasal airway. These results are surprising, as we would have expected to observe smaller nasal airways in the populations living in colder regions (e.g. the Russian sample). This reduced volume would indeed increase the efficiency of air conditioning: an acoustic rhinometry study (Lindemann et al., 2009) found that a healthy but relatively less voluminous airway has a more efficient air conditioning function than a more voluminous nasal airway.

Nasal SA/V ratio variation

Regarding the nasal cavity, the relation between surface-area-to-volume ratio (SA/V) and climatic adaptation was first suggested by Franciscus and Long (1991). The authors hypothesized that individuals from populations that evolved in cold and/or dry climates would have a greater SA/V ratio than individuals from warmer and more humid environments, as this would allow for more efficient heat and moisture exchange between the inspired air and the nasal mucosa during respiration. This hypothesis was then confirmed by Yokley (2009), who demonstrated that the European Americans group of his study had a greater SA/V ratio than the African Americans group. Evteev and Grosheva (2019) also demonstrated that all the north Asian groups they studied displayed increased SA/V compared to east Asians and Aleuts from temperate climates.

Concerning the nasal airway, our study did not allow us to measure a significant difference in SA/V ratio between our five populations. This result echoes what was described by Yokley (2009) who recorded no significant differences between groups of European Americans and African Americans for the congested nasal cavity, *i.e.*, the functional nasal airway.

Nasal shape variation

Variation in nasal cavity shape in relation with climate has long been demonstrated: several studies have showed that populations living in colder climates display narrower, longer and higher nasal cavities (e.g. Carey & Steegmann, 1981; Yokley, 2009; Fukase et al., 2016; Maddux et al., 2016; Butaric & Klocke, 2018). Similarly to volume and SA/V ratio variation, shape variation has been explained in the sense that narrower nasal passages facilitate heat and moisture exchange by increasing the SA/V ratio, while longer nasal passages influence the overall amount of mucosa and occurrence time of the airflow in the nasal cavity (Inthavong et al., 2007; Noback et al., 2011). However, the shape variation of the nasal cavity might not be only explainable by climatic factors. In their study, Eevtev and Grosheva (2019) showed that the correlation of shape variation with climatic variables is moderate, and even loses statistical significance when controlling for genetic distances. In addition, shape differences between groups inhabiting cold climates may be variable, such as, in the latter study, Eskimo-Aleutian groups versus other Siberian groups. The authors suggest two explanations for these shape

variation: a different population history implying some selective-neutral factors, or an adaptation to coastal Arctic environments versus inland Siberian climate requiring different morphological features.

Regarding the nasal airway, our results show a shape variation between modern populations (Maréchal et al., 2023). At first glance, some general observations in terms of width, length, and height are consistent with what is observed in the nasal cavity (e.g.: the Cambodian sample has a shorter and wider nasal airway, which is consistent with what was previously described as a warm-adapted phenotype). However, the shape variation we observe clearly reflects genetic proximity between the populations rather than eco-geographic patterns (see aso Hubbe et al., 2009).

6.2. Beyond morphology: evolutionary mechanisms

The most striking aspect of this brief overview is that the nasal cavity shows a quite clear inter-population variation both in volume, SA/V ratio and shape, while the nasal airway only shows a modest, yet significant, inter-population variation in shape. This observation should come with no real surprise, knowing that the strict co-variation between these two anatomical structures as never been accurately demonstrated. A study by Heuzé (2019) actually reported a low correlation between these two structures ($R^2 = 0.1408$, $p = 0.0349$), which is quite consistent with the fact that the variation in volume and SA/V ratio of the nasal cavity is not associated with a variation in volume and SA/V ratio of the nasal airway. However, it is still unexpected to find such results despite the genetic, geographical and climatic differences of the five human groups we studied.

One asset we can use to discuss the mechanisms behind the variation of these morphological features is the results obtained on the mice experimental sample. In order to transpose these results to humans, we have to keep in mind that Hallgrímsson et al. (2004) have questioned the inferences from how developmental perturbations produce phenotypic effects in model organisms to how the same perturbations would affect craniofacial morphology in primates and, by extension, in humans. Among their results, they showed that the effect of both breeding structure and environmental conditions on the configuration of phenotypic variation is a potential confounding factor in the comparisons between a variation that would be

observed within an inbred mouse model and a naturally occurring variation in primates. We will therefore be extremely cautious in concluding on these results.

First, how can we try to explain the mechanisms behind the variation in the volume of the nasal cavity? It seems that integration plays an important role in this variation, as some studies demonstrated that the volume of the nasal cavity co-varied with the overall size of the craniofacial skeleton (Butaric et al., 2010; Evteev & Grosheva, 2019), which seems to suggest a rather structural, *i.e.*, not adaptive, explanation for volume variation. But this volume variation has also been linked to climatic factors (Evteev & Grosheva, 2019; Kelly et al., 2023) and could imply a process of natural selection for beneficial phenotypes during the evolution of these populations (see also Yokley 2009). Our results also highlight the possibility that part of this variation may be explained by a mechanism of phenotypic – or developmental – plasticity when subject to a strong environmental constraint, in this case environmental temperature. In our murine sample, the signal of variation, *i.e.*, smaller nasal cavities in cold-reared mice, goes in the opposite direction as the signal observed in primates, including humans (see also Rae et al. 2006). This phenomenon could be explained by the aforementioned differences in patterns of morphological integration and modularity between rodents and primates and naturally raises the question of the applicability of this result to our reflections on human variation. But the very fact that a plastic response has been observed for the volume of the nasal cavity is a novel and valuable information. We can also imagine that this plastic response might be achieved through one or several temperature-sensitive developmental pathways that we discussed in chapter 2, e.g. by directly altering the activity of preosteoblast cells, osteoblasts or osteoclasts, or indirectly, by inducing proteins or hormones involved in bone cells activity.

We believe that, as for all the mechanisms involved in the variation and evolution of human phenotypes, these factors are not mutually exclusive and probably interact throughout evolution in ways that are beyond our current knowledge. If the hypothesis of a phenotypic plasticity is confirmed, we can imagine that this mechanism played a role at some point for some populations, creating beneficial phenotypes that would then be selected for their environmental fitness. Moreover, these phenotypic responses might be continuous and follow temperature variation, while others might be expressed when a threshold is reached, which means that perhaps the response would be different according to the human groups and the time scale we are considering. All these factors probably also result in the shape of the nasal

cavity. One can imagine that integration and natural selection have also influenced this shape. Finally, we did not record a clear temperature-driven plastic response for the shape of the nasal cavity, as the biomechanical stress related to mastication was the factor that mainly drove the signal on the PCA, perhaps because it is the “dominant” stress in our sample. This does not imply, however, that phenotypic plasticity is not influencing nasal cavity shape and we expect further studies will attempt to address that question.

Regarding the volume of the nasal airway, we argue that it is influenced by respiratory energetics related to a size/dimorphic effect, but also by other biological phenomena such as the age-related shrinkage of the nasal mucosa. Unfortunately, the temperature influence on the nasal mucosa morphology and the corresponding nasal airway shape on an intra-population scale has been poorly explored in our study, as we did not have the appropriate sample to explore that path. This piece of the puzzle is, to our knowledge, still missing, and we believe that this aspect also constitutes a promising avenue of research. As was previously mentioned, nasal airway volume does not vary between geographic groups and we can make two assumptions to try to explain this result. Either the climates in which the individuals of our samples were not extreme enough and different enough to generate a clear response. The scanning environment might also have affected this signal. The second hypothesis is that climates are sufficiently different in our sample to produce a mucosal response, but the nasal airway volume is not the main proxy to look at to understand this response to temperature. Instead, one would rather look at how this volume is distributed, *i.e.*, the shape of the nasal airway. The SA/V ratio is closely related, as it represents the complexity of the surface area of a structure, which more or less comes down to measuring the complexity of its shape.

In either case, the shape of the nasal airway probably varies to some extent via integration with craniofacial anatomy and is obviously constrained by the shape of the nasal cavity. The first hypothesis we mentioned for the volume of the nasal airway does not involve a climatic response to temperature. In this scenario, what other factors could drive the variation? We can hypothesize that, in addition to integration with the craniofacial skeleton, and in the absence of major morphological or functional constraints as it is the case for our murine sample, for example, the shape variation would also be likely to be influenced by various "secondary" factors (e.g. temperature oscillation within a day, diet, air pollution…). It is known that in the absence of major functional constraint, the shape of the different cranial parts of modern individuals can indeed be relatively modular (Eyquem et al., 2019). This would imply

that the cranial structures of modern individuals have a freedom in variation, under the obvious condition of respecting basic requirements such as the space provided for the brain, air inspiration, swallowing, or for the eyeballs. This also implies that some factors may affect one group of individuals, and other factors, other individuals. Finally, our second hypothesis put forward a response of the airway to temperature that would not be expressed in the volume of the nasal airway but rather in its shape. Unfortunately, we cannot test this hypothesis with our data since it brings us back to our lack of knowledge on the temperature-related reactivity of the nasal mucosa, which still remains poorly defined.

6.3. Research prospects

Research has demonstrated that climate has directly influenced the morphological, physiological, and genetic variation of the human species. This variation can occur through a process of acclimatization, both in the short and long term, and through the process of natural selection. But there are still many unknown factors in the study of climatic adaptation in humans. For example, while morphological differences between populations have been identified, the mechanisms at the origin of these potentially functional traits need to be explored, as they are yet not properly understood. In this perspective, we also have to keep in mind the cultural component of climatic adaptation, formulated by Steegmann (1979) as follows: “Do thermally protective behaviors make special biological adaptations unnecessary?”. There is still much to learn about nasal morphology and how it can be related to climatic factors, although many studies are still in progress (e.g. among the most recent publications: Campbell et al. 2022; Laitman & Smith 2022; Shah & Frank-Ito 2022; Kelly et al. 2023). At the conclusion of this work, we suggest some promising avenues that should, in our opinion, be explored in the future to stimulate the discussions on these questions.

On several occasions, we have mentioned the reactivity of the nasal mucosa to temperature, as we believe that it is an important and still poorly understood element of nasal morphology. We need to know how rapidly and to what extent the nasal mucosa is likely to react to external temperature. Is there a temperature threshold that the nasal mucosa is able to withstand, beyond which its ability to warm and humidify the air is affected? We believe that these questions are equally important in order to validate our observations of the nasal airway, but also to better understand how the various tissues of the nasal region react, and ultimately potentially adapt, to climatic variations. We suggest that the best way to answer these

questions would be to conduct an experimental study on modern humans of known age, sex, health conditions and placed under different temperature conditions, so that we can observe the reactivity of their nasal mucosa. This could be achieved by a volume quantification by acoustic rhinometry (Kiemle Trindade et al., 2007), although we have to be mindful of the important limitation pointed out by Tomkinson & Eccles (1996), stating that acoustic rhinometry data should always be collected under the same stable environmental conditions. Both the volume and the shape of the airway could also be studied by implementing a study based on 3D imaging, e.g. using MRI in order to avoid the exposure to X-rays related to the practice of CT-scanning.

Another approach, more and more frequently used and that should be extensively pursued thereafter, is simulation by computational fluid dynamics (CFD). These methods allow to connect morphology and function and have the potential to answer many questions about the functional aspects of the nasal airway at the population scale. For example: is the absence of volume variation between the human samples of our study indicative of identical inspired air volumes in these five populations? How does the shape of the nasal airway influence the distribution of the inspired air in the nasal airway and, by extension, the efficiency of the warming and humidification processes? Based on the previous question, can we interpret shape as an immediate response of the nasal mucosa to the environment? We are currently involved in the development of these questions, which will hopefully soon yield new results to allow us to discuss the connections between form and function (Sanz-Prieto et al., In review).

Finally, the last aspect we will discuss here is the burning question, namely the application of these results to the fossil record. The interest in Neanderthal morphology, in particular, has led many researchers to question the factors that influenced the morphology of its nasal cavity. Recently, computational fluid dynamics methods have been used to study Neanderthal's nasal cavity after virtually reconstructing it and morphing a modern human mucosa on the bone cavity (Wroe et al., 2018). Based on our study, we are convinced that the complexity of the factors influencing the morphology of this nasal mucosa does not *yet* allow us to apply this kind of method to fossils. While we acknowledge the obvious interest of trying to apply this approach, we would however recommend to cautiously pursue the research on modern humans, in order to understand in details the intricacies of nasal morphological variation. We are convinced that by doing so, step by step, we will one day unravel the puzzling complexity of these phenomena in human species.

BIBLIOGRAPHIC REFERENCES
RÉFÉRENCES BIBLIOGRAPHIQUES

Ackermann RR, Cheverud JM (2004) Detecting genetic drift versus selection in human evolution. *Proceedings of the National Academy of Sciences* 101, 17946-17951.

Adhikari K, Fuentes-Guajardo M, Quinto-Sánchez M, et al. (2016) A genome-wide association scan implicates DCHS2, RUNX2, GLI3, PAX1 and EDAR in human facial variation. *Nat Commun* 7, 11616.

Al Dayeh AA, Rafferty KL, Egbert M, et al. (2013) Real-time monitoring of the growth of the nasal septal cartilage and the nasofrontal suture. *American Journal of Orthodontics and Dentofacial Orthopedics* 143, 773-783.

Albert AM, Ricanek K, Patterson E (2007) A review of the literature on the aging adult skull and face: Implications for forensic science research and applications. *Forensic Science International* 172, 1-9.

Alexander CM, Kasza I, Yen C-LE, et al. (2015) Dermal white adipose tissue: a new component of the thermogenic response. *Journal of Lipid Research* 56, 2061-2069.

Alhajeri BH, Steppan SJ (2016) Association between climate and body size in rodents: A phylogenetic test of Bergmann's rule. *Mammalian Biology* 81, 219-225.

Allen JA (1877) *The Influence of Physical Conditions in the Genesis of Species* Université de Harvard.,

Al-Sayed AA, Agu RU, Massoud E (2017) Models for the study of nasal and sinus physiology in health and disease: A review of the literature: Models for Sinonasal Physiology and Pathology. *Laryngoscope Investigative Otolaryngology* 2, 398-409.

Ashton KG, Tracy MC, Queiroz A de (2000) Is Bergmann's Rule Valid for Mammals? *The American Naturalist* 156, 390-415.

Aubin JE, Bonnelye E (2000) Osteoprotegerin and its Ligand: A New Paradigm for Regulation of Osteoclastogenesis and Bone Resorption. *Osteoporosis International* 11, 905-913.

de Azevedo S, González MF, Cintas C, et al. (2017) Nasal airflow simulations suggest convergent adaptation in Neanderthals and modern humans. *Proc Natl Acad Sci USA* 114, 12442-12447.

Balanoff AM, Bever GS, Colbert MW, et al. (2016) Best practices for digitally constructing endocranial casts: examples from birds and their dinosaurian relatives. *J Anat* 229, 173-190.

Barna J, Princz A, Kosztelnik M, et al. (2012) Heat shock factor-1 intertwines insulin/IGF-1, TGF-β and cGMP signaling to control development and aging. *BMC Dev Biol* 12, 32.

Barnett SA (1965) Adapation of mice to cold. *Biological Reviews* 40, 5-51.

Bassett JHD, Williams GR (2016) Role of Thyroid Hormones in Skeletal Development and Bone Maintenance. *Endocrine Reviews* 37, 135-187.

Bastir M (2019) Big Choanae, Larger Face: Scaling Patterns Between Cranial Airways in Modern Humans and African Apes and Their Significance in Middle and Late Pleistocene Hominin Facial Evolution. *BMSAP* 31, 5-13.

Bastir M, Godoy P, Rosas A (2011) Common features of sexual dimorphism in the cranial airways of different human populations. *Am J Phys Anthropol* 146, 414-422.

Bastir M, Megía I, Torres‐Tamayo N, et al. (2020) Three‐dimensional analysis of sexual dimorphism in the soft tissue morphology of the upper airways in a human population. *Am J Phys Anthropol* 171, 65-75.

Bastir M, Rosas A (2013) Cranial airways and the integration between the inner and outer facial skeleton in humans: Facial Modularity and Integration. *Am J Phys Anthropol* 152, 287-293.

Bastir M, Rosas A (2016) Cranial base topology and basic trends in the facial evolution of Homo. *Journal of Human Evolution* 91, 26-35.

Beall CM, Jablonski NG, Steegmann AT (2012) Human Adaptation to Climate: Temperature, Ultraviolet Radiation, and Altitude. In S. Stinson, B. Bogin, & D. O'Rourke, éd. *Human Biology*. Hoboken, NJ, USA: John Wiley & Sons, Inc., 175-250.

Beaudet A (2015) *Caractérisation des structures crânio-dentaires internes des cercopithécoïdes et étude diachronique de leurs variations morphologiques dans la séquence Plio-Pléistocène sud-africaine*. Thèse de doctorat. Université de Toulouse.

Beaudet A, Clarke RJ, Heaton JL, et al. (2020) The atlas of StW 573 and the late emergence of human-like head mobility and brain metabolism. *Sci Rep* 10, 4285.

Beaudet A, Dumoncel J, de Beer F, et al. (2016) Morphoarchitectural variation in South African fossil cercopithecoid endocasts. *Journal of Human Evolution* 101, 65-78.

Bergmann C (1847) Über die Verhältnisse der Wärmeökonomie der Thiere zu ihrer Größe. *Göttinger Studien* 3, 595-708.

Besl PJ, McKay ND (1992) A method for registration of 3-D shapes. *IEEE Trans Pattern Anal Mach Intell* 14, 239-256.

Blackburn TM, Hawkins BA (2004) Bergmann's rule and the mammal fauna of northern North America. *Ecography* 27, 715-724.

Bookstein FL (1991) *Morphometric Tools for Landmark Data: Geometry and Biology* 1re éd., Cambridge University Press.

Bougeard S, Dray S (2018) Supervised Multiblock Analysis in R with the ade4 Package. *J Stat Soft* 86.

Bourke JM, Ruger Porter Wm, Ridgely RC, et al. (2014) Breathing Life Into Dinosaurs: Tackling Challenges of Soft-Tissue Restoration and Nasal Airflow in Extinct Species: Dinosaur Nasal Airflow. *Anat Rec* 297, 2148-2186.

Brachetta-Aporta N, Toro-Ibacache V (2021) Differences in masticatory loads impact facial bone surface remodeling in an archaeological sample of South American individuals. *Journal of Archaeological Science*, 10.

Braga J, Zimmer V, Dumoncel J, et al. (2019) Efficacy of diffeomorphic surface matching and 3D geometric morphometrics for taxonomic discrimination of Early Pleistocene hominin mandibular molars. *Journal of Human Evolution* 130, 21-35.

Brookes M, Revell WJ (1998) *Blood Supply of Bone: Scientific Aspects*, London: Springer London.

Brown JS, Kotler BP, Porter WP (2017) How foraging allometries and resource dynamics could explain Bergmann's rule and the body-size diet relationship in mammals. *Oikos* 126.

Buck LT, Stringer CB, MacLarnon AM, et al. (2019) Variation in Paranasal Pneumatisation between Mid-Late Pleistocene Hominins. *BMSAP* 31, 14-33.

Buikstra JE, Ubelaker DH (1994) *Standards for data collection from human skeletal remains* Arkansas Archaeological Survey.,

Burgos MA, Sanmiguel-Rojas E, del Pino C, et al. (2017) New CFD tools to evaluate nasal airflow. *Eur Arch Otorhinolaryngol* 274, 3121-3128.

Butaric LN (2015) Differential Scaling Patterns in Maxillary Sinus Volume and Nasal Cavity Breadth Among Modern Humans. *Anat Rec* 298, 1710-1721.

Butaric LN, Klocke RP (2018) Nasal variation in relation to high-altitude adaptations among Tibetans and Andeans. *Am J Hum Biol* 30, e23104.

Butaric LN, Maddux SD (2016) Morphological Covariation between the Maxillary Sinus and Midfacial Skeleton among Sub-Saharan and Circumpolar Modern Humans: Maxillary Sinus Shape in Humans. *Am J Phys Anthropol* 160, 483-497.

Butaric LN, McCarthy RC, Broadfield DC (2010) A preliminary 3D computed tomography study of the human maxillary sinus and nasal cavity. *Am J Phys Anthropol* 143, 426-436.

Buzi C, Profico A, Liang C, et al. (2023) *Icex*: Advances in the automatic extraction and volume calculation of cranial cavities. *Journal of Anatomy*, joa.13843.

Campbell HL (1945) Seasonal changes in food consumption and rate of growth of the albino rat. *American Journal of Physiology* 143, 428-433.

Campbell RM, Vinas G, Henneberg M (2022) Relationships between the hard and soft dimensions of the nose in Pan troglodytes and Homo sapiens reveal the positions of the nasal tips of Plio-Pleistocene hominids C. Wilkinson, éd. *PLoS ONE* 17, e0259329.

Cannon B, Nedergaard J (2004) Brown Adipose Tissue: Function and Physiological Significance. *Physiological Reviews* 84, 277-359.

Caputa M (2004) Selective brain cooling: a multiple regulatory mechanism. *Journal of Thermal Biology* 29, 691-702.

Carey JW, Steegmann AT (1981) Human nasal protrusion, latitude, and climate. *Am J Phys Anthropol* 56, 313-319.

Cauna N (1982) Blood and nerve supply of the nasal lining. In D. F. Proctor & I. Andersen, éd. *The Nose: Upper Airway Physiology and the Atmospheric Environment*. New York: Elsevier Biomedical Press, 45-69.

Cavalli-Sforza LL, Piazza A (1993) Human Genomic Diversity in Europe: A Summary of Human Genomic Diversity in Europe: A Summary of Recent Research and Prospects for the Future. *Eur J Hum Genet* 1, 3-18.

Chae Y, Aguilar G, Lavernia EJ, et al. (2003) Characterization of temperature dependent mechanical behavior of cartilage. *Lasers Surg Med* 32, 271-278.

Charles CM (1930) The cavum nasi of the American negro. *Am J Phys Anthropol* 14, 177-253.

Chen XB, Lee HP, Chong VFH, et al. (2010) Numerical Simulation of the Effects of Inferior Turbinate Surgery on Nasal Airway Heating Capacity. *Am J Rhinol Allergy* 24, e118-e122.

Chessel D, Dufour AB, Thioulouse J (2004) The ade4 Package – I: One-Table Methods. *R News* 4, 5-10.

Choudhury A, Ramsay M, Hazelhurst S, et al. (2017) Whole-genome sequencing for an enhanced understanding of genetic variation among South Africans. *Nat Commun* 8, 2062.

Chung E, Rylander MN (2012) Response of preosteoblasts to thermal stress conditioning and osteoinductive growth factors. *Cell Stress and Chaperones* 17, 203-214.

Churchill SE, Shackelford LL, Georgi JN, et al. (2004) Morphological variation and airflow dynamics in the human nose. *Am J Hum Biol* 16, 625-638.

Claes P, Roosenboom J, White JD, et al. (2018) Genome-wide mapping of global-to-local genetic effects on human facial shape. *Nat Genet* 50, 414-423.

Clauss M, Dittmann MT, Müller DWH, et al. (2013) Bergmann's rule in mammals: a cross-species interspecific pattern. *Oikos*, no-no.

Cohen MM, MacLean RE éd. (2000) *Craniosynostosis: diagnosis, evaluation, and management* 2nd ed., New York: Oxford University Press.

Cole P (1982a) Upper respiratory airflow. In *The Nose: Upper Airway Physiology and the Atmospheric Environment*. New York: Elsevier Biomedical Press, 163-190.

Cole P (1982b) Modification of inspired air. In D. F. Proctor & I. Andersen, éd. *The Nose: Upper Airway physiology and the Atmospheric Environment*. New York: Elsevier Biomedical Press, 351-375.

Collins JC, Pilkington TC, Schmidt-Nielsen K (1971) A Model of Respiratory Heat Transfer in a Small Mammal. *Biophysical Journal* 11, 886-914.

Cooper LF, Uoshima K (1994) Differential estrogenic regulation of small M(r) heat shock protein expression in osteoblasts. *J Biol Chem* 269, 7869-7873.

Cottle MH (1955) The Structure and Function of the Nasal Vestibule. *Archives of Otolaryngology - Head and Neck Surgery* 62, 173-181.

Crameri F, Shephard GE, Heron PJ (2020) The misuse of colour in science communication. *Nat Commun* 11, 5444.

Croen KD (1993) Evidence for antiviral effect of nitric oxide. Inhibition of herpes simplex virus type 1 replication. *J Clin Invest* 91, 2446-2452.

Crognier E (1981a) Climate and anthropometric variations in Europe and the Mediterranean area. *Annals of Human Biology* 8, 99-107.

Crognier É (1981b) The Influence of Climate on the Physical Diversity of European and Mediterranean Populations. *Journal of Human Evolution*, 611-614.

Dag O, Dolgun A, Konar N Meric (2018) onewaytests: An R Package for One-Way Tests in Independent Groups Designs. *The R Journal* 10, 175.

Dai J, Rabie ABM (2007) VEGF: an Essential Mediator of Both Angiogenesis and Endochondral Ossification. *J Dent Res* 86, 937-950.

Davies A (1932) A Re-Survey of the Morphology of the Nose in Relation to Climate. *The Journal of the Royal Anthropological Institute of Great Britain and Ireland* 62, 337.

Degroot D, Anchukaitis KJ, Tierney JE, et al. (2022) The history of climate and society: a review of the influence of climate change on the human past. *Environ Res Lett* 17, 103001.

Devlin MJ (2015) The “Skinny” on brown fat, obesity, and bone: The “Skinny” on Brown Fat, Obesity, and Bone. *Am J Phys Anthropol* 156, 98-115.

Devlin MJ (2022) Brown Adipose Tissue, Nonshivering Thermogenesis, and Energy Availability. In K. M. Pitirri & J. T. Richtsmeier, éd. *Evolutionary Cell Processes in Primates*. Boca Raton: CRC Press.

Doorly DJ, Taylor DJ, Gambaruto AM, et al. (2008) Nasal architecture: form and flow. *Phil Trans R Soc A* 366, 3225-3246.

Dray S, Dufour A-B (2007) The ade4 Package: Implementing the Duality Diagram for Ecologists. *J Stat Soft* 22.

Dray S, Dufour AB, Chessel D (2007) The ade4 Package – II: Two-Table and K-Table Methods. *R News* 7, 47-52.

Dryden IL, Mardia KV (2016) *Statistical shape analysis with applications in R* Second edition., Chichester, UK⍰; Hoboken, NJ: John Wiley & Sons.

Dumoncel J (2017) *Analyse morphométrique 3D de structures anatomiques pour la paléoanthropologie*. Thèse de doctorat. Université de Toulouse.

Dumoncel J (2020) RToolsForDeformetrica: R script for Deformetrica ouput. R package version 0.1.

Dumoncel J, Subsol G, Durrleman S, et al. (2016) How to Build an Average Model When Samples are Variably Incomplete? Application to Fossil Data. 2016 IEEE Conference on Computer Vision and Pattern Recognition Workshops (CVPRW). Las Vegas, NV, USA: IEEE, 541-548.

Durrleman S (2010) *Statistical models of currents for measuring the variability of anatomical curves, surfaces and their evolution*. PhD thesis. Université de Nice - Sophia Antipolis.

Durrleman S, Pennec X, Trouvé A, et al. (2013) Toward a Comprehensive Framework for the Spatiotemporal Statistical Analysis of Longitudinal Shape Data. *Int J Comput Vis* 103, 22-59.

Durrleman S, Prastawa M, Charon N, et al. (2014) Morphometry of anatomical shape complexes with dense deformations and sparse parameters. *NeuroImage* 101, 35-49.

Durrleman S, Prastawa M, Korenberg JR, et al. (2012) Topology Preserving Atlas Construction from Shape Data without Correspondence Using Sparse Parameters. In N. Ayache, H. Delingette, P. Golland, et al., éd. *Medical Image Computing and Computer-Assisted Intervention – MICCAI 2012*. Lecture Notes in Computer Science. Berlin, Heidelberg: Springer Berlin Heidelberg, 223-230.

Eccles R (1982) Neurological and pharmacological considerations. In D. F. Proctor & I. Andersen, éd. *The Nose: Upper Airway Physiology and the Atmospheric Environment*. Amsterdam: Elsevier, 191-214.

Eccles R (1996) A role for the nasal cycle in respiratory defence. *European Respiratory Journal* 9, 371-376.

Eccles R (2002) An Explanation for the Seasonality of Acute Upper Respiratory Tract Viral Infections. *Acta Oto-Laryngologica* 122, 183-191.

Egeli E, Demirci L, Yaz??c?? B, et al. (2004) Evaluation of the Inferior Turbinate in Patients With Deviated Nasal Septum by Using Computed Tomography: *The Laryngoscope* 114, 113-117.

Elad D, Wolf M, Keck T (2008) Air-conditioning in the human nasal cavity. *Respiratory Physiology & Neurobiology* 163, 121-127.

Enerbäck S, Jacobsson A, Simpson EM, et al. (1997) Mice lacking mitochondrial uncoupling protein are cold-sensitive but not obese. *Nature* 387, 90-94.

Enlow DH (1990) *Facial Growth* Third Edition., Philadelphia: Saunders WB Co.

Evteev A, Anikin A, Satanin L (2018) Midfacial growth patterns in males from newborn to 5 years old based on computed tomography. *Am J Hum Biol* 30, e23132.

Evteev A, Cardini AL, Morozova I, et al. (2014) Extreme climate, rather than population history, explains mid-facial morphology of northern asians: MID-Facial Cold Adaptation in Northern Asians. *Am J Phys Anthropol* 153, 449-462.

Evteev AA, Grosheva AN (2019) Nasal cavity and maxillary sinuses form variation among modern humans of Asian descent. *Am J Phys Anthropol* 169, 513-525.

Evteev AA, Heuzé Y (2018) Impact of sampling strategies and reconstruction protocols in nasal airflow simulations in fossil hominins. *Proc Natl Acad Sci USA* 115, E4737-E4738.

Eyheramendy S, Martinez FI, Manevy F, et al. (2015) Genetic structure characterization of Chileans reflects historical immigration patterns. *Nat Commun* 6, 6472.

Eyquem AP, Kuzminsky SC, Aguilera J, et al. (2019) Normal and altered masticatory load impact on the range of craniofacial shape variation: An analysis of pre-Hispanic and modern populations of the American Southern Cone. *PLoS ONE* 14, e0225369.

Feldhamer GA (2020) *Mammalogy: adaptation, diversity, ecology* Fifth edition., Baltimore: Johns Hopkins University Press.

Finlayson C, Giles Pacheco F, Rodríguez-Vidal J, et al. (2006) Late survival of Neanderthals at the southernmost extreme of Europe. *Nature* 443, 850-853.

Fischer AW, Csikasz RI, von Essen G, et al. (2016) No insulating effect of obesity. *American Journal of Physiology-Endocrinology and Metabolism* 311, E202-E213.

Fishbaugh J, Durrleman S, Prastawa M, et al. (2017) Geodesic shape regression with multiple geometries and sparse parameters. *Medical Image Analysis* 39, 1-17.

Flour M-P, Ronot X, Vincent F, et al. (1992) Differential temperature sensitivity of cultured cells from cartilaginous or bone origin. *Biology of the Cell* 75, 83-87.

Fontanari P, Burnet H, Zattara-Hartmann MC, et al. (1996) Changes in airway resistance induced by nasal inhalation of cold dry, dry, or moist air in normal individuals. *Journal of Applied Physiology* 81, 1739-1743.

Foster F, Collard M (2013) A Reassessment of Bergmann's Rule in Modern Humans K. Rosenberg, éd. *PLoS ONE* 8, e72269.

Franciscus RG (1995) *Later Pleistocene nasofacial variation in western Eurasia and Africa and modern human origins*. Albuquerque: University of New Mexico.

Franciscus RG, Churchill SE (2002) The costal skeleton of Shanidar 3 and a reappraisal of Neandertal thoracic morphology. *Journal of Human Evolution* 42, 303-356.

Franciscus RG, Long JC (1991) Variation in human nasal height and breadth. *Am J Phys Anthropol* 85, 419-427.

Franciscus RG, Trinkaus E (1988) Nasal morphology and the emergence ofHomo erectus. *Am J Phys Anthropol* 75, 517-527.

Froehle AW (2008) Climate variables as predictors of basal metabolic rate: New equations. *Am J Hum Biol* 20, 510-529.

Froehle AW, Yokley TR, Churchill SE (2013) Energetics and the Origin of Modern Humans. In F. H. Smith & J. C. M. Ahern, éd. *The Origins of Modern Humans*. Hoboken, NJ: John Wiley & Sons, Inc, 285-320.

Fukase H, Ito T, Ishida H (2016) Geographic variation in nasal cavity form among three human groups from the Japanese Archipelago: Ecogeographic and functional implications. *Am J Hum Biol* 28, 343-351.

de Gabory L, Kérimian M, Baux Y, et al. (2020) Computational fluid dynamics simulation to compare large volume irrigation and continuous spraying during nasal irrigation. *Int Forum Allergy Rhinol* 10, 41-48.

Gannon PJ, Doyle WJ, Ganjian E, et al. (1997) Maxillary Sinus Mucosal Blood Flow During Nasal vs Tracheal Respiration. *Archives of Otolaryngology - Head and Neck Surgery* 123, 1336-1340.

García-Martínez D, Torres-Tamayo N, Torres-Sánchez I, et al. (2018) Ribcage measurements indicate greater lung capacity in Neanderthals and Lower Pleistocene hominins compared to modern humans. *Commun Biol* 1, 117.

Garrett SC, Rosenthal JJC (2012) A Role for A-to-I RNA Editing in Temperature Adaptation. *Physiology* 27, 362-369.

Gee AH, Treece GM (2014) Systematic misregistration and the statistical analysis of surface data. *Medical Image Analysis* 18, 385-393.

Gluckman P, Hanson M éd. (2006) *Developmental Origins of Health and Disease* 1re éd., Cambridge University Press.

Gohli J, Voje KL (2016) An interspecific assessment of Bergmann's rule in 22 mammalian families. *BMC Evol Biol* 16, 222.

Golozoubova V, Hohtola E, Matthias A, et al. (2001) Only UCP1 can mediate adaptive nonshivering thermogenesis in the cold. *FASEB j* 15, 2048-2050.

Gossan N, Zeef L, Hensman J, et al. (2013) The Circadian Clock in Murine Chondrocytes Regulates Genes Controlling Key Aspects of Cartilage Homeostasis. *Arthritis & Rheumatism* 65, 2334-2345.

Grenander U (1996) *Elements of pattern theory*, Baltimore: Johns Hopkins University Press.

Hall BK (2015) *Bones and cartilage: developmental and evolutionary skeletal biology* Second edition., Amsterdam: Elsevier/AP, Academic Press is an imprint of Elsevier.

Hall BK, Eckhard Witten P (2018) Plasticity and Variation of Skeletal Cells and Tissues and the Evolutionary Development of Actinopterygian Fishes. In Z. Johanson, C. Underwood, & M. Richter, éd. *Evolution and Development of Fishes*. Cambridge University Press, 126-143.

Hall BK, Precious DS (2013) Cleft lip, nose, and palate: the nasal septum as the pacemaker for midfacial growth. *Oral Surgery, Oral Medicine, Oral Pathology and Oral Radiology* 115, 442-447.

Hall RL (2005) Energetics of nose and mouth breathing, body size, body composition, and nose volume in young adult males and females. *Am J Hum Biol* 17, 321-330.

Hallgrímsson B, Willmore K, Dorval C, et al. (2004) Craniofacial variability and modularity in macaques and mice. *J Exp Zool* 302B, 207-225.

Hancock AM, Witonsky DB, Alkorta-Aranburu G, et al. (2011) Adaptations to Climate-Mediated Selective Pressures in Humans M. W. Nachman, éd. *PLoS Genet* 7, e1001375.

Hang K, Ye C, Chen E, et al. (2018) Role of the heat shock protein family in bone metabolism. *Cell Stress and Chaperones* 23, 1153-1164.

Hanna JM, Brown DE (1983) Human Heat Tolerance: An Anthropological Perspective. *Annu Rev Anthropol* 12, 259-284.

Hanna LM, Scherer PW (1986) A Theoretical Model of Localized Heat and Water Vapor Transport in the Human Respiratory Tract. *Journal of Biomechanical Engineering* 108, 19-27.

Harrison GA, Clegg EJ (1969) Environmental factors infuencing mammalian growth. In E. Bajusz, éd. *Physiology and Pathology of Adaptation Mechanisms*. Oxford: Pergamon Press, 74.

Hartman C, Holton N, Miller S, et al. (2016) Nasal Septal Deviation and Facial Skeletal Asymmetries: Nasal Septal Deviation. *Anat Rec* 299, 295-306.

Harvati K, Weaver TD (2006a) Reliability of cranial morphology in reconstructing Neanderthal phylogeny. In J.-J. Hublin, K. Harvati, & T. Harrison, éd. *Neanderthals Revisited: New Approaches and Perspectives*. Vertebrate Paleobiology and Paleoanthropology. Dordrecht: Springer Netherlands, 239-254.

Harvati K, Weaver TD (2006b) Human cranial anatomy and the differential preservation of population history and climate signatures. *Anat Rec* 288A, 1225-1233.

Hasegawa M, Kern EB (1977) The human nasal cycle. *Mayo Clin Proc* 52, 28-34.

Hatakeyama D, Kozawa O, Niwa M, et al. (2002) Upregulation by retinoic acid of transforming growth factor-⊠-stimulated heat shock protein 27 induction in osteoblasts: involvement of mitogen-activated protein kinases. *Biochimica et Biophysica Acta (BBA) - Molecular Cell Research* 1589, 15-30.

Havenith G (2005) Temperature Regulation, Heat Balance and Climatic Stress. In W. Kirch, R. Bertollini, & B. Menne, éd. *Extreme Weather Events and Public Health Responses*. Berlin/Heidelberg: Springer-Verlag, 69-80.

Heuzé Y (2019) What Does Nasal Cavity Size Tell us about Functional Nasal Airways? *BMSAP* 31, 69-76.

Hiernaux J, Froment A (1976) The correlations between anthropobiological and climatic variables in sub-Saharan Africa: revised estimates. *Hum Biol* 48, 757-767.

Hildebrandt T, Heppt W, Kertzscher U, et al. (2013) The Concept of Rhinorespiratory Homeostasis—A New Approach to Nasal Breathing. *Facial plast Surg* 29, 085-092.

Holden WE, Wilkins JP, Harris M, et al. (1999) Temperature conditioning of nasal air: effects of vasoactive agents and involvement of nitric oxide. *Journal of Applied Physiology* 87, 1260-1265.

Holliday TW (1997) Body proportions in Late Pleistocene Europe and modern human origins. *Journal of Human Evolution* 32, 423-448.

Holliday TW, Hilton CE (2009) Body proportions of circumpolar peoples as evidenced from skeletal data: Ipiutak and Tigara (Point Hope) versus Kodiak Island Inuit. *Am J Phys Anthropol*, NA-NA.

Holton N, Yokley T, Butaric L (2013) The Morphological Interaction Between the Nasal Cavity and Maxillary Sinuses in Living Humans. *Anat Rec* 296, 414-426.

Holton NE, Alsamawi A, Yokley TR, et al. (2016) The ontogeny of nasal shape: An analysis of sexual dimorphism in a longitudinal sample: The Ontogeny of Nasal Shape. *Am J Phys Anthropol* 160, 52-61.

Holton NE, Piche A, Yokley TR (2018) Integration of the nasal complex: Implications for developmental and evolutionary change in modern humans. *Am J Phys Anthropol* 166, 791-802.

Holton NE, Yokley TR, Franciscus RG (2011a) Climatic adaptation and Neandertal facial evolution: A comment on Rae et al. (2011). *Journal of Human Evolution* 61, 624-627.

Holton NE, Yokley TR, Franciscus RG (2011b) Climatic adaptation and Neandertal facial evolution: A comment on Rae et al. (2011). *Journal of Human Evolution* 61, 624-627.

Holton NE, Yokley TR, Froehle AW, et al. (2014) Ontogenetic scaling of the human nose in a longitudinal sample: Implications for genus *Homo* facial evolution: Ontogenetic Scaling of the Human Nose. *Am J Phys Anthropol* 153, 52-60.

Hounsfield GN (1980) Computed Medical Imaging. *Science* 210, 22-28.

Hoyme LE (1965) The nasal index and climate – A spurious case of natural selection in man. *American Journal of Physical Anthropology* 23, 336-337.

Hubbe M, Hanihara T, Harvati K (2009) Climate Signatures in the Morphological Differentiation of Worldwide Modern Human Populations. *Anat Rec* 292, 1720-1733.

Ingelstedt S (1956) Studies on the conditioning of air in the respiratory tract. *Acta Otolaryngol Suppl* 131, 1-80.

Inthavong K, Chetty A, Shang Y, et al. (2018) Examining mesh independence for flow dynamics in the human nasal cavity. *Computers in Biology and Medicine* 102, 40-50.

Inthavong K, Tian ZF, Tu JY (2007) CFD Simulations on the Heating Capability in a Human Nasal Cavity. In 16th Australasian Fluid Mechanics Conference. Crown Plaza, Gold Coast, Australia, 842-847.

IPCC (2023) *Climate Change 2023: Synthesis Report. A Report of the Intergovernmental Panel on Climate Change. Contribution of Working Groups I, II and III to the Sixth Assessment Report of the Intergovernmental Panel on Climate Change*, Geneva, Switzerland.

Irmak MK, Korkmaz A, Erogul O (2004) Selective brain cooling seems to be a mechanism leading to human craniofacial diversity observed in different geographical regions. *Medical Hypotheses* 63, 974-979.

Iwen KA, Oelkrug R, Brabant G (2018) Effects of thyroid hormones on thermogenesis and energy partitioning. *Journal of Molecular Endocrinology* 60, R157-R170.

Jain B, Rubinstein I, Robbins RA, et al. (1993) Modulation of Airway Epithelial Cell Ciliary Beat Frequency by Nitric Oxide. *Biochemical and Biophysical Research Communications* 191, 83-88.

James FC (1970) Geographic Size Variation in Birds and Its Relationship to Climate. *Ecology* 51, 365-390.

James GD (2010) Climate-Related Morphological Variation and Physiological Adaptations inHomo sapiens. In C. S. Larsen, éd. *A Companion to Biological Anthropology*. Oxford, UK: Wiley-Blackwell, 153-166.

Jankowski R (2013) *The Evo-Devo Origin of the Nose, Anterior Skull Base and Midface*, Paris: Springer Paris.

Jaskulska E (2014) *Adaptation to Cold Climate in the Nasal Cavity Skeleton. A Comparison of Archaeological Crania from Different Climatic Zones*. University of Warsaw.

Jelinek AJ (1994) Hominids, Energy, Environment, and Behavior in the Late Pleistocene. In M. H. Nitecki & D. V. Nitecki, éd. *Origins of Anatomically Modern Humans*. Interdisciplinary Contributions to Archaeology. Boston, MA: Springer US, 67-92.

Joganic JL, Heuzé Y (2019) Allometry and advancing age significantly structure craniofacial variation in adult female baboons. *J Anat* 235, 217-232.

Joshi AA, Leahy RM, Badawi RD, et al. (2016) Registration-Based Morphometry for Shape Analysis of the Bones of the Human Wrist. *IEEE Trans Med Imaging* 35, 416-426.

Kalyakulina A, Iannuzzi V, Sazzini M, et al. (2020) Investigating Mitonuclear Genetic Interactions Through Machine Learning: A Case Study on Cold Adaptation Genes in Human Populations From Different European Climate Regions. *Front Physiol* 11, 575968.

Kasza I, Hernando D, Roldán-Alzate A, et al. (2016) Thermogenic profiling using magnetic resonance imaging of dermal and other adipose tissues. *JCI Insight* 1.

Kasza I, Suh Y, Wollny D, et al. (2014) Syndecan-1 Is Required to Maintain Intradermal Fat and Prevent Cold Stress G. S. Barsh, éd. *PLoS Genet* 10, e1004514.

Katzmarzyk PT, Leonard WR (1998) Climatic influences on human body size and proportions: ecological adaptations and secular trends. *American Journal of Physical Anthropology*, 483-503.

Keck T, Leiacker R, Riechelmann H, et al. (2000) Temperature Profile in the Nasal Cavity. *Laryngoscope* 110, 651-654.

Keck T, Lindemann J (2010) Numerical simulation and nasal air-conditioning. *GMS Current Topics in Otorhinolaryngology - Head and Neck Surgery; 9:Doc08; ISSN 1865-1011*.

Keir J (2009) Why do we have paranasal sinuses? *J Laryngol Otol* 123, 4-8.

Kelly AP, Ocobock C, Butaric LN, et al. (2023) Metabolic demands and sexual dimorphism in human nasal morphology: A test of the respiratory‐energetics hypothesis. *American Journal of Biological Anthropology* 180, 453-471.

Keustermans W, Huysmans T, Danckaers F, et al. (2018) High quality statistical shape modelling of the human nasal cavity and applications. *R Soc open sci* 5, 181558.

Keustermans W, Huysmans T, Schmelzer B, et al. (2020) The effect of nasal shape on the thermal conditioning of inhaled air: Using clinical tomographic data to build a large-scale statistical shape model. *Computers in Biology and Medicine* 117, 103600.

Keyhani K, Scherer PW, Mozell MM (1995) Numerical Simulation of Airflow in the Human Nasal Cavity. *Journal of Biomechanical Engineering* 117, 429-441.

Kiemle Trindade IE, Oliveira Camargo Gomes AD, Martins Sampaio-Teixeira AC, et al. (2007) Adult nasal volumes assessed by acoustic rhinometry. *Brazilian Journal of Otorhinolaryngology* 73, 32-39.

Kiliaridis S, Engstr m C, Thilander B (1985) The relationship between masticatory function and craniofacial morphology: I. A cephalometric longitudinal analysis in the growing rat fed a soft diet. *The European Journal of Orthodontics* 7, 273-283.

Kim D-W, Chung S-K, Na Y (2017) Numerical study on the air conditioning characteristics of the human nasal cavity. *Computers in Biology and Medicine* 86, 18-30.

Kishida Y, Hirao M, Tamai N, et al. (2005) Leptin regulates chondrocyte differentiation and matrix maturation during endochondral ossification. *Bone* 37, 607-621.

Klatzow J, Dalmasso G, Martínez-Abadías N, et al. (2022) Match: 3D Shape Correspondence for Biological Image Data. *Front Comput Sci* 4, 777615.

Kloss-Brandstätter A, Summerer M, Horst D, et al. (2021) An in-depth analysis of the mitochondrial phylogenetic landscape of Cambodia. *Sci Rep* 11, 10816.

Korhonen T, Mustonen A-M, Nieminen P, et al. (2008) Effects of cold exposure, exogenous melatonin and short-day treatment on the weight-regulation and body temperature of the Siberian hamster (Phodopus sungorus). *Regulatory Peptides* 149, 60-66.

Kottek M, Grieser J, Beck C, et al. (2006) World Map of the Köppen-Geiger climate classification updated. *Meteorol Z*, 5.

Kozawa O, Tokuda H (2002) Heat shock protein 27 in osteoblasts. *Folia Pharmacol Jpn* 119, 89-94.

Kushniarevich A, Utevska O, Chuhryaeva M, et al. (2015) Genetic Heritage of the Balto-Slavic Speaking Populations: A Synthesis of Autosomal, Mitochondrial and Y-Chromosomal Data F. Calafell, éd. *PLoS ONE* 10, e0135820.

Laitman JT, Smith HF (2022) *The Anatomical Record* sheds light on the world of the nasopharynx, a most important, yet underappreciated, realm, in a novel *Special Issue*. *The Anatomical Record* 305, 1825-1828.

Leitch VD, Bassett JHD, Williams GR (2020) Role of thyroid hormones in craniofacial development. *Nat Rev Endocrinol* 16, 147-164.

Leong SC, Eccles R (2009) A systematic review of the nasal index and the significance of the shape and size of the nose in rhinology. *Clinical Otolaryngology* 34, 191-198.

Lesciotto KM, Richtsmeier JT (2019) Craniofacial skeletal response to encephalization: How do we know what we think we know? *Am J Phys Anthropol* 168, 27-46.

Li C, Farag AA, Leach J, et al. (2017) Computational fluid dynamics and trigeminal sensory examinations of empty nose syndrome patients: Computational and Trigeminal Studies of ENS. *The Laryngoscope* 127, E176-E184.

Lieberman D (2011) *The evolution of the human head*, Cambridge, Mass: Belknap Press of Harvard University Press.

Lindemann J, Tsakiropoulou E, Keck T, et al. (2009) Nasal air conditioning in relation to acoustic rhinometry values. *am j rhinol allergy* 23, 575-577.

Lipson M, Ribot I, Mallick S, et al. (2020) Ancient West African foragers in the context of African population history. *Nature* 577, 665-670.

Lorensen WE, Cline HE (1987) Marching cubes: A high resolution 3D surface construction algorithm. In *Proceedings of the 14th annual conference on Computer graphics and interactive techniques - SIGGRAPH '87*. the 14th annual conference. ACM Press, 163-169.

Lovejoy CO, McCollum MA, Reno PL, et al. (2003) Developmental Biology and Human Evolution. *Annu Rev Anthropol* 32, 85-109.

Lowell BB, Spiegelman BM (2000) Towards a molecular understanding of adaptive thermogenesis. *Nature* 404, 652-660.

Lundberg JO (2008) Nitric Oxide and the Paranasal Sinuses. *Anat Rec* 291, 1479-1484.

Lundberg JON, Farkas-Szallasi T, Weitzberg E, et al. (1995) High nitric oxide production in human paranasal sinuses. *Nat Med* 1, 370-373.

Lundberg JON, Weitzberg E, Rinder J, et al. (1996) Calcium-independent and steroid-resistant nitric oxide synthase activity in human paranasal sinus mucosa. *European Respiratory Journal* 9, 1344-1347.

Ma J, Dong J, Shang Y, et al. (2018) Air conditioning analysis among human nasal passages with anterior anatomical variations. *Medical Engineering & Physics* 57, 19-28.

Maddux SD, Butaric LN (2017) Zygomaticomaxillary Morphology and Maxillary Sinus Form and Function: How Spatial Constraints Influence Pneumatization Patterns among Modern Humans. *Anat Rec* 300, 209-225.

Maddux SD, Butaric LN, Yokley TR, et al. (2016a) Ecogeographic variation across morphofunctional units of the human nose. *Am J Phys Anthropol* 162, 103-119.

Maddux SD, Yokley TR, Svoma BM, et al. (2016b) Absolute humidity and the human nose: A reanalysis of climate zones and their influence on nasal form and function: Absolute Humidity and the Human Nose. *Am J Phys Anthropol* 161, 309-320.

Maier W, Ruf I (2014) Morphology of the Nasal Capsule of Primates-With Special Reference to *Daubentonia* and *Homo*. *Anat Rec* 297, 1985-2006.

Mancinelli RL, McKay CP (1983) Effects of nitric oxide and nitrogen dioxide on bacterial growth. *Appl Environ Microbiol* 46, 198-202.

Maréchal L, Dumoncel J, Santos F, et al. (2023) New insights into the variability of upper airway morphology in modern humans. *Journal of Anatomy* 242, 781-795.

Maréchal L, Heuzé Y (2022) Interaction Between Environmental Temperature and Craniofacial Morphology in Human Evolution. In *Evolutionary Cell Processes in Primates*. Boca Raton: CRC Press, 161-188.

Marks R (2018) Circadian clock: potential role in cartilage integrity and disruption. *International Journal of Orthopaedics* 5.

Marks TN, Maddux SD, Butaric LN, et al. (2019) Climatic adaptation in human inferior nasal turbinate morphology: Evidence from Arctic and equatorial populations. *Am J Phys Anthropol* 169, 498-512.

Márquez S, Laitman JT (2008) Climatic Effects on the Nasal Complex: A CT Imaging, Comparative Anatomical, and Morphometric Investigation of *Macaca mulatta* and *Macaca fascicularis*. *Anat Rec* 291, 1420-1445.

Márquez S, Pagano AS, Delson E, et al. (2014) The Nasal Complex of Neanderthals: An Entry Portal to their Place in Human Ancestry. *Anat Rec* 297, 2121-2137.

Martin JM, Leece AB, Neubauer S, et al. (2021) Drimolen cranium DNH 155 documents microevolution in an early hominin species. *Nat Ecol Evol* 5, 38-45.

Martinez Arbizu P (2020) pairwiseAdonis: Pairwise multilevel comparison using adonis. R package version 0.4.

Massaro EJ, Rogers JM éd. (2004) *The Skeleton*, Totowa, NJ: Humana Press.

Masuda S (1992) Role of the maxillary sinus as a resonant cavity. *Nippon Jibiinkoka Gakkai Kaiho* 95, 71-80.

Mayr E (1963) *Animal Species and Evolution*, Cambridge, Mass: Harvard University Press.

McDonald RB (2009) Thermoregulation: Autonomic, Age-Related Changes. In *Encyclopedia of Neuroscience*. Elsevier, 977-986.

McNab BK (1971) On the Ecological Significance of Bergmann's Rule. *Ecology* 52, 845-854.

McNab BK (2010) Geographic and temporal correlations of mammalian size reconsidered: a resource rule. *Oecologia* 164, 13-23.

McNab BK (2012) *Extreme measures: the ecological energetics of birds and mammals*, Chicago: The University of Chicago Press.

Meiri S, Dayan T (2003) On the validity of Bergmann's rule: On the validity of Bergmann's rule. *Journal of Biogeography* 30, 331-351.

Meiri S, Dayan T, Simberloff D (2004) Carnivores, biases and Bergmann's rule: CARNIVORES, BIASES AND BERGMANN's RULE. *Biological Journal of the Linnean Society* 81, 579-588.

Menéndez L, Bernal V, Novellino P, et al. (2014) Effect of bite force and diet composition on craniofacial diversification of Southern South American human populations: Diet and Cranial Variation in South America. *Am J Phys Anthropol* 155, 114-127.

Mlynski G, Grützenmacher S, Plontke S, et al. (2001) Correlation of nasal morphology and respiratory function. *Rhinology* 39, 197-201.

Moore WJ (1981) *The Mammalian Skull*, Cambridge: Cambridge University Press.

Moreland K (2016) Why We Use Bad Color Maps and What You Can Do About It. *Electronic Imaging* 2016, 1-6.

Moss ML, Young RW (1960) A functional approach to craniology. *Am J Phys Anthropol* 18, 281-292.

Mouse Genome Sequencing Consortium (2002) Initial sequencing and comparative analysis of the mouse genome. *Nature* 420, 520-562.

Myers P, Lundrigan BL, Gillespie BW, et al. (1996) Phenotypic plasticity in skull and dental morphology in the prairie deer mouse (Peromyscus maniculatus bairdii). *J Morphol* 229, 229-237.

Na Y, Chung KS, Chung S-K, et al. (2012) Effects of single-sided inferior turbinectomy on nasal function and airflow characteristics. *Respiratory Physiology & Neurobiology* 180, 289-297.

Naclerio RM, Pinto J, Assanasen P, et al. (2007) Observations on the ability of the nose to warm and humidify inspired air. *Rhinology* 45, 102-111.

Naftali S, Rosenfeld M, Wolf M, et al. (2005) The Air-Conditioning Capacity of the Human Nose. *Ann Biomed Eng* 33, 545-553.

Nedergaard J, Bengtsson T, Cannon B (2007) Unexpected evidence for active brown adipose tissue in adult humans. *American Journal of Physiology-Endocrinology and Metabolism* 293, E444-E452.

Neff EP (2020) A point on thermoneutrality for mice. *Lab Anim* 49, 169-169.

Negus V (1960) Further observations on the air conditioning mechanism of the nose. *Ann R Coll Surg Engl* 27, 171-204.

Negus VE (1952) Humidification of the Air Passages. *Thorax* 7, 148-151.

Noback ML, Harvati K, Spoor F (2011) Climate-related variation of the human nasal cavity. *Am J Phys Anthropol* 145, 599-614.

Noback ML, Samo E, van Leeuwen CHA, et al. (2016) Paranasal sinuses: A problematic proxy for climate adaptation in Neanderthals. *Journal of Human Evolution* 97, 176-179.

Nunes GT, Mancini PL, Bugoni L (2017) When Bergmann's rule fails: evidences of environmental selection pressures shaping phenotypic diversification in a widespread seabird. *Ecography* 40, 365-375.

Ochocińska D, Taylor JRE (2003) Bergmann's rule in shrews: geographical variation of body size in Palearctic Sorex species. *Biological Journal of the Linnean Society* 78, 365-381.

Oksanen J, Blanchet G, Friendly M, et al. (2020) vegan: Community Ecology Package. R package version 2.5-7.

Olsson P, Bende M (1985) Influence of Environmental Temperature on Human Nasal Mucosa. *Ann Otol Rhinol Laryngol* 94, 153-155.

O'malley JF (1923) Evolution of the Nasal Cavities and Sinuses in Relation to Function. *Proceedings of the Royal Society of Medicine* 16, 83-84.

OpenStreetMap (2022) Open-Elevation API.

Opperman LA, Gakunga PT, Carlson DS (2005) Genetic Factors Influencing Morphogenesis and Growth of Sutures and Synchondroses in the Craniofacial Complex. *Seminars in Orthodontics* 11, 199-208.

Oreskovich SM, Ong FJ, Ahmed BA, et al. (2019) Magnetic resonance imaging reveals human brown adipose tissue is rapidly activated in response to cold. *Journal of the Endocrine Society*, 18.

Palmer RI, Xie X, Tam G (2015) Finding complete 3D vertex correspondence for statistical shape modeling. In *2015 37th Annual International Conference of the IEEE Engineering in Medicine and Biology Society (EMBC)*. 37th Annual International Conference of the IEEE Engineering in Medicine and Biology Society (EMBC). Milan: IEEE, 2912-2915.

Paschetta C, de Azevedo S, Castillo L, et al. (2010) The influence of masticatory loading on craniofacial morphology: A test case across technological transitions in the Ohio valley: Masticatory Stress and Technological Transitions. *Am J Phys Anthropol* 141, 297-314.

Patel JJ, Utting JC, Key ML, et al. (2012) Hypothermia inhibits osteoblast differentiation and bone formation but stimulates osteoclastogenesis. *Experimental Cell Research* 318, 2237-2244.

Patel RG, Garcia GJM, Frank-Ito DO, et al. (2015) Simulating the Nasal Cycle with Computational Fluid Dynamics. *Otolaryngol Head Neck Surg* 152, 353-360.

Patil S, Paul S (2014) A Comprehensive Review on the Role of Various Materials in the Osteogenic Differentiation of Mesenchymal Stem Cells with a Special Focus on the Association of Heat Shock Proteins and Nanoparticles. *Cells Tissues Organs* 199, 81-102.

Pendolino AL, Lund VJ, Nardello E, et al. (2018) The nasal cycle: a comprehensive review. *RHINOL* 1, 67-76.

Percival CJ, Richtsmeier JT (2013) Angiogenesis and intramembranous osteogenesis: Angiogenesis and Intramembranous Osteogenesis. *Dev Dyn* 242, 909-922.

Pickrell JK, Berisa T, Liu JZ, et al. (2016) Detection and interpretation of shared genetic influences on 42 human traits. *Nat Genet* 48, 709-717.

Ponganis PJ, Van Dam RP, Levenson DH, et al. (2003) Regional heterothermy and conservation of core temperature in emperor penguins diving under sea ice. *Comparative Biochemistry and Physiology Part A: Molecular & Integrative Physiology* 135, 477-487.

Potts R, Faith JT (2015) Alternating high and low climate variability: The context of natural selection and speciation in Plio-Pleistocene hominin evolution. *Journal of Human Evolution* 87, 5-20.

Proctor DF (1982) The upper airway. In D. F. Proctor & I. Andersen, éd. *The Nose: Upper Airway Physiology and the Atmospheric Environment*. New York: Elsevier Biomedical Press., 23-43.

Proetz AW (1951) Air Currents in the Upper Respiratory Tract and Their Clinical Importance. *Ann Otol Rhinol Laryngol* 60, 439-467.

Proetz AW (1953) *Applied Physiology of the Nose*, St. Louis: Annals Publishing Co.

R Core Team (2021) R: A language and environment for statistical computing. R Foundation for Statistical Computing, Vienna, Austria.

Rae TC, Hill RA, Hamada Y, et al. (2003) Clinal variation of maxillary sinus volume in Japanese macaques (Macaca fuscata). *Am J Primatol* 59, 153-158.

Rae TC, Koppe T, Stringer CB (2011) The Neanderthal face is not cold adapted. *Journal of Human Evolution* 60, 234-239.

Rae TC, Viðarsdóttir US, Jeffery N, et al. (2006) Developmental response to cold stress in cranial morphology of *Rattus*: implications for the interpretation of climatic adaptation in fossil hominins. *Proc R Soc B* 273, 2605-2610.

Reppert SM, Weaver DR (2001) Molecular Analysis of Mammalian Circadian Rhythms. *Annu Rev Physiol* 63, 647-676.

Rezai-Zadeh K, Münzberg H (2013) Integration of sensory information via central thermoregulatory leptin targets. *Physiology & Behavior* 121, 49-55.

Richtsmeier J, Lesciotto KM (2020) From Phenotype to Genotype And Back Again. *BMSAP* 32, 8-17.

Richtsmeier JT, Aldridge K, DeLeon VB, et al. (2006) Phenotypic integration of neurocranium and brain. *J Exp Zool* 306B, 360-378.

Robbins A, Tom CATMB, Cosman MN, et al. (2018) Low temperature decreases bone mass in mice: Implications for humans. *Am J Phys Anthropol* 167, 557-568.

Rodríguez MÁ, López-Sañudo IL, Hawkins BA (2006) The geographic distribution of mammal body size in Europe: Mammal body size gradient. *Global Ecology and Biogeography* 15, 173-181.

Rohlf JF, Marcus LF (1993) A revolution morphometrics. *Trends in Ecology & Evolution* 8, 129-132.

Romano GH, Harari Y, Yehuda T, et al. (2013) Environmental Stresses Disrupt Telomere Length Homeostasis J.-Q. Zhou, éd. *PLoS Genet* 9, e1003721.

Romanovsky AA (2018) The thermoregulation system and how it works. In *Handbook of Clinical Neurology*. Elsevier, 3-43.

Roseman CC (2004) Detecting interregionally diversifying natural selection on modern human cranial form by using matched molecular and morphometric data. *Proceedings of the National Academy of Sciences* 101, 12824-12829.

Roseman CC, Weaver TD (2004) Multivariate apportionment of global human craniometric diversity. *Am J Phys Anthropol* 125, 257-263.

Rothman KJ (1990) No adjustments are needed for multiple comparisons. *Epidemiology* 1, 43-46.

Rubel F, Brugger K, Haslinger K, et al. (2017) The climate of the European Alps: Shift of very high resolution Köppen-Geiger climate zones 1800–2100. *metz* 26, 115-125.

Ruff C (2002) Variation in Human Body Size and Shape. *Annu Rev Anthropol* 31, 211-232.

Ruff CB (1994) Morphological adaptation to climate in modern and fossil hominids. *Am J Phys Anthropol* 37, 65-107.

Rylander MN (2005) Thermally Induced Injury and Heat-Shock Protein Expression in Cells and Tissues. *Annals of the New York Academy of Sciences* 1066, 222-242.

Sahin-Yilmaz A, Naclerio RM (2011) Anatomy and Physiology of the Upper Airway. *Proceedings of the American Thoracic Society* 8, 31-39.

Saito M, Okamatsu-Ogura Y, Matsushita M, et al. (2009) High Incidence of Metabolically Active Brown Adipose Tissue in Healthy Adult Humans. *Diabetes* 58, 1526-1531.

Salman SD, Proctor DF, Swift DL, et al. (1971) Nasal Resistance: Description of a Method and Effect of Temperature and Humidity Changes. *Ann Otol Rhinol Laryngol* 80, 736-743.

Sanz-Prieto D, Bastir M, Pérez-Ramos A, et al. (In review) Testing sex and geographic differences in dimensionless parameters for human nasal airflow. *Laryngoscope Investigative Otolaryngology*.

Sardi ML (2018) Craniofacial morphology and adaptation. In W. Trevathan, M. Cartmill, D. Dufour, et al., éd. *The International Encyclopedia of Biological Anthropology*. Hoboken, NJ, USA: John Wiley & Sons, Inc., 1-2.

Sardi ML, Joosten GG, Pandiani CD, et al. (2018) Frontal sinus ontogeny and covariation with bone structures in a modern human population. *Journal of Morphology* 279, 871-882.

Sargis EJ, Millien V, Woodman N, et al. (2018) Rule reversal: Ecogeographical patterns of body size variation in the common treeshrew (Mammalia, Scandentia). *Ecol Evol* 8, 1634-1645.

Schlebusch CM, Malmström H, Günther T, et al. (2017) Southern African ancient genomes estimate modern human divergence to 350,000 to 260,000 years ago. *Science* 358, 652-655.

Schmidt-Nielsen K, Hainsworth FR, Murrish DE (1970) Counter-current heat exchange in the respiratory passages: Effect on water and heat balance. *Respiration Physiology* 9, 263-276.

Scholander PF (1955) Evolution of Climatic Adaptation in Homeotherms. *Evolution* 9, 15-26.

Schrödter S, Biermann E, Halata Z (2003) Histological evaluation of age-related changes in human respiratory mucosa of the middle turbinate. *Anatomy and Embryology* 207, 19-27.

Schroter RC, Watkins NV (1989) Respiratory heat exchange in mammals. *Respiration Physiology* 78, 357-367.

Scott NA, Strauss A, Hublin J-J, et al. (2018) Covariation of the endocranium and splanchnocranium during great ape ontogeny C. Meloro, éd. *PLoS ONE* 13, e0208999.

Serrat MA (2014) Environmental Temperature Impact on Bone and Cartilage Growth. *Comprehensive Physiology* 4, 35.

Serrat MA, King D, Lovejoy CO (2008) Temperature regulates limb length in homeotherms by directly modulating cartilage growth. *Proceedings of the National Academy of Sciences* 105, 19348-19353.

Serrat MA, Schlierf TJ, Efaw ML, et al. (2015) Unilateral heat accelerates bone elongation and lengthens extremities of growing mice. *J Orthop Res* 33, 692-698.

Serrat MA, Williams RM, Farnum CE (2010) Exercise mitigates the stunting effect of cold temperature on limb elongation in mice by increasing solute delivery to the growth plate. *Journal of Applied Physiology* 109, 1869-1879.

Shaffer JR, Orlova E, Lee MK, et al. (2016) Genome-Wide Association Study Reveals Multiple Loci Influencing Normal Human Facial Morphology G. S. Barsh, éd. *PLoS Genet* 12, e1006149.

Shah R, Frank-Ito DO (2022) The role of normal nasal morphological variations from race and gender differences on respiratory physiology. *Respiratory Physiology & Neurobiology* 297, 103823.

Shea BT (1977) Eskimo craniofacial morphology, cold stress and the maxillary sinus. *Am J Phys Anthropol* 47, 289-300.

Shi L, Ma J, Deng Y, et al. (2021) Cold□inducible RNA□binding protein contributes to tissue remodeling in chronic rhinosinusitis with nasal polyps. *Allergy* 76, 497-509.

Shui C, Scutt A (2001) Mild Heat Shock Induces Proliferation, Alkaline Phosphatase Activity, and Mineralization in Human Bone Marrow Stromal Cells and Mg-63 Cells In Vitro. *J Bone Miner Res* 16, 731-741.

Shum AY, Liao FY, Chen CF, et al. (1991) The role of interscapular brown adipose tissue in cold acclimation in the rat. *Chin J Physiol* 34, 427-437.

Silva JE (2006) Thermogenic Mechanisms and Their Hormonal Regulation. *Physiological Reviews* 86, 435-464.

Slice DE éd. (2005) *Modern morphometrics in physical anthropology*, New York: Kluwer Academic/Plenum Publishers.

Smith T, Rossie J, Doherty P (2006) Primate Olfaction: Anatomy and Evolution. In W. J. Brewer, D. Castle, & C. Pantelis, éd. *Olfaction and the Brain*. Cambridge: Cambridge University Press, 135-166.

Sommer F, Kroger R, Lindemann J (2012) Numerical simulation of humidification and heating during inspiration within an adult nose. *Rhinology* 50, 157-164.

St. Hoyme LE, Işcan MY (1989) Determination of sex and race: accuracy and assumptions. In M. Y. Işcan & K. A. R. Kennedy, éd. *Reconstruction of life from the skeleton*. New York: Alan R. Liss Inc.

Steegmann AT (1979) Human facial temperatures in natural and laboratory cold. *Aviat Space Environ Med* 50, 227-232.

Steegmann AT, Cerny FJ, Holliday TW (2002) Neandertal cold adaptation: Physiological and energetic factors. *Am J Hum Biol* 14, 566-583.

Steegmann AT, Platner WS (1968) Experimental cold modification of cranio-facial morphology. *Am J Phys Anthropol* 28, 17-30.

Steindal IA, Whitmore D (2019) Circadian clocks in fish: what have we learned so far? *Biology* 8, 17.

Swift DL, Proctor DF (1977) Access of air to the respiratory tract. In J. Brain, D. F. Proctor, & L. Reid, éd. *Respiratory defense mechanisms*. New York: Dekker M, 63-91.

Takarada T, Kodama A, Hotta S, et al. (2012) Clock Genes Influence Gene Expression in Growth Plate and Endochondral Ossification in Mice. *Journal of Biological Chemistry* 287, 36081-36095.

Tansey EA, Johnson CD (2015) Recent advances in thermoregulation. *Advances in Physiology Education* 39, 139-148.

Tattersall GJ, Sinclair BJ, Withers PC, et al. (2012) Coping with Thermal Challenges: Physiological Adaptations to Environmental Temperatures. In R. Terjung, éd. *Comprehensive Physiology*. Wiley, 2151-2202.

Taubin G (1995) Curve and surface smoothing without shrinkage. In *Proceedings of IEEE International Conference on Computer Vision*. IEEE International Conference on Computer Vision. Cambridge, MA, USA: IEEE Comput. Soc. Press, 852-857.

The World Bank Group (2021) Climate Change Knowledge Portal for Development Practitioners and Policy Makers.

Thioulouse J, Dray S, Dufour A-B, et al. (2018) *Multivariate Analysis of Ecological Data with ade4*, New York, NY: Springer New York.

Thomson A (1913) The correlations of isotherms with variations in the nasal index. *International Congress of Medicine London* 17, 89-90.

Thomson A, Buxton LHD (1923) Man's Nasal Index in Relation to Certain Climatic Conditions. *The Journal of the Royal Anthropological Institute of Great Britain and Ireland* 53, 92.

Tillier A-M (1977) La pneumatisation du massif cranio-facial chez les hommes actuels et fossiles. *bmsap* 4, 177-189.

Tokuda H, Niwa M, Ito H, et al. (2003) Involvement of stress-activated protein kinase/c-Jun N-terminal kinase in endothelin-1-induced heat shock protein 27 in osteoblasts. *European Journal of Endocrinology*, 239-245.

Tomkinson A, Eccles R (1996) The effect of changes in ambient temperature on the reliability of acoustic rhinometry data. *Rhinology* 34, 75-77.

Toppozada H (1988) The human nasal mucosa in the menopause (a histochemical and electron microscopic study). *J Laryngol Otol* 102, 314-318.

Tos M (1982) Goblet cells and glands in the nose and paranasal sinuses. In D. F. Proctor & I. Andersen, éd. *The Nose: Upper Airway Physiology and the Atmospheric Environment*. New York: Elsevier Biomedical Press, 99-144.

Trinkaus E (1981) Neanderthal limb proportions and cold adaptation. In *Aspects of Human Evolution*. Taylor & Francis Ltd., 187-224.

Urciuoli A, Zanolli C, Beaudet A, et al. (2020) The evolution of the vestibular apparatus in apes and humans. *eLife* 9, e51261.

Vaillant M, Qiu A, Glaunès J, et al. (2007) Diffeomorphic metric surface mapping in subregion of the superior temporal gyrus. *NeuroImage* 34, 1149-1159.

Walker JEC, Wells RE (1961) Heat and water exchange in the respiratory tract. *The American Journal of Medicine* 30, 259-267.

van der Walt S, Smith N MPL Colour Maps. *https://bids.github.io/colormap*.

Wang B, Sudijono T, Kirveslahti H, et al. (2021) A statistical pipeline for identifying physical features that differentiate classes of 3D shapes. *Ann Appl Stat* 15.

Wang K, Denney TS, Morrison EE, et al. (2005) Numerical Simulation of Air Flow in the Human Nasal Cavity. In *2005 IEEE Engineering in Medicine and Biology 27th Annual Conference*. 2005 IEEE Engineering in Medicine and Biology 27th Annual Conference. Shanghai, China: IEEE, 5607-5610.

Warner A, Rahman A, Solsjo P, et al. (2013) Inappropriate heat dissipation ignites brown fat thermogenesis in mice with a mutant thyroid hormone receptor 1. *Proceedings of the National Academy of Sciences* 110, 16241-16246.

Washburn SL (1951) The New Physical Anthropology. *Transactions of the New York Academy of Sciences* 13, 298-304.

Watelet JB, Cauwenberge PV (1999) Applied anatomy and physiology of the nose and paranasal sinuses. *Allergy* 54, 14-25.

Wealthall RJ, Herring SW (2006) Endochondral ossification of the mouse nasal septum. *Anat Rec* 288A, 1163-1172.

Weaver T, Roseman C, Stringer C (2007) Were neandertal and modern human cranial differences produced by natural selection or genetic drift? *Journal of Human Evolution* 53, 135-145.

Weaver TD (2009) The meaning of Neandertal skeletal morphology. *Proceedings of the National Academy of Sciences* 106, 16028-16033.

Weinberg SM, Cornell R, Leslie EJ (2018) Craniofacial genetics: Where have we been and where are we going? *PLoS Genet* 14, e1007438.

Weiner JS (1954) Nose shape and climate. *Am J Phys Anthropol* 12, 615-618.

Welch BL (1951) On the Comparison of Several Mean Values: An Alternative Approach. *Biometrika* 38, 330.

Wen J, Inthavong K, Tu J, et al. (2008) Numerical simulations for detailed airflow dynamics in a human nasal cavity. *Respiratory Physiology & Neurobiology* 161, 125-135.

West-Eberhard MJ (2005) Developmental plasticity and the origin of species differences. *Proc Natl Acad Sci USA* 102, 6543-6549.

White DE, Bartley J, Nates RJ (2015) Model demonstrates functional purpose of the nasal cycle. *BioMed Eng OnLine* 14, 38.

White MD (2006) Components and mechanisms of thermal hyperpnea. *Journal of Applied Physiology* 101, 655-663.

Wickham H, Averick M, Bryan J, et al. (2019) Welcome to the Tidyverse. *JOSS* 4, 1686.

Williams RB (1998) The effects of excessive humidity. *Respir Care Clin N Am* 4, 215-228.

Winder IC, Devès MH, King GCP, et al. (2015) Evolution and dispersal of the genus Homo : A landscape approach. *Journal of Human Evolution* 87, 48-65.

de Wit E, Delport W, Rugamika CE, et al. (2010) Genome-wide analysis of the structure of the South African Coloured Population in the Western Cape. *Hum Genet* 128, 145-153.

Wolf M, Naftali S, Schroter RC, et al. (2004) Air-conditioning characteristics of the human nose. *J Laryngol Otol* 118, 87-92.

Wolpoff MH (1968) Climatic influence on the skeletal nasal aperture. *Am J Phys Anthropol* 29, 405-423.

Woo TL, Morant GM (1934) A Biometric Study of the « Flatness » of the Facial Skeleton in Man. *Biometrika* 26, 196-250.

Wroe S, Parr WCH, Ledogar JA, et al. (2018) Computer simulations show that Neanderthal facial morphology represents adaptation to cold and high energy demands, but not heavy biting. *Proc R Soc B* 285, 20180085.

Xiong G-X, Zhan J-M, Jiang H-Y, et al. (2008) Computational Fluid Dynamics Simulation of Airflow in the Normal Nasal Cavity and Paranasal Sinuses. *American Journal of Rhinology* 22, 477-482.

Xiong Z, Dankova G, Howe LJ, et al. (2019) Novel genetic loci affecting facial shape variation in humans. *eLife* 8, e49898.

Xu R, Li S, Guo S, et al. (2020) Environmental temperature and human epigenetic modifications: A systematic review. *Environmental Pollution* 259, 113840.

Yokley TR (2006) *The functional and adaptive significance of anatomical variation in recent and fossil human nasal passages*. Duke University.

Yokley TR (2009) Ecogeographic variation in human nasal passages. *Am J Phys Anthropol* 138, 11-22.

Zaidi AA, Mattern BC, Claes P, et al. (2017) Investigating the case of human nose shape and climate adaptation G. Gibson, éd. *PLoS Genet* 13, e1006616.

Zanolli C, Bouchet F, Fortuny J, et al. (2023) A reassessment of the distinctiveness of dryopithecine genera from the Iberian Miocene based on enamel-dentine junction geometric morphometric analyses. *Journal of Human Evolution* 177, 103326.

Zhang M, Golland P (2016) Statistical shape analysis: From landmarks to diffeomorphisms. *Medical Image Analysis* 33, 155-158.

Zhao K (2004) Effect of Anatomy on Human Nasal Air Flow and Odorant Transport Patterns: Implications for Olfaction. *Chemical Senses* 29, 365-379.

Zhao K, Jiang J (2014) What is normal nasal airflow? A computational study of 22 healthy adults: Normal human nasal airflow. *International Forum of Allergy & Rhinology* 4, 435-446.

Zhao Z-J (2011) Serum Leptin, Energy Budget, and Thermogenesis in Striped Hamsters Exposed to Consecutive Decreases in Ambient Temperatures. *Physiological and Biochemical Zoology* 84, 560-572.

Zhu JH, Lee HP, Lim KM, et al. (2011) Evaluation and comparison of nasal airway flow patterns among three subjects from Caucasian, Chinese and Indian ethnic groups using computational fluid dynamics simulation. *Respiratory Physiology & Neurobiology* 175, 62-69.

Zimmerman DW (2004) A note on preliminary tests of equality of variances. *British Journal of Mathematical and Statistical Psychology* 57, 173-181.

Zollikofer CPE, Weissmann JD (2008) A Morphogenetic Model of Cranial Pneumatization Based on the Invasive Tissue Hypothesis. *Anat Rec* 291, 1446-1454.

Zuckerkandl E (1893) *Normale und pathologishe Anatomie der Nasenhöle und ihrer pneumatischen Anhänge* W. Braumuller., Wien.

Appendix A. Supplementary information of article 2

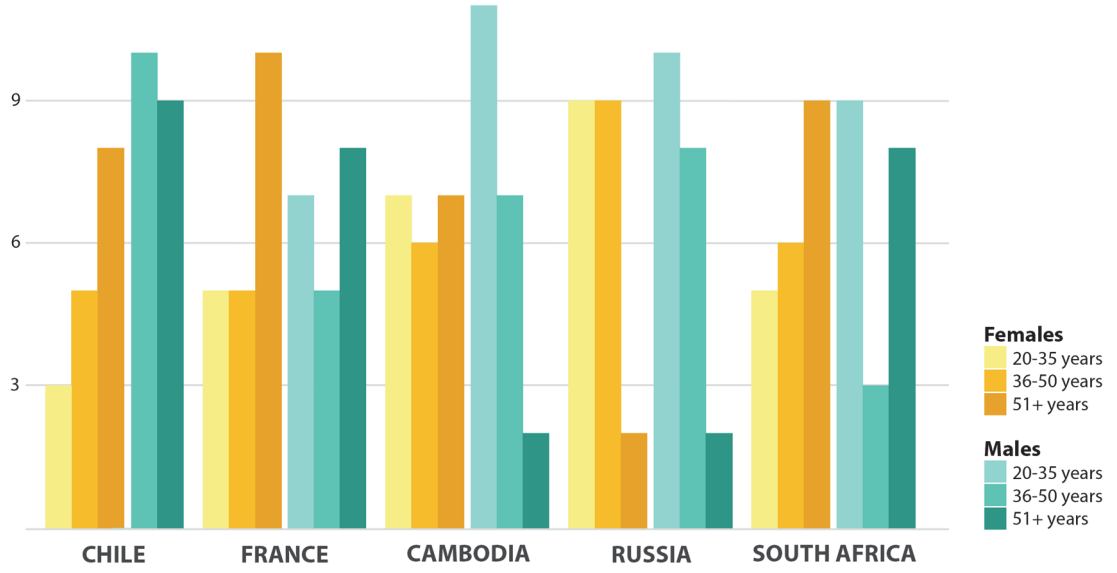

Figure A1. Sample composition by population, sex and age categories.

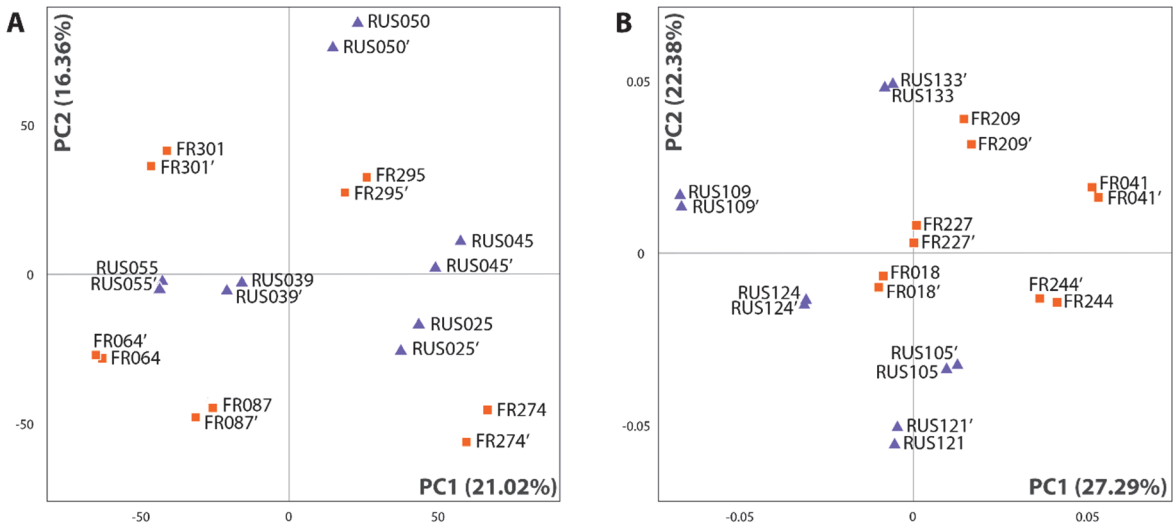

Figure A2. Intra-observer test on NA segmentation (A) and facial skeleton landmarking (B). For both tests, 10 individuals were randomly selected in the samples from France and from Russia. These individuals were segmented (A) or landmarked (B) twice at several weeks interval. Then we made a PCA on the deformation-based shape comparison of the NA (A) and a PCA on the Procrustes coordinates of the 3D landmarks measured on the facial skeleton (B). For each individual, the first measurement is represented by the ID of the individual and the second measurement by ID'. We consider both tests to be validated because the first and second measures of each individual are all closer to each other in the morphospace than to a measure of another individual. Furthermore, the distances between individuals are always greater than the distances between two measurements of the same individual.

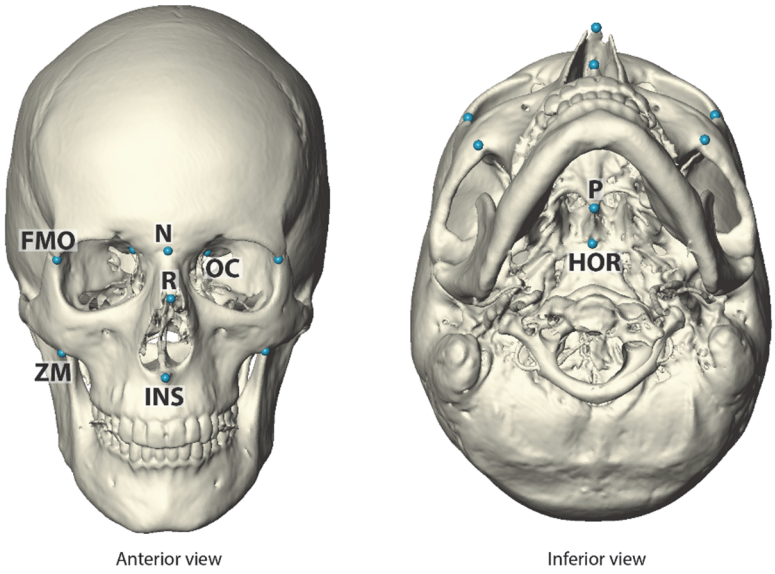

Figure A3. 11 landmarks measured on the facial skeleton: nasion (N), rhinion (R), inferior nasal spine (INS), frontomalare orbitale (FMO), zygomaxillare (ZM), optic canal (OC), palatine (P) and hormion (HOR).

A

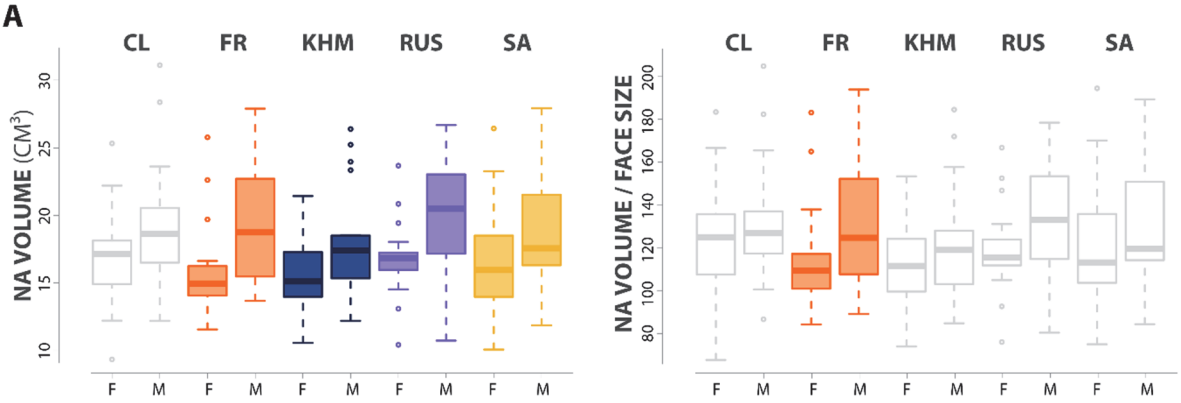

B

	N	NA volume (cm^3)	Centroid size	NA volume/face size
Chile				
Females	16	16.90 *(3.8)*	136.37 *(3.9)*	124.14 *(28.5)*
Males	19	19.18 *(4.7)*	145.04 *(5.7)*	131.66 *(28.6)*
France				
Females	20	15.70 *(3.5)*	137.91 *(4.1)*	113.81 *(24.3)*
Males	20	19.28 *(4.1)*	147.30 *(4.9)*	130.93 *(27.7)*
Cambodia				
Females	20	15.72 *(2.6)*	138.82 *(3.4)*	113.28 *(18.4)*
Males	20	17.99 *(3.9)*	147.44 *(4.3)*	122.07 *(26.6)*
Russia				
Females	20	16.80 *(2.7)*	141.07 *(5.4)*	119.22 *(19.8)*
Males	20	19.83 *(4.1)*	149.34 *(5.4)*	132.49 *(26.4)*
South Africa				
Females	20	16.16 *(4.0)*	135.49 *(4.8)*	119.30 *(29.5)*
Males	20	18.80 *(4.3)*	144.31 *(4.4)*	130.13 *(28.6)*

Figure A4. Box-whisker plots representing sexual dimorphism within each population in NA volume and in NA volume normalized by the centroid size of the facial skeleton (A). The boxplots are colored when the influence of sex is significant ($p < 0.05$) (see Table A4). Mean values of the raw and scaled NA volumes for the five population groups divided by sexes (B).

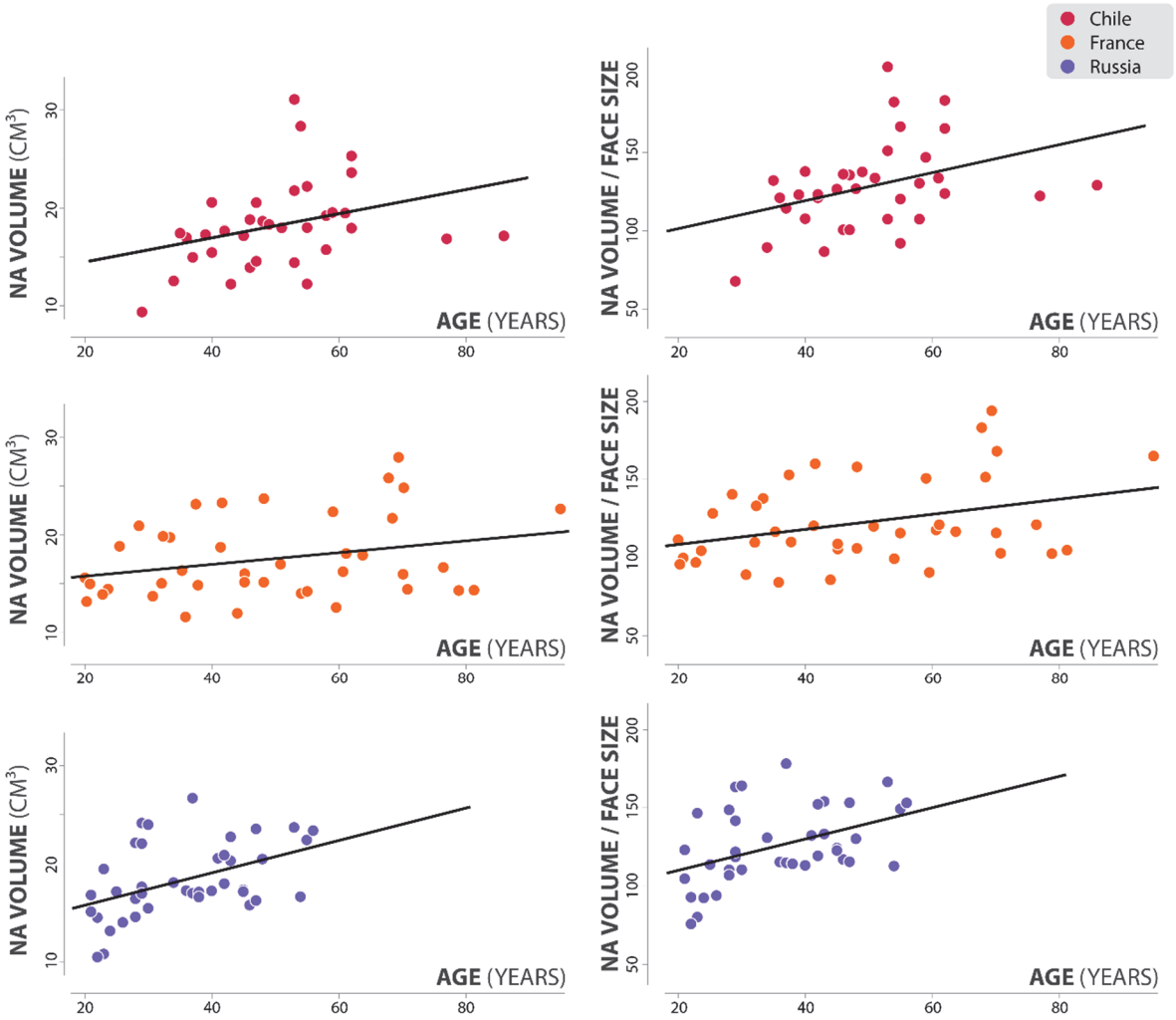

Figure A5. Regression plots representing age influence within each population in NA volume (left) and in NA volume normalized by the centroid size of the facial skeleton (right). Age influence is significant for these 3 populations (Chile, France and Russia) (see Table A4) except for France when considering (non-normalized) NA volume.

Table A1. Results of the PERMANOVAs performed on all the PCs and on the 5 populations (N = 195) to quantify the effect of sex, age and temperature and humidity at the time of scan on the distribution of the sample in the morphospace. F and R^2 values and associated p values are indicated for each test. When the results were considered significant ($p < 0.05$) and the factor being tested included more than two groups, we performed a post-hoc test to quantify the pairwise distances.

			F	R^2	p
Geographical group			6.500	0.120	0.001*
Sex			1.655	0.009	0.040*
Age			1.228	0.013	0.142
Temperature			4.271	0.083	0.001*
	>25°C	0-9°C	10.071	0.148	0.002*
	>25°C	<0°C	8.760	0.142	0.002*
	>25°C	20-24°C	7.862	0.086	0.002*
	>25°C	10-19°C	5.533	0.047	0.002*
	10-19°C	0-9°C	3.369	0.035	0.002*
	10-19°C	<0°C	3.127	0.035	0.003*
	0-9°C	20-24°C	1.930	0.029	0.046*
	10-19°C	20-24°C	1.864	0.016	0.065
	<0°C	20-24°C	1.782	0.029	0.065
	<0°C	0-9°C	0.927	0.027	0.567
Humidity			1.315	0.020	0.059

Table A2. Results of the PERMANOVAs of the effect of geographical group, age and sex on the distribution of the sample on each PC from PC1 to PC8. F and R^2 values and associated p values are indicated for each PC. Correlations are considered significant when $p < 0.05$.

		F	R^2	p
Geographical group				
PC1	(18.59%)	34.700	0.422	0.001*
PC2	(6.91%)	6.194	0.115	0.001*
PC3	(5.26%)	4.674	0.090	0.003*
PC4	(3.99%)	5.294	0.100	0.001*
PC5	(3.8%)	0.696	0.014	0.605
PC6	(3.64%)	4.539	0.087	0.001*
PC7	(3.36%)	4.197	0.081	0.003*
PC8	(3%)	2.962	0.059	0.020*
Sex				
PC1	(18.59%)	0.023	0.001	0.879
PC2	(6.91%)	0.208	0.001	0.656
PC3	(5.26%)	4.447	0.023	0.032*
PC4	(3.99%)	0.687	0.004	0.402
PC5	(3.8%)	0.014	0.001	0.910
PC6	(3.64%)	0.137	0.001	0.702
PC7	(3.36%)	2.795	0.014	0.096
PC8	(3%)	2.587	0.013	0.100
Age				
PC1	(18.59%)	1.742	0.018	0.183
PC2	(6.91%)	0.069	0.001	0.938
PC3	(5.26%)	1.566	0.016	0.192
PC4	(3.99%)	0.510	0.005	0.608
PC5	(3.8%)	1.081	0.011	0.358
PC6	(3.64%)	0.950	0.010	0.406
PC7	(3.36%)	0.654	0.007	0.529
PC8	(3%)	1.572	0.016	0.212

Table A3. Results of the bivariate regressions between each of the first three PCs and the log-transformed volume of NA, to quantify the effect of allometry on the sample distribution in the morphospace. Correlations are considered significant when p <0.05.

	PC eigenvalue	R^2	p
5 populations *(N=195)*			
PC1 vs. ln(Vol)	18.59%	0.005	0.167
PC2 vs. ln(Vol)	6.91%	0.057	0.001*
PC3 vs. ln(Vol)	5.26%	0.069	0.001*
Chile *(N=35)*			
PC1 vs. ln(Vol)	21.02%	0.023	0.629
PC2 vs. ln(Vol)	8.27%	0.186	0.006*
PC3 vs. ln(Vol)	7.64%	0.006	0.278
France *(N=40)*			
PC1 vs. ln(Vol)	12.82%	0.156	0.007*
PC2 vs. ln(Vol)	8.54%	0.015	0.527
PC3 vs. ln(Vol)	7.52%	0.018	0.200
Cambodia *(N=40)*			
PC1 vs. ln(Vol)	14.93%	0.181	0.004*
PC2 vs. ln(Vol)	10.98%	0.139	0.010*
PC3 vs. ln(Vol)	8.86%	0.022	0.678
Russia (N=40)			
PC1 vs. ln(Vol)	11.25%	0.017	0.552
PC2 vs. ln(Vol)	10.19%	0.002	0.302
PC3 vs. ln(Vol)	8.57%	0.124	0.014*
South Africa *(N=40)*			
PC1 vs. ln(Vol)	18.67%	0.004	0.293
PC2 vs. ln(Vol)	9.14%	0.026	0.908
PC3 vs. ln(Vol)	7.23%	0.0006	0.330

Table A4. Results of the ANOVAs performed on NA volume (left) and on NA volume normalized by the centroid size of the facial skeleton (right) to test the influence of geographical group, sex, age, and temperature and humidity at the time of scan. Correlations are considered significant when p <0.05.

	NA volume			Ratio NA volume / face size		
	F	R^2	p	F	R^2	p
5 populations *(N=195)*						
Geographical group	0.826		0.510	0.883		0.475
Sex	26.570		0.001*	10.100		0.002*
Age	9.163	0.045	0.003*	12.990	0.063	0.001*
Temperature	0.874	0.005	0.351	0.431	0.002	0.512
Humidity	0.000	0.001	0.989	0.129	0.001	0.720
Chile *(N=35)*						
Sex	2.439		0.128	0.601		0.444
Age	4.126	0.111	0.050*	5.263	0.138	0.028*
Temperature	2.432	0.069	0.128	2.155	0.061	0.152
Humidity	1.160	0.034	0.289	0.860	0.025	0.361
France *(N=40)*						
Sex	8.979		0.005*	4.313		0.045*
Age	3.249	0.079	0.080	5.077	0.118	0.030*
Temperature	2.476	0.061	0.124	3.822	0.091	0.058
Humidity	0.848	0.022	0.363	1.270	0.032	0.267
Cambodia *(N=40)*						
Sex	4.702		0.037*	1.474		0.232
Age	0.243	0.006	0.625	0.183	0.005	0.671
Temperature	N/A	N/A	N/A	N/A	N/A	N/A
Humidity	0.032	0.001	0.859	0.035	0.001	0.853
Russia (N=40)						
Sex	7.606		0.009*	3.222		0.081
Age	10.21	0.212	0.003*	8.845	0.189	0.005*
Temperature	0.001	0.001	0.979	0.028	0.001	0.869
Humidity	0.117	0.003	0.734	0.073	0.002	0.789
South Africa *(N=40)*						
Sex	4.036		0.052*	1.390		0.246
Age	1.851	0.046	0.182	2.153	0.054	0.151
Temperature	N/A	N/A	N/A	N/A	N/A	N/A
Humidity	N/A	N/A	N/A	N/A	N/A	N/A

Table A5. Results of the PERMANOVAs performed on all the PCs and on each population separately to quantify the effect of sex, age and temperature and humidity at the time of scan on the distribution of each sample in the morphospace. F and R^2 values and associated p values are indicated for each test. When the results were considered significant ($p < 0.05$) and the factor being tested included more than two groups, we performed a post-hoc test to quantify the pairwise distances.

			F	R^2	p
Chile *(N=35)*					
Sex			1.455	0.042	0.081
Age			1.008	0.059	0.404
Temperature			1.106	0.065	0.267
Humidity			1.056	0.031	0.326
France *(N=40)*					
Sex			1.243	0.032	0.147
Age			1.134	0.058	0.208
Temperature			0.762	0.040	0.945
Humidity			0.773	0.040	0.935
Cambodia *(N=40)*					
Sex			0.609	0.016	0.971
Age			1.108	0.057	0.250
Temperature			N/A	N/A	N/A
Humidity			1.318	0.067	0.069
Russia (N=40)					
Sex			1.056	0.027	0.360
Age			1.068	0.055	0.312
Temperature			1.306	0.098	0.031*
	>20°C	<0°C	1.857	0.085	0.038*
	>20°C	10-19°C	1.857	0.117	0.038*
	>20°C	0-9°C	1.689	0.108	0.062
	<0°C	10-19°C	1.093	0.047	0.925
	<0°C	0-9°C	0.938	0.041	1.000
	0-9°C	10-19°C	0.622	0.037	1.000
Humidity			1.173	0.060	0.135
South Africa *(N=40)*					
Sex			0.869	0.022	0.621
Age			0.715	0.037	0.960
Temperature			N/A	N/A	N/A
Humidity			N/A	N/A	N/A

Appendix B. Supplementary information of article 3

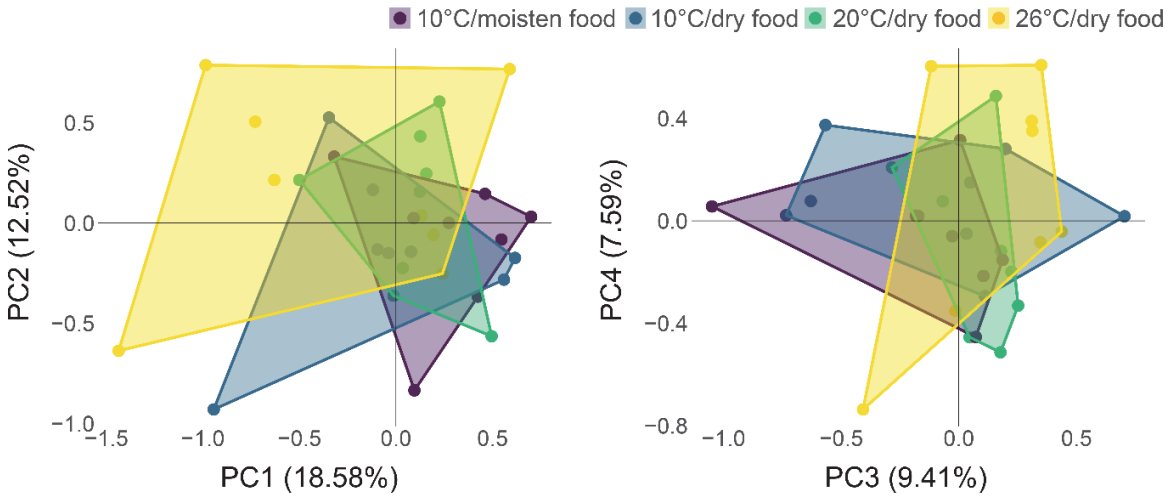

Figure B1. Principal Component Analysis (PCA) based on the anatomical landmarks measured on the craniofacial skeleton of the 4 mice groups.

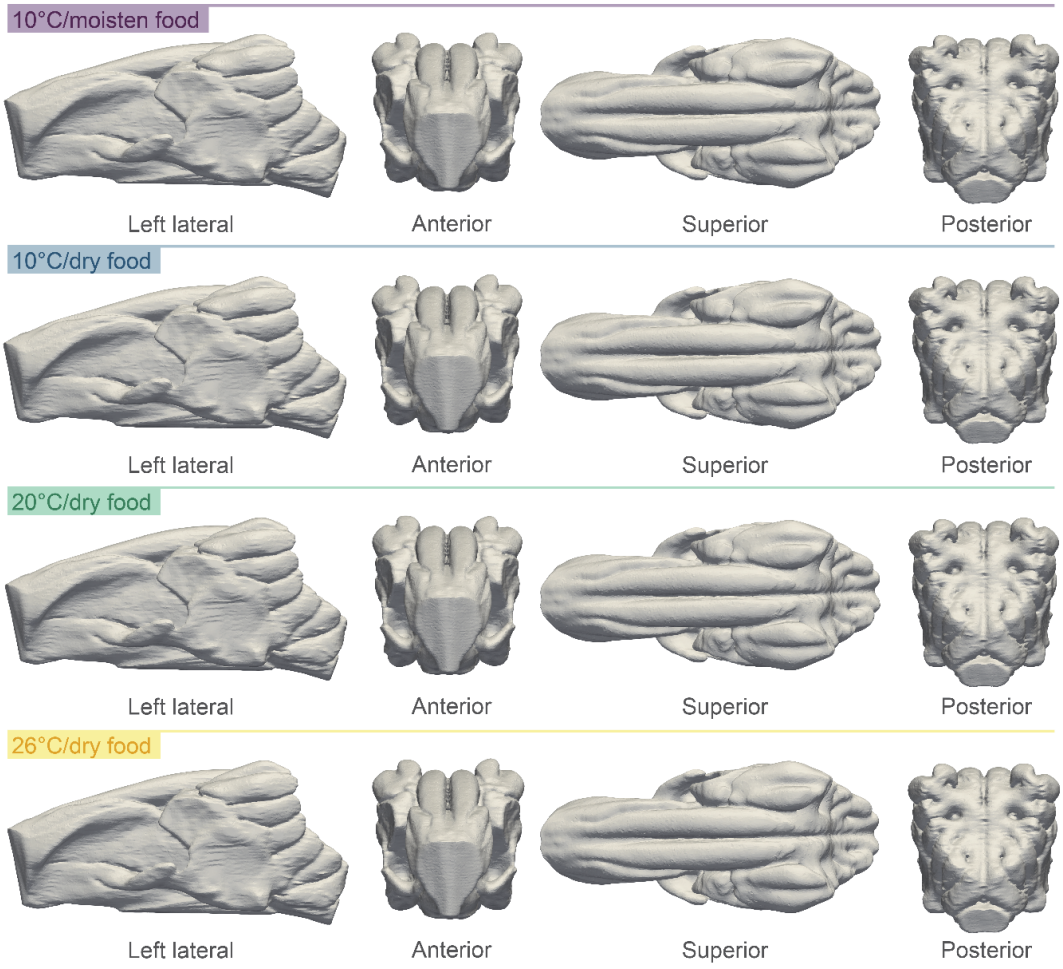

Figure B2. Nasal cavity mean shape per group, computed through the deformation-based shape comparison.

Table B1. Description and characteristics of the craniofacial landmarks measured on the reconstructed skulls of the mice.

#	Landmark description	Location
1	Most anterio-superior point of the intersection of the L and R anterior turbinates	Midline
2	Most posterior point of the intersection of the posterior turbinates	Midline
3	Most anterior point of the indentation in the center of the presphenoid	Midline
4/5	Most postero-lateral point on the body of the presphenoid	Bilateral
6	Most antero-medial point on the body of the sphenoid	Midline
7	Most anterior point in the center of the basioccipital	Midline
8/9	Most postero-lateral point on the sphenoid	Bilateral
10	Mid-point on the anterior margin of the foramen magnum, taken on basioccipital	Midline
11	Mid-point on the posterior margin of the foramen magnum, taken on squamous occipital	Midline
12/13	Most anterior point of the anterior palatine foramen	Bilateral
14/15	Most posterior point of the anterior palatine foramen	Bilateral
16/17	Most infero-lateral point of the premaxillary-maxillary suture, taken on premaxilla	Bilateral
18	Most posterior point on the center of the premaxilla	Midline
19/20	Most antero-lateral identation at the posterior edge of the palatine plate	Bilateral
21/22	Post molar point taken on the palatine	Bilateral
23/24	Most medial point on the formanen inferior to the foramen magnum	Bilateral
25/26	Most lateral point on the foramen magnum (depression posterior to the condyle)	Bilateral
27	Nasale on left nasal bone	Midline
28	Nasion on nasal suture	Midline
29/30	Most postero-lateral point of the nasal bone	Bilateral
31	Bregma	Midline
32	Lambda taken on intraparietal	Midline
33/34	Most lateral superior point of the intraparietal	Bilateral
35	Most superior point in the center of the sqamous occipital	Midline
36/37	Most infero-posterior point on the parietal	Bilateral
38/48	Most supero-anterior point of the maxilla on the lateral part of the nasal aperture	Bilateral
39/49	Most distal point of the infraorbital hiatus	Bilateral
40/50	Intersection of maxilla frontal process with frontal and lacrimal bones, taken on the maxilla	Bilateral
41/51	Intersection of zygoma with zygomatic process of maxilla, taken on zygoma	Bilateral
42/52	Intersection of zygoma with zygomatic process of temporal, taken on zygoma	Bilateral
43/53	Basis of the zygomatic process of the temporal	Bilateral
44/54	Most supero-posterior point of the sphenoid canal	Bilateral
45/55	Intersection between frontal, sphenoid and squamous part of the temporal on sphenoid	Bilateral
46/56	Most superior point on the squamous temporal, intersection of the coronal suture	Bilateral
47/57	Most infero-posterior point of the external auditory meatus	Bilateral

Table B2. Body mass differences between groups: results of the Welch's F-test and the Kruskal-Wallis test. The results are considered significant (*) when p<0.05.

Welch F test (F=3.91, p=0.031)		p		**Kruskal-Wallis test** (χ^2=10.85, p=0.013)		
Cold (dry food)	Control	0.522		Cold (dry food)	Control	
Cold (dry food)	Thermoneutrality	0.153		Cold (dry food)	Thermoneutrality	*****
Cold (dry food)	Cold (moist food)	0.201		Cold (dry food)	Cold (moist food)	
Control	Thermoneutrality	0.351		Control	Thermoneutrality	
Control	Cold (moist food)	0.167		Control	Cold (moist food)	*
Thermoneutrality	Cold (moist food)	0.033	*	Thermoneutrality	Cold (moist food)	*

Table B3. Lean mass differences between groups: results of the Welch's F-test and the Kruskal-Wallis test. The results are considered significant (*) when p<0.05.

Welch F test (F=4.98, p=0.013)		p		**Kruskal-Wallis test** (χ^2=8.18, p=0.042)		
Cold (dry food)	Control	0.988		Cold (dry food)	Control	
Cold (dry food)	Thermoneutrality	0.076		Cold (dry food)	Thermoneutrality	*****
Cold (dry food)	Cold (moist food)	0.391		Cold (dry food)	Cold (moist food)	
Control	Thermoneutrality	0.218		Control	Thermoneutrality	
Control	Cold (moist food)	0.421		Control	Cold (moist food)	
Thermoneutrality	Cold (moist food)	0.013	*	Thermoneutrality	Cold (moist food)	*

Table B4. Skull centroid size difference between groups: results of the Welch's F-test and the Kruskal-Wallis test.

Welch F test (F=2.28, p=0.119)	**Kruskal-Wallis test** (χ^2=6.47, p=0.091)

Table B5. Pairwise PERMANOVA testing for shape differences between groups for the first six principal components. The results are considered significant (*) when p<0.05.

PC1 (15.58%)			F	p	
PERMANOVA (testing for group differences)			20.453	<0.001	*
Pairwise comparison	Cold (dry food)	Control	33.693	<0.001	*
	Cold (dry food)	Thermoneutrality	27.238	<0.001	*
	Cold (dry food)	Cold (moist food)	48.608	<0.001	*
	Control	Thermoneutrality	0.136	0.719	
	Control	Cold (moist food)	3.331	0.088	
	Thermoneutrality	Cold (moist food)	1.237	0.296	

PC2 (11.14%)			F	p	
PERMANOVA (testing for group differences)			4.333	0.017	*
Pairwise comparison	Cold (dry food)	Control	0.176	0.672	
	Cold (dry food)	Thermoneutrality	1.801	0.192	
	Cold (dry food)	Cold (moist food)	3.819	0.071	
	Control	Thermoneutrality	4.329	0.062	
	Control	Cold (moist food)	3.327	0.092	
	Thermoneutrality	Cold (moist food)	12.045	0.002	*

PC3 (9.32%)			F	p	
PERMANOVA (testing for group differences)			5.973	0.005	*
Pairwise comparison	Cold (dry food)	Control	7.136	0.021	*
	Cold (dry food)	Thermoneutrality	0.752	0.393	
	Cold (dry food)	Cold (moist food)	5.748	0.034	*
	Control	Thermoneutrality	1.452	0.249	
	Control	Cold (moist food)	18.809	0.002	*
	Thermoneutrality	Cold (moist food)	5.869	0.034	*

PC4 (7.92%)	F	p
PERMANOVA (testing for group differences)	0.228	0.882

PC5 (6.25%)	F	p
PERMANOVA (testing for group differences)	0.779	0.531

PC6 (4.94%)	F	p
PERMANOVA (testing for group differences)	0.318	0.823

Table B6. Nasal cavity volume differences between groups: results of the Welch's F-test and the Kruskal-Wallis test. The results are considered significant (*) when p<0.05.

Welch F test (F=10.03, p<0.001)		p		**Kruskal-Wallis test** (χ^2=15.20, p=0.001)		
Cold (dry food)	Control	0.103		Cold (dry food)	Control	*
Cold (dry food)	Thermoneutrality	0.478		Cold (dry food)	Thermoneutrality	
Cold (dry food)	Cold (moist food)	0.003	*	Cold (dry food)	Cold (moist food)	*
Control	Thermoneutrality	0.478		Control	Thermoneutrality	
Control	Cold (moist food)	0.340		Control	Cold (moist food)	*
Thermoneutrality	Cold (moist food)	0.042	*	Thermoneutrality	Cold (moist food)	*

Table B7. Nasal cavity volume (normalized by body mass) differences between groups: results of the Welch's F-test and the Kruskal-Wallis test. The results are considered significant (*) when p<0.05.

Welch F test (F=7.60, p=0.002)		p		**Kruskal-Wallis test** (χ^2=13.38, p=0.004)		
Cold (dry food)	Control	0.049	*	Cold (dry food)	Control	*
Cold (dry food)	Thermoneutrality	0.004	*	Cold (dry food)	Thermoneutrality	*
Cold (dry food)	Cold (moist food)	0.806		Cold (dry food)	Cold (moist food)	
Control	Thermoneutrality	0.410		Control	Thermoneutrality	
Control	Cold (moist food)	0.194		Control	Cold (moist food)	*
Thermoneutrality	Cold (moist food)	0.054		Thermoneutrality	Cold (moist food)	*

Table B8. Nasal cavity volume (normalized by lean mass) differences between groups: results of the Welch's F-test and the Kruskal-Wallis test. The results are considered significant (*) when p<0.05.

Welch F test (F=10.95, p<0.001)		p		**Kruskal-Wallis test** (χ^2=12.07, p=0.007)		
Cold (dry food)	Control	0.279		Cold (dry food)	Control	*
Cold (dry food)	Thermoneutrality	<0.001	*	Cold (dry food)	Thermoneutrality	*
Cold (dry food)	Cold (moist food)	0.425		Cold (dry food)	Cold (moist food)	
Control	Thermoneutrality	0.425		Control	Thermoneutrality	
Control	Cold (moist food)	0.578		Control	Cold (moist food)	
Thermoneutrality	Cold (moist food)	0.147		Thermoneutrality	Cold (moist food)	*

Table B9. Maxilloturbinate volume differences between groups: results of the Welch's F-test and the Kruskal-Wallis test.

Welch F test (F=2.60, p=0.090)	**Kruskal-Wallis test** (χ^2=5.32, p=0.149)

Table B10. Nasoturbinate volume differences between groups: results of the Welch's F-test and the Kruskal-Wallis test.

Welch F test (F=0.37, p=0.775)	**Kruskal-Wallis test** (χ^2=1.10, p=0.777)

Table B11. Maxilloturbinate volume (normalized by nasal cavity volume) differences between groups: results of the Welch's F-test and the Kruskal-Wallis test. The results are considered significant (*) when p<0.05.

Welch F test (F=3.03, p=0.060)		**Kruskal-Wallis test** (χ^2=7.87, p=0.049)		
Cold (dry food)	Control	Cold (dry food)	Control	
Cold (dry food)	Thermoneutrality	Cold (dry food)	Thermoneutrality	*
Cold (dry food)	Cold (moist food)	Cold (dry food)	Cold (moist food)	*
Control	Thermoneutrality	Control	Thermoneutrality	
Control	Cold (moist food)	Control	Cold (moist food)	
Thermoneutrality	Cold (moist food)	Thermoneutrality	Cold (moist food)	

Table B12. Nasoturbinate volume (normalized by nasal cavity volume) differences between groups: results of the Welch's F-test and the Kruskal-Wallis test.

Welch F test (F=0.32, p=0.813)	**Kruskal-Wallis test** (χ^2=2.31, p=0.511)

Table B13. Maxilloturbinate surface area differences between groups: results of the Welch's F-test and the Kruskal-Wallis test.

Welch F test (F=0.85, p=0.490)	**Kruskal-Wallis test** (χ^2=2.09, p=0.553)

Table B14. Nasoturbinate surface area differences between groups: results of the Welch's F-test and the Kruskal-Wallis test.

Welch F test (F=2.79, p=0.078)	**Kruskal-Wallis test** (χ^2=6.40, p=0.094)

Table B15. Maxilloturbinate surface area (normalized by nasal cavity volume) differences between groups: results of the Welch's F-test and the Kruskal-Wallis test. The results are considered significant (*) when p<0.05.

Welch F test (F=6.38, p=0.006)		p		**Kruskal-Wallis test** (χ^2=9.87, p=0.019)		
Cold (dry food)	Control	0.835		Cold (dry food)	Control	
Cold (dry food)	Thermoneutrality	0.835		Cold (dry food)	Thermoneutrality	
Cold (dry food)	Cold (moist food)	0.042	*	Cold (dry food)	Cold (moist food)	*
Control	Thermoneutrality	0.835		Control	Thermoneutrality	
Control	Cold (moist food)	0.103		Control	Cold (moist food)	*
Thermoneutrality	Cold (moist food)	0.357		Thermoneutrality	Cold (moist food)	*

Table B16. Nasoturbinate surface area (normalized by nasal cavity volume) differences between groups: results of the Welch's F-test and the Kruskal-Wallis test. The results are considered significant (*) when p<0.05.

Welch F test (F=10.81, p=0<0.001)		p		**Kruskal-Wallis test** (χ^2=12.41, p=0.006)		
Cold (dry food)	Control	0.740		Cold (dry food)	Control	
Cold (dry food)	Thermoneutrality	0.432		Cold (dry food)	Thermoneutrality	
Cold (dry food)	Cold (moist food)	0.238		Cold (dry food)	Cold (moist food)	*
Control	Thermoneutrality	0.740		Control	Thermoneutrality	
Control	Cold (moist food)	0.054		Control	Cold (moist food)	*
Thermoneutrality	Cold (moist food)	0.002	*	Thermoneutrality	Cold (moist food)	*